Molecular insights into the mechanism of sensing and signal transduction of the thermosensor DesK

Joost Ballering

Colofon

J. Ballering

Molecular insights into the mechanism of sensing and signal transduction of the thermosensor DesK

PhD Thesis, Utrecht University, 2016
In English, with summary in Dutch

ISBN: 978-90-393-6534-2

Cover design:	Joost Ballering
Cover image:	Science meets culture: methamorphosis from Chateau de Blois to membrane cartoon.
Printed by:	Proefschriftmaken.nl || Uitgeverij BOXPress
Published by:	Uitgeverij BOXPress, 's-Hertogenbosch

The research presented in this thesis was performed at the Membrane Biochemistry and Biophysics group, Bijvoet Center for Biomolecular Research, Faculty of Science, Utrecht University, the Netherlands. The printing of this thesis was financially supported by Avanti Polar Lipids, Eurogentec and the J.E. Jurriaanse Stichting.

Molecular insights into the mechanism of sensing and signal transduction of the thermosensor DesK

Moleculaire inzichten in het mechanisme van detectie en signaaltransductie van de thermosensor DesK

(met een samenvatting in het Nederlands)

Proefschrift

ter verkrijging van de graad van doctor aan de Universiteit Utrecht op gezag van de rector magnificus, prof. dr. G.J. van der Zwaan, ingevolge het besluit van het college voor promoties in het openbaar te verdedigen op woensdag 20 april 2016 des middags te 2.30 uur

door

Joost Ballering

geboren op 1 maart 1981
te Leiden

Promotor

Prof. dr. J.A. Killian

The research described in this thesis was supported by an ECHO grant of the Netherlands Organization for Scientific Research (NWO)

Table of contents

Chapter 1	General introduction	**9**
Chapter 2	Activation of the bacterial thermosensor DesK involves a serine zipper dimerization motif that is modulated by bilayer thickness	**33**
Chapter 3	Structural properties of the transmembrane helices of the thermosensor DesK are regulated by both length and phase state of the surrounding lipids	**61**
Chapter 4	Cold adaptation of *Bacillus subtilis* by regulation of lipid composition	**81**
Chapter 5	Exploring the use of a styrene-maleic acid polymer to determine the oligomerization state of MS-DesK	**99**
Chapter 6	Summarizing discussion	**115**
Addendum		**129**
	Nederlandse samenvatting	**131**
	List of publications	**137**
	Curriculum Vitae	**139**
	Dankwoord	**141**

1

General introduction

1. Cell membrane architecture

Marvel and wonder about the universe and the life within is immemorial and may underlie our continuous quest of understanding the world around us. Contributions to our understanding of nature were made all throughout human history. The development of mathematics, philosophy and astronomy dates back to the ancient civilizations of Greece, Egypt, Mesopotamia, the Indus valley, China and the Mayans. During the European Renaissance, scientists gradually changed traditional methods and proclaim their faith in logic as a measure of all things [1-3]. The drive of artists and scientists alike to display matters as they are – contrary to adding to the teachings of predecessors – lead them to observe carefully and experiment under controlled conditions [1, 2]. To improve the quality of his paintings, Leonardo da Vinci systematically dissected dozens of corpses and made beautiful, realistic drawings with which he described the human anatomy in more detail than ever before [4]. Vesalius, a famous anatomist had artists to make visualizations of his dissections [3, 4]. In the 17th century, the new opinions and methods of the Renaissance culminated in the scientific revolution and modern fact-finding, practice-oriented experimental science came into the world [1, 2]. New paradigms arose in physics and astronomy, and the invention of the microscope enabled the observation of cells. Cells were recognized as the basic units of all organisms and a theory emerged, consisting of three theorems: 1) all living organisms are composed of one or more cells, 2) the cell is the basic unit of structure and organization in organisms and 3) all cells rise from pre-existing cells. In the 19th century this cell theory became generally accepted. However, an intriguing question remained: what is the nature of the cell membrane, the outer defining barrier of the cell, which allows for selective transport of substances into and out of the cell? It would take until the 20th century, to unravel both the chemical composition and the structure of the cell membrane. We now know that it is a sheet-like structure consisting mainly of lipids and proteins. Some common membrane components and their properties, which are relevant for the research in this thesis will be discussed below.

1.1 Lipids

Many properties of a biological membrane are defined by the lipids, biomolecules which are water-insoluble, but highly soluble in organic solvents. Lipids are amphipathic molecules that contain both a hydrophobic tail and a hydrophilic head group. In aqueous solutions, hydrophobic moieties tend to cluster together, minimizing the disturbance of energetically favorable hydrogen bonds. This phenomenon is called the hydrophobic effect and it drives amphiphilic molecules to form structures such as micelles or bilayers. Most lipids in aqueous environment spontaneously form bilayers, i.e. two layers with the tails clustered together in a hydrophobic core, and the hydrophilic head groups facing the aqueous environment. In biological membranes the lipids are arranged in such bilayers, also referred to as lamellae, a concept first proposed by the Dutch scientists Gorter and Grendel [5].

Common lipids in biomembranes are glycerophospholipids, sphingophospholipids, glycolipids and sterols. This thesis will mainly focus on glycerophospholipids, which belong to the most common type of lipids in cell membranes. Glycerophospholipids are composed of a glycerol backbone, with two esterified fatty acids attached, which form the hydrophobic tail of the lipid. Common structures are illustrated in Table 1. The hydrophilic head group consists of a phosphate moiety, often esterified to an alcohol. The phosphate of the head group is esterified to the C-3 hydroxyl group of the glycerol. The fatty acid chains differ in length, branching pattern and degree of saturation, giving rise to an enormous diversity in lipid species. The variety in alcohols attached to the head group, some of which can be glycosylated, further increases the complexity.

Lipid bilayers are highly impermeable to ions and most polar molecules, except for water, which crosses the bilayer relatively easily. These characteristics qualify the lipid bilayer as an excellent barrier to separate the inside from the outside of cells. However, many substances need to enter and exit the cell in a controlled way. For these and other functions cells are dependent on different components of the membrane: the membrane proteins.

1.2 Membrane proteins

Most of the dynamic processes which take place in biological membranes are carried out by membrane proteins. These associate with the membrane in various ways, classified as either integral or peripheral. Integral membrane proteins are embedded in the membrane, interacting extensively with the hydrophobic acyl chains of the lipids. Peripheral membrane proteins are more transiently associated to the membrane, mainly interacting with the lipid head groups by electrostatic and hydrogen-bond interactions. Integral membrane proteins either embed part of their structure in the membrane, or they protrude through the membrane with one or more α-helices or β-sheets. The membrane-spanning α-helix is the most common structural motif

Table 1. Structure of common phospholipids at physiological conditions.

Basic phospholipid structure	Substituent (X)	Name
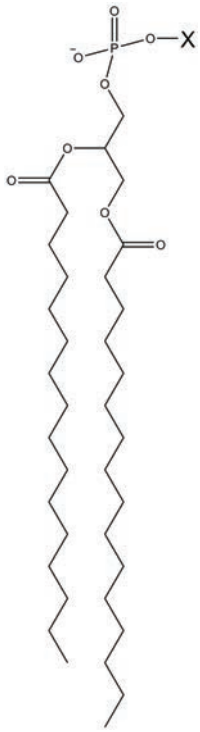	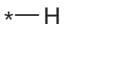 hydrogen	phosphatidic acid (PA)
	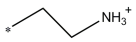 ethanolamine	phosphatidylethanolamine (PE)
	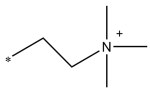 choline	phosphatidylcholine (PC)
	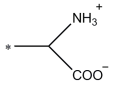 serine	phosphatidylserine (PS)
	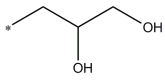 glycerol	phosphatidylglycerol (PG)
	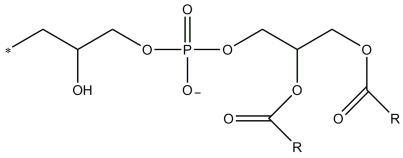 phosphatidylglycerol	cardiolipin (CL)
	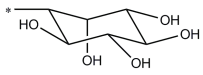 inositol	phosphatidylinositol (PI)

in membrane proteins. Helices are involved in the formation of channels and pumps that allow for selective transport over the membrane and are responsible for energy generation. Furthermore, in receptors and sensors, transmembrane helices are responsible for transporting information over the membrane, resulting in activation or de-activation of vital cellular processes. These processes depend on the intimate interplay between proteins and lipids [6-9]. Therefore, next to studies on membrane proteins, it is very important to investigate how they are affected by the lipid environment.

1.3 Membrane fluidity

Cell membranes are highly dynamic structures. Figure 1 shows a cartoon representation of the fluid mosaic model, a simplified description of the organization and dynamics of the membrane [10]. In this model, the membrane is proposed to behave as a two-dimensional fluid. Individual lipid and protein molecules can diffuse freely in a lateral fashion. On the other hand, the transverse diffusion, which is the transloca-

tion of a molecule from one monolayer to the opposing monolayer in the membrane, also referred to as flip-flop, is a much slower process. The viscosity or fluidity of the membrane is a biologically important property. Membrane proteins require a fluid membrane to perform their functions correctly. In more rigid membranes, crucial functions such as transport and signal transduction are disturbed, ultimately resulting in cell death. Therefore membrane fluidity is carefully regulated in all organisms.

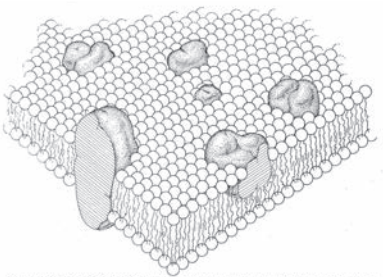

Figure 1. The fluid mosaic model describes the membrane as a two-dimensional liquid in which phospholipid and protein molecules diffuse easily. Adapted from [10].

Membrane fluidity depends largely on the packing of the lipid acyl chains. The fatty acids can exist either in a relatively disordered state, resulting in fluid membranes or in an ordered and tightly packed state, resulting in a more rigid and thicker phase, referred to as the gel phase. The water permeability is decreased in the gel phase and the membranes are less hydrated [11]. Figure 2 illustrates key properties of the fluid-to-gel phase transition, which is temperature dependent and rather abrupt, demonstrating cooperativity, when the temperature approaches the melting temperature (T_m). The T_m of a lipid bilayer depends on the length, the degree of unsaturation and the branching pattern of the fatty acids. Acyl chain packing is disrupted by branches and by *cis* double bonds, which introduce kinks, thereby decreasing T_m. In addition, longer acyl chains have stronger Van der Waals interactions between the chains, which increases T_m.

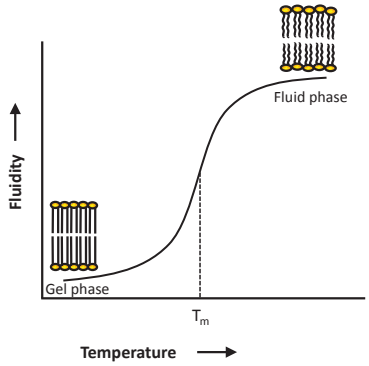

Figure 2. Membrane phase behavior is temperature dependent. At low temperatures, in the gel phase, the membrane lipids form a regular structure with ordered acyl chains. At high temperatures the acyl chains are disordered and the lipids are in the fluid phase. The melting of the chains or the fluid-to-gel phase transition of membrane lipids is a cooperative process and therefore rather abrupt.

In principle, membrane fluidity can also be regulated by sterols such as cholesterol, which inserts in-between the fatty acid tails, changing the interactions between them. Thus cholesterol can moderate the membrane fluidity, making the gel phase less rigid, allowing for lateral diffusion in a so-called liquid-ordered state [12]. Membranes of warm-blooded animals commonly contain cholesterol and their stable body temperature excludes major temperature fluctuations at the membrane level. However, the situation is very different for bacteria. With very few exceptions, bacteria are unable to synthesize sterols in their membranes [13] and they are poikilothermic organisms, which means that their membranes adopt the temperature of the surroundings, and hence are subject to large fluctuations in temperature. In order to tune their membrane properties to the environmental temperature they need to react quickly. An important membrane fluidity regulation mechanism for bacteria is adaption of their lipid acyl chain composition. Since the regulation of membrane fluidity in bacteria is the main topic of this thesis, we will focus on bacterial membranes below.

2. Bacterial membranes

The function and architecture of the bacterial cell membrane are similar to its counterpart in animal cells. However, unlike animal cell membranes, the bacterial cell membrane is not the only cell barrier. Bacteria possess more complex cell envelopes, consisting of multiple layers [14]. A major categorization, based on cell envelop architecture, divides the bacteria in two classes: gram-positive and gram-negative bacteria. This division is based on staining of the peptidoglycan of the cell wall when it is the outer layer of the bacterium [15]. Gram-positive bacteria possess a thick cell wall, consisting of peptidoglycan and teichoic acids, but lack an outer membrane. The cell wall provides structural support and extra protection for the bacteria. In gram-negative bacteria, the cell wall is relatively thin, consisting of a few layers of peptidoglycan surrounded by the outer membrane, which forms an extra permeability barrier and contains lipopolysaccharides that help bacteria adhere to host cells. Some species of both gram-positive and gram-negative bacteria possess an additional surface layer of proteins surrounding their cell wall, called the S-layer [16].

2.1 Lipid biosynthesis machinery

In bacteria, fatty acids are commonly synthesized by a highly conserved set of genes, together forming the type II fatty acid biosynthetic pathway [17]. The structures of fatty acids in bacteria are very diverse. Common modifications are illustrated in Table 2. The length of the fatty acids can vary from 12 up to 22 carbon atoms [18]. The biosynthesis of a new acyl chain is initiated by the enzyme FabH, which condenses an acyl-CoA with a malonyl moiety, effectively elongating the initial acyl-CoA by two carbons. The FabH specificity for acetyl-CoA produces straight

chain fatty acids. However, FabH of gram-positive bacteria prefers larger branched substrates, resulting in iso- and anteiso-branched fatty acids [19, 20]. Gram-positive bacteria are able to produce these branched substrates from leucine, valine and isoleucine. After initiation, the fatty acid intermediate is transferred to the elongation module, which consists of four enzymes that work together to elongate the acyl chain. Each new round, another malonyl moiety is added to the growing acyl chain, effectively increasing it by two carbons. Finally, the fatty acids are transferred to glycerol-3-phosphate creating phosphatidic acid (PA). The competition between the elongation module and phospholipid acyltransferases for the fatty acid intermediates determines the final lengths of the fatty acids [21].

Table 2. Structure of common fatty acids in bacteria.

Fatty acid	Structure
Palmitic acid (C16:0)	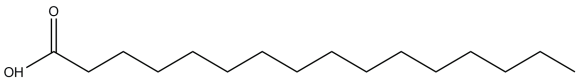
cis-Vaccenic acid (cis-11-C18:1)	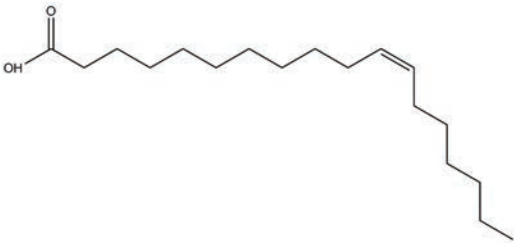
Iso-C17:0	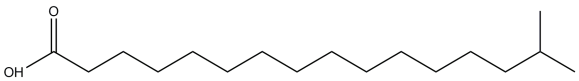
Anteiso-C17:0	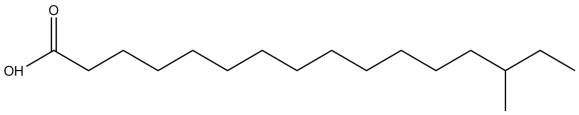
Cyclopropane-C17:0	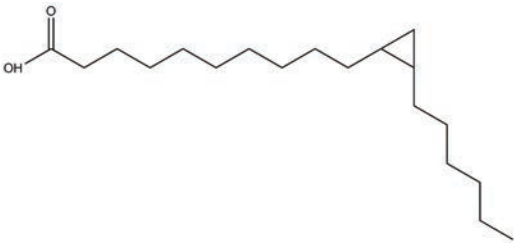
trans-Vaccenic acid (*trans*-C18:1)	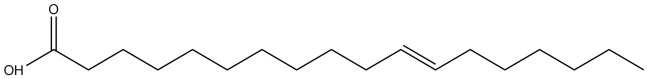

PA is the universal core structure of most bacterial membrane lipids. Various types of polar head groups can be attached to PA, adding considerably to the diversity of bacterial phospholipids. The balance of these head groups influences the charge of the membrane, which is crucial for many integral membrane proteins to adopt the correct topology [22, 23]. This is one of the main reasons why the synthesis of the different head groups is strictly regulated. The most common membrane lipids are acquired via the condensation of serine and glycerol, yielding phosphatidylserine (PS) and phosphatidylglycerol (PG) respectively. The rapid decarboxylation of PS yields phosphatidylethanol (PE) and two PG molecules can be condensed to cardiolipin (Table 1). Most gram-positive bacteria have the ability to decrease the negative charge of the membrane by amino acylation of PG, mostly with alanine or lysine, which diminishes their vulnerability to cationic antimicrobial agents [24]. Additionally, the glycolipids glucosyl- and diglucosyl-diacylglycerol are abundant in gram-positive bacteria [25]. These lipids are involved in maintaining the bilayer character of the membrane and function as membrane anchors for lipoteichoic acid constituents of the cell wall [26].

The cell membrane of *Bacillus subtilis* is the focus of this thesis. *B. subtilis* is a gram-positive, rod-shaped bacterium commonly found in the upper layers of the soil. Genetic modification of *B. subtilis* is straightforward, which is an important reason why it is so well-studied and considered a model organism among gram-positive bacteria. Furthermore, enzyme secretion in *B. subtilis* is very versatile, and it is therefore widely used by biotechnology companies to produce various enzymes on an industrial scale.

2.2 Membrane fluidity regulation

Many bacterial cells are continuously exposed to a changing environment. Not only temperature, but also osmolarity, salinity and pH have an effect on the physical properties of the cell membrane. Crucial for the survival of bacteria is their ability to control these membrane properties by actively remodeling the lipid composition of the cell membrane, a process termed membrane homeostasis. The fluidity of the membrane is an important regulated membrane property that is dependent on temperature.

B. subtilis maintains its membrane fluidity by a switch in fatty acid synthesis from iso-branched fatty acids to anteiso-branched fatty acids [27]. This strategy provides an increase in fluidity over time, as it requires incorporation of *de novo* synthesized fatty acids. Additionally, *B. subtilis* possesses a Δ-5 desaturase that is able to incorporate double bonds in existing lipids. This desaturase is expressed under the control of the two-component system DesKR that immediately responds to a cold shock [28].

3. Sensing and signaling by two component systems

Two-component systems are generally used by bacteria to respond to various environmental stimuli. These systems play a role in fundamental processes such as chemotaxis and phototaxis. Furthermore, adaption to changes in osmolarity, pH and temperature involve two-component systems [29]. Two-component systems convert a signal, which is sensed by a histidine kinase to a modification of a response factor by transfer of a phosphoryl group. The DesKR system in *B. subtilis* is an example of a two-component system. It is involved in membrane fluidity maintenance and its components and mode of action are described below.

3.1 Thermosensor DesK

The two-component system DesKR controls the expression of the *B. subtilis* desaturase (Des) [28]. The mode of action of the DesKR system is described in Figure 3. Low ambient temperatures are sensed within the membrane, by the thermosensor DesK. This protein consists of a sensing domain of five transmembrane helices connected to an intracellular catalytic domain, containing a dimerization domain and an ATP-binding domain (ABD) [30]. DesK becomes kinase active by autophosphorylation of a conserved histidine residue on a temperature drop [31]. The phosphorylated DesK then immediately transfers the phosphoryl group to the response regulator DesR. Phosphorylated DesR (DesR-P) forms tetramers that bind to the DNA, activating the transcription of the *des* gene [32, 33], whereupon Des is expressed. Des incorporates double bonds in existing membrane lipids, resulting in increased membrane fluidity [28]. Presumably, this increased fluidity is sensed by DesK and the kinase activity is switched off. Additionally, DesK gains phosphatase activity, removing the phosphoryl group from DesR-P. In conclusion, the DesKR mechanism is based on a switch between kinase and phosphatase activity that appears to be regulated by ambient temperature via changes in membrane fluidity.

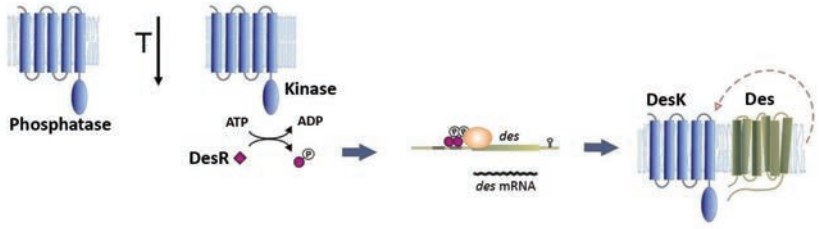

Figure 3. General mechanism of fluidity maintenance via DesK thermosensor. On a decrease in temperature, the intracellular domain of DesK acquires kinase activity and it phosphorylates DesR. Phosphorylated DesR binds to the promotor site of des, resulting in expression of a desaturase, which incorporates double bonds to increase the fluidity of the membrane.

There is evidence that DesK is directly sensitive to the fluidity of the membrane, rather than sensing the temperature. When the supply of precursors for branched-chain fatty acids is limited, which results in more ordered membranes with a higher transition temperature, DesK independently of temperature, becomes active [34, 35]. Furthermore, DesK is sensitive to the incorporation of double bonds by Des, which results in switching to phosphatase activity, again independently of temperature [28].

Structural studies of the intracellular catalytic domain of DesK (DesKC) have given insight into the general architecture of DesK (Fig. 4) and the structural mechanism of autophosphorylation and phosphotransferase activity of DesK [30, 36]. DesKC was crystallized in several states, as a dimer. It was found that a central four-helix bundle (4-HB) contains the conserved histidine residue that can be phosphorylated. The 4-HB is connected to the N-terminal membrane-embedded sensing domain with a two-helix coiled-coil. At the C-terminus, the 4-HB is connected to the ABD with a short flexible loop. Crystal structures showed three distinctly different conformations, which were hypothesized to represent a phosphatase-competent state, a kinase-competent state and a phosphotransferase-competent state of DesKC, respectively (Fig. 5). The phosphatase-competent state has a stable coiled-coil and a compact structure of the 4-HB. The ABD is attached to the 4-HB with multiple interactions. This compact, rigid conformation would on the one hand prohibit auto phosphorylation, which requires a flexible ABD, and on the other hand enable DesR-P binding for phosphatase activity. In the kinase-competent state the ABDs are released from the 4-HB and would be flexible to phosphorylate the conserved histidine residue. This phosphorylation would induce a different, asymmetric conformation, which is able to bind DesR and would therefore represent the phosphotransferase-competent state. In this model, the two-helix coiled-coil transduces the signal from the membrane to rearrangements in the 4-HB. Helical coiled-coils are indeed commonly found to induce conformational changes via subtle reorientation, resulting in a signaling event [37-40]. Nevertheless, no structural information was obtained on the membrane embedded signaling domain of DesK. Thus, an intriguing question remains: how does a drop in temperature result in the transmembrane helix rearrangements underlying the catalytic mechanism?

3.2 The minimal sensor DesK (MS-DesK)

In 2010, a simplified membrane-embedded signaling domain of DesK was discovered. A number of observations resulted in this intriguing discovery. It was demonstrated that deletion of the first transmembrane helix from the sensor caused permanent inactivity, showing the importance of the first transmembrane helix. Furthermore, the fifth transmembrane was hypothesized to play a crucial role in signal transduction because it is directly connects to the two-helix coiled-coil. Therefore, a fusion protein was constructed, consisting of the N-terminal part of the first transmembrane

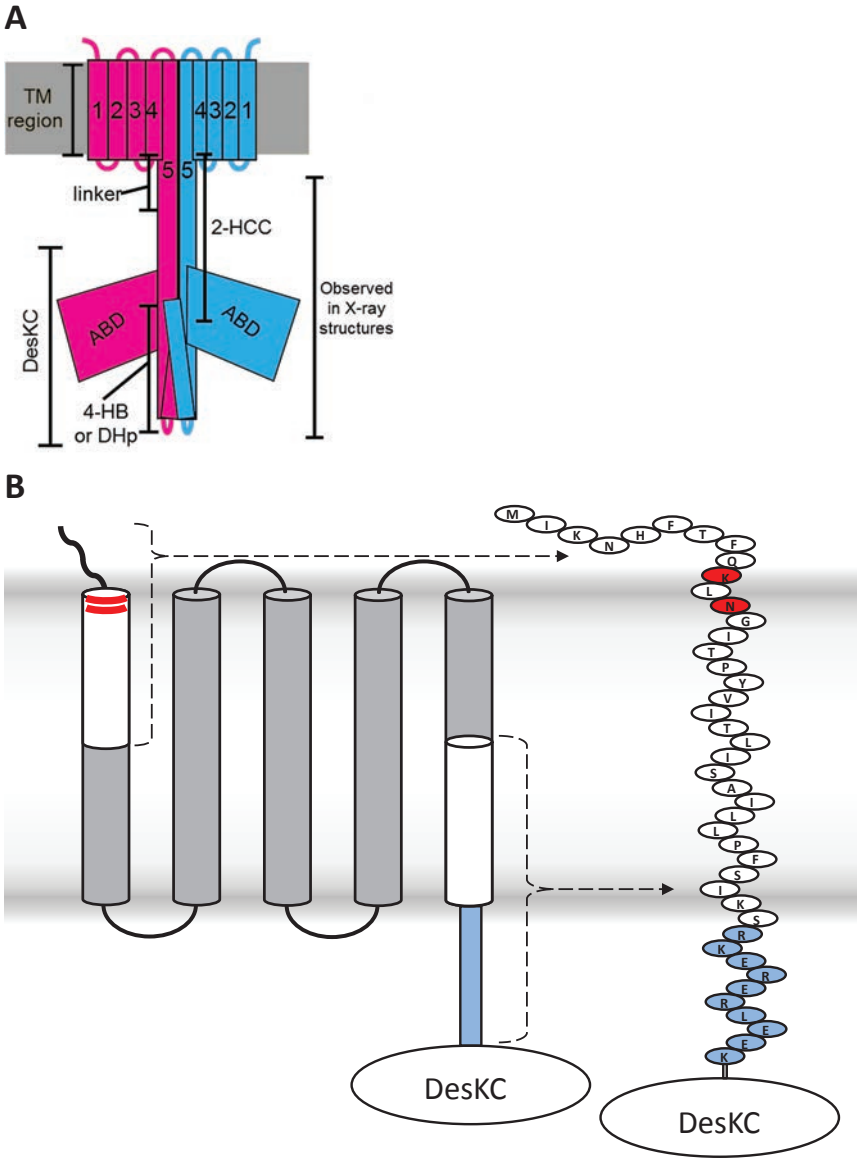

Figure 4. General architecture of the DesK homodimer and MS-DesK. A) The DesK sensing domain consists of five transmembrane helices, connected to a 2-helix coiled-coil (2-HCC) via a charged linker region. The 2-HCC is connected to the core 4-helix bundle (4-HB), which contains the conserved phosphorylatable histidine residue and is also referred to as the Dimerization and Histidine phosphotransfer (DHp) domain. The 4-HB is connected to the ATP-binding domain (ABD) via a flexible linker. B) The combination of the first half of the first DesK transmembrane helix with the second half of the fifth helix, resulted in an active construct, called the minimal sensor DesK (MS-DesK). Two essential motives are highlighted: the sunken-buoy (SB) motif (red) and the charged linker region (blue).

helix and the C-terminal part of the fifth transmembrane helix, continuing into the intracellular domain as depicted in Figure 4B. Interestingly, this fusion protein showed temperature-dependent activity similar to the wildtype, so it was called minimal sensor DesK (MS-DesK) [41]. When reconstituted in protein-free lipid bilayers, MS-DesK retained the kinase activity switch, showing that MS-DesK activity does not require other proteins. Furthermore, the sensing mechanism of MS-DesK was shown to be located in the membrane, because the activity of DesKC proved to be independent of temperature [41].

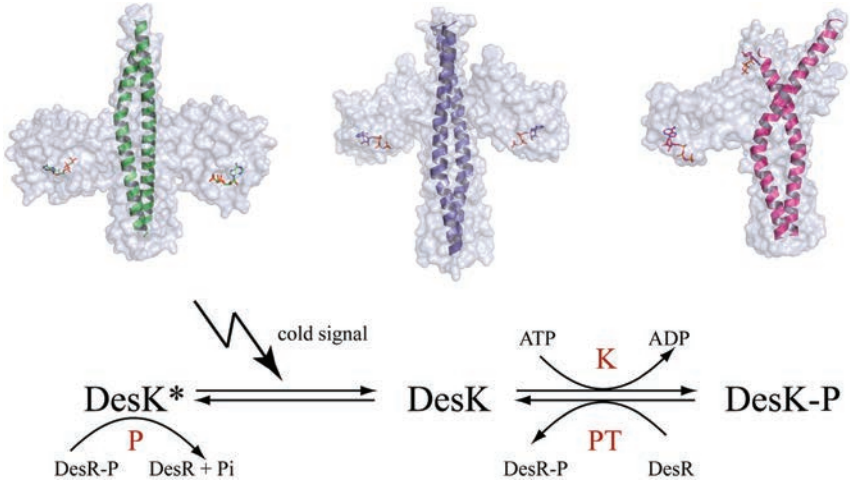

Figure 5. Model of DesK catalysis regulation. The crystal structures, ascribed to three functional states of DesK: phosphatase-competent state (DesK*), kinase-competent state (DesK) and phosphotransferase-competent state (DesK-P). The corresponding reactions are indicated in the lower panel. Adapted from [30].

It was hypothesized that MS-DesK senses membrane fluidity through changes in membrane thickness, because membrane thickness in the gel phase is significantly increased with respect to the fluid phase [42, 43]. Furthermore, membrane proteins have been shown to adapt to situations, where the hydrophobic length of the transmembrane segment does not match the hydrophobic thickness of the membrane. A positive mismatch situation arises when the hydrophobic length of the transmembrane segment exceeds the hydrophobic thickness of the membrane and vice versa in the negative mismatch situation. The adaptations to these mismatch situations could lead to structural rearrangements, resulting in a signaling event [44, 45]. In the thickness sensing hypothesis, a difference in the extent of mismatch would result in the switch from phosphatase to kinase activity of MS-DesK. Several observations supported this thickness sensing hypothesis of MS-DesK. Mismatch situations were

introduced by modifying either the protein or the lipids. In the protein, an essential lysine was identified at the N-terminal lipid-water interface. When this residue was moved one residue towards the C-terminus, effectively shortening the hydrophobic length of the transmembrane helix, creating negative mismatch, the sensor was active, independent of temperature. However, when the hydrophobic length of the transmembrane segment was lengthened by four valine residues, DesK remained inactive [41]. Furthermore both DesK and MS-DesK show increasing activity when reconstituted in membranes with increasing thickness [41, 46]. Additionally, *in vivo* experiments showed stimulated DesK activity with increased incorporation of long-chain fatty acids and loss of activity when levels of short-chain fatty acids were increased. [47]

3.3 Preliminary model of sensing and signaling of MS-DesK

Two motifs were discovered to be essential for the activity switch of MS-DesK (Fig. 4B). The first motif, which stabilizes the transmembrane segment at the N-terminal lipid-water interface on the outside of the cell, consists of a conserved asparagine and the conserved lysine that was used for the mismatch experiments described above. Because it was reasoned that this motif could sink partially in the membrane, with the side chains snorkeling to the interface it was called the sunken buoy (SB) motif [41]. The second motif would stabilize the transmembrane segment at the inside of the cell consists of several conserved charged residues. This motif could also be involved in signaling by adapting different conformations and is called the linker region [48]. Both motifs could act together as a molecular gauge that is sensitive to the thickness of the membrane, generating a signal that is passed down to the intracellular domain.

3.4 MS-DesK and model membrane systems

The essence of model membrane systems is reducing the complexity of the membrane to allow systematic studies. The DesK system is ideally suited for studies in model membrane systems for several reasons. Firstly, the sensing and signaling mechanism is reduced to only one transmembrane helix. Secondly, both sensing and signal transduction take place inside the membrane and furthermore, specific membrane properties are sensed which can be systematically varied and so the contribution of each property can be explored. Protein-lipid interactions are of crucial importance because these interactions are directly responsible for the activity switch of MS-DesK. Physical properties and behavior of these model membrane systems can be studied with multiple biophysical and biochemical techniques, providing insight in the mechanism on a molecular level. An overview of suitable model membrane systems and biophysical and biochemical techniques will be given below, with an emphasis on the systems used in this study.

4. Studying membranes at a molecular level

4.1 Model systems

Tremendous variations exist in the composition of biological membranes and in addition they are very dynamic which allows them to mediate and modulate conformational changes, signaling, transport, and recognition. The investigation of such complex systems is therefore an enormous challenge. In order to increase the experimental accessibility of biological membranes, it is necessary to reduce their complexity, while retaining essential properties, such as the bilayer structure. This can be achieved by using various model membrane systems to investigate different aspects of the membrane. Not only the characterization of the membrane proteins is facilitated by such model systems, but they also allow systematic studies of the protein-lipid interactions under various controlled conditions. The model membrane systems used in this study are described below.

4.1.1 Vesicles

The characteristics of phospholipid membrane vesicles or liposomes have been extensively studied [49-51] since they were first observed and investigated by Bangham and coworkers in the 1960s [52, 53]. Liposomes are versatile in composition, size and possibilities of embedding and encapsulating material, which enabled their use in applied research of drug delivery, cosmetics and food technology [54, 55]. Liposomes are spherical particles consisting of one or more bilayers, generally composed of phospholipids enclosing a volume of aqueous medium. Liposomes used as analogs of biomembranes are commonly assembled by spontaneous self-organization from pure synthetic lipids or lipid extracts from the organism of interest. Liposomes can be used to study lipid characteristics and behavior under various controlled conditions, but model transmembrane peptides or entire proteins can also be embedded in the liposomes. Synthetic peptides corresponding to a single transmembrane segment are easily incorporated and make it possible to systematically vary the sequence and incorporate labels, which increases analytical possibilities [56]. These peptides can be chemically synthesized by solid-phase peptide synthesis. Furthermore model transmembrane peptides have been studied extensively, and their behavior is well characterized [57-65]. Thus, these systems allow systematic investigation of how lipids influence properties of protein transmembrane segments, such as that of DesK.

4.1.2 Nanodiscs

Nanodiscs represent a recently developed type of model membrane systems. Nanodiscs are self-assembled disc-like fragments of lipid bilayers with sizes in the order of 10 nm, stabilized in solution by a scaffold. Both specially engineered membrane scaffolding proteins (MSPs) [66] and amphipathic styrene-maleic acid polymers (SMA) [67] are used as scaffolds to yield stable nanodiscs. Due to their small size and high solubility in aqueous solution, these nanodiscs represent an attractive model system, allowing for analysis with a wide range of biophysical and biochemical techniques [68, 69]. Furthermore bilayer organization is maintained within the nanodiscs [70, 71]. However, in contrast to nanodiscs with MSPs, the formation of nanodiscs with SMA, referred to as Styrene Maleic Acid Lipid Particles (SMALPs) does not require the use of detergents [69]. As shown in Figure 6, addition of SMA to synthetic or biological lipid membranes, or even whole cell lysates results in the spontaneous formation of the nanodiscs [72]. This allows the study of proteins in their native bilayer environment, where native protein-lipid and protein-protein interactions are preserved. Therefore these native nanodiscs can be useful to study these interactions and thus, native oligomerization states of membrane proteins or model peptides thereof can be studied.

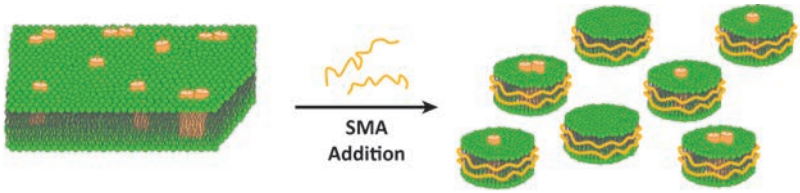

Figure 6. When styrene-maleic acid polymer (SMA) is added to membranes, nanodiscs are formed spontaneously.

4.1.3 In silico bilayers

In addition to an experimental approach, membranes can also be modeled computationally. Molecular modeling is especially interesting for biomembranes because they are not easily accessible experimentally. Computational modeling of cell membranes ranges in complexity from full-atomistic to continuum descriptions and so the level of detail which is chosen depends on the system of study. Full-atomistic modeling provides a high level of detail and is now feasible for membranes [73-76]. However, due to the enormous degree of freedom of the system the simulation is computationally very challenging. In full-atomistic descriptions compromises on system size, timescale and complexity are inevitable. Mesoscopic or coarse grained (CG) simulations provide less detail, but allow modeling of bigger membrane systems on a microsecond timescale, which is sufficient to investigate different types

of protein-protein and protein-lipid interactions. In a CG model several atoms are united into one particle, while the interaction properties of the new particle are modeled as closely as possible to those of the original atoms it represents [77]. Thus, the degrees of freedom are reduced and larger simulation steps are possible, allowing for longer simulation times. These longer simulations however, are not necessarily more realistic, because they can get trapped in local energy minima. Therefore, other modeling approaches have been developed [78-80], in which a large number of simulations are performed. The results are analyzed by clustering of resembling ending structures of the simulations. Thus, insight is provided in the relevance of each structure. Docking Assay For Transmembrane components (DAFT), is a method based on multiple simulations, especially developed to identify preferred binding orientations within the membrane [81].

4.2 Analysis tools

Structural information on model membrane systems can be acquired by various biophysical and biochemical techniques. Below, the applications of the main techniques, used to investigate the molecular mode of action of MS-DesK are briefly described. Circular dichroism (CD) is used in this study to determine the secondary structure of transmembrane peptides in model systems [82]. This technique is based on dissimilar absorption of right and left circularly polarized light. The absorption of light in the far-UV region by the backbone amide bonds of a peptide or protein is dependent on its secondary structure. Therefore each type of secondary structure yields a CD spectrum with a characteristic shape. Percentages of secondary structural elements can be determined by deconvolution of these spectra [83]. Thus, subtle differences in folding of the MS-DesK transmembrane peptides can be detected and the dependence on various properties of the membrane and mutation of essential residues can be investigated.

Tryptophan fluorescence spectroscopy is used in this study to investigate the position of peptides within the membrane systems. Trp fluorescence spectroscopy is based on fluorescence properties of tryptophan. The emission maximum exhibits a significant blue shift on a decrease in polarity of its environment, thus providing information on the location of the tryptophan with respect to the membrane [84]. Therefore, a tryptophan residue was incorporated into the MS-DesK transmembrane peptides as a substitution of a phenylalanine residue at the intracellular membrane-water interface. This mutation has no effect on *in vivo* thermo-sensing behavior of MS-DesK [41] and allows the investigation of the relative position of the Trp residue and its dependence on various properties of the membrane and mutation of essential residues.

Furthermore, gas chromatography is used to analyze the fatty acid composition of the *B. subtilis* membrane lipids. Chromatography is a separation technique, based on different partitioning of the analytes between a stationary and a mobile phase. This results in different elution times for each compound. Gas chromatography uses an inert carrier gas as mobile phase and a porous column as a stationary phase. This technique is often used for fatty acids, which are analyzed in their methylated form [85]. The analysis of the polar head groups of the membrane lipids was performed with thin-layer chromatography. Separation is achieved with a carefully selected solvent mixture as a mobile phase which is applied on a stationary phase, consisting of silica-gel, coated on a glass plate. This technique is routinely used for the analysis of lipids [86].

The melting trajectory of the *B. subtilis* membrane lipids was analyzed by differential scanning calorimetry. This technique is based on the principle that energy is required for phase transitions. Therefore, the heat required to increase the temperature of a sample and a reference is measured. The temperature range, in which the measured amounts of heat actually differ from each other, represents the melting trajectory of the sample [87].

5. Scope of this thesis

DesK is a well-studied thermosensor, but its molecular mode of action has remained elusive. The aim of the research presented here is to elucidate the molecular mechanism of sensing and signal transduction of DesK. To this end we aimed to investigate which properties of the membrane are sensed by studying the influence of the membrane lipids on conformational properties and membrane localization of DesK. The minimal sensor DesK (MS-DesK) preserves the sensing and signaling mechanism in only one transmembrane segment [41]. Therefore MS-DesK is a convenient tool for the study in model membrane systems, in which it was observed to react to changes in thickness of the bilayer [41].

In **chapter 2**, the mode of action of DesK was studied by investigating functional and non-functional transmembrane segments of MS-DesK in model membrane systems. The molecular mechanism was examined as a reaction to changes in thickness of the bilayer with circular dichroism, tryptophan fluorescence and molecular modeling. Together with *in vivo* functional studies with specific MS-DesK mutants, these experiments resulted in a molecular model of sensing and signal transduction of DesK, involving a serine zipper dimerization motif. In **chapter 3**, this model was explored further with experiments in model membrane systems. It was shown that the MS-DesK transmembrane segment reacts similar to a lipid phase transition as to changes in thickness of the bilayer. Therefore, MS-DesK is likely to sense the physiologically relevant phase transition with a similar mechanism to the thickness sensitivity, which would imply that the thickness sensitivity is part of the mechanism of MS-DesK temperature sensing *in vivo*.

In **chapter 4**, the *B. subtilis* membrane lipids and their influence on the structure of MS-DesK were studied. The lipid composition was investigated and the results show temperature-dependent regulation of the lipid acyl chain composition. Both an iso-anteiso switching mechanism [88] and the activity of a desaturase [28] were observed. Next to the characterization, the extracted *B. subtilis* lipids were also used in model membrane studies with incorporated synthetic peptides of the transmembrane segment of MS-DesK. These systems were analyzed with circular dichroism and Trp fluorescence spectroscopy. The results show that no temperature-dependent change in conformation of the MS-DesK transmembrane helix can be induced. These results indicate that the *B. subtilis* lipids may stabilize both the active and the inactive conformation, and that the energetic barrier for switching from one state to the other may be relatively high in these more native-like membrane systems.

In **chapter 5**, we explored the use of a styrene-maleic acid polymer (SMA) to determine the oligomerization state of MS-DesK. SMA solubilizes membranes into Styrene-Maleic Acid Lipid Particles (SMALPs) [69]. Two approaches with SMALPs were investigated in this study. The first approach is based on the biochemical characterization of purified SMALPs with transmembrane peptides. The second approach uses chemical cross-linking of the peptides. The results show that both of these approaches are promising tools for the characterization of oligomerization states. However, these methods require further optimization.

The results of this thesis are discussed in relation to literature in **chapter 6**. Furthermore implications and perspectives for future research are described.

1

References

[1] Cohen HF (2010) How modern science came into the world – Four civilizations, one 17th-century breakthrough. (Amsterdam University Press, Amsterdam).

[2] Dijksterhuis EJ (1950) De mechanisering van het wereldbeeld. (Meulenhoff, Amsterdam).

[3] Hart-Davis A (2009) Science: the definitive visual guide. (Dorling Kindersley, London).

[4] Nicholl C (2004) Leonardo da Vinci – The flights of the mind. (Allen Lane, London).

[5] Gorter E & Grendel F (1925) On bimolecular layers of lipoids on the chromocytes of the blood. *J Exp Med* 41(4): 439-443.

[6] Dowhan W, Mileykovskaya E & Bogdanov M (2004) Diversity and versatility of lipid-protein interactions revealed by molecular genetic approaches. *Biochim Biophys Acta* 1666(1-2): 19-39.

[7] Dowhan W & Bogdanov M (2009) Lipid-dependent membrane protein topogenesis. *Annu Rev Biochem* 78: 515-540.

[8] Goldenberg NM & Steinberg BE (2010) Surface charge: A key determinant of protein localization and function. *Cancer Res* 70: 1277–1280.

[9] Lee AG (2011) Biological membranes: The importance of molecular detail. *Trends Biochem Sci* 36: 493–500.

[10] Singer SJ & Nicolson GL (1972) The fluid mosaic model of the structure of cell membranes. *Science* 175(4023): 720-731.

[11] Cevc G & Marsh D (1987) Phospholipid Bilayers: Physical Principles and Models (Wiley-Interscience, New York)

[12] Mouritsen OG (1991) Theoretical models of phospholipid phase transitions. *Chem Phys Lipids* 57(2-3): 179-194.

[13] Volkman JK (2003) Sterols in microorganisms. *Appl Microbiol Biotechnol* 60(5): 495-506.

[14] Dufresne K & Paradis-Bleau C (2015) Biology and assembly of the bacterial envelope. *Adv Exp Med Biol* 883: 41-76.

[15] HC Gram (1884). Über die isolierte Färbung der Schizomyceten in Schnitt- und Trockenpräparaten. *Fortschritte der Medizin* 2: 185–189

[16] Sleytr UB, Messner P, Pum D & Sara M (1999) Crystalline bacterial cell surface layers (S-layers): From supramolecular cell structure to biomimetics and nanotechnology. *Angew Chem Int Ed Engl* 38(8): 1034-1054.

[17] Parsons JB & Rock CO (2013) Bacterial lipids: Metabolism and membrane homeostasis. *Prog Lipid Res* 52(3): 249-276.

[18] Zhang Z & Hendrickson WA (2010) Structural characterization of the predominant family of histidine kinase sensor domains. *J Mol Biol* 400(3): 335-353.

[19] Choi KH, Heath RJ & Rock CO (2000) Beta-ketoacyl-acyl carrier protein synthase III (FabH) is a determining factor in branched-chain fatty acid biosynthesis. *J Bacteriol* 182(2): 365-370.

[20] Qiu X, et al (2005) Crystal structure and substrate specificity of the beta-ketoacyl-acyl carrier protein synthase III (FabH) from staphylococcus aureus. *Protein Sci*14(8): 2087-2094.

[21] Zhang YM & Rock CO (2008) Membrane lipid homeostasis in bacteria. *Nat Rev Microbiol* 6(3): 222-233.

[22] Zhang W, Campbell HA, King SC & Dowhan W (2005) Phospholipids as determinants of membrane protein topology. phosphatidylethanolamine is required for the proper topological organization of the gamma-aminobutyric acid permease (GabP) of *escherichia coli*. *J Biol Chem* 280(28): 26032-26038.

[23] Xie J, Bogdanov M, Heacock P & Dowhan W (2006) Phosphatidylethanolamine and monoglucosyldiacylglycerol are interchangeable in supporting topogenesis and function of the polytopic membrane protein lactose permease. *J Biol Chem* 281(28): 19172-19178.

[24] Ernst CM & Peschel A (2011) Broad-spectrum antimicrobial peptide resistance by MprF-mediated aminoacylation and flipping of phospholipids. *Mol Microbiol* 80(2): 290-299.

[25] Jorasch P, Wolter FP, Zahringer U & Heinz E (1998) A UDP glucosyltransferase from *bacillus subtilis* successively transfers up to four glucose residues to 1,2-diacylglycerol: Expression of ypfP in *escherichia coli* and structural analysis of its reaction products. *Mol Microbiol* 29(2): 419-430.

[26] Neuhaus FC & Baddiley J (2003) A continuum of anionic charge: Structures and functions of D-alanyl-teichoic acids in gram-positive bacteria. *Microbiol Mol Biol Rev* 67(4): 686-723.

[27] Klein W, Weber MH & Marahiel MA (1999) Cold shock response of *bacillus subtilis*: Isoleucine-dependent switch in the fatty acid branching pattern for membrane adaptation to low temperatures. *J Bacteriol* 181(17): 5341-5349.

[28] Aguilar PS, Hernandez-Arriaga AM, Cybulski LE, Erazo AC & de Mendoza D (2001) Molecular basis of thermosensing: A two-component signal transduction thermometer in *bacillus subtilis*. *Embo J* 20(7): 1681-1691.

[29] Gao R & Stock AM (2009) Biological insights from structures of two-component proteins. *Annu Rev Microbiol* 63: 133-154.

[30] Albanesi D, et al (2009) Structural plasticity and catalysis regulation of a thermosensor histidine kinase. *Proc Natl Acad Sci U S A* 106(38): 16185-16190.

[31] Albanesi D, Mansilla MC & de Mendoza D (2004) The membrane fluidity sensor DesK of *bacillus subtilis* controls the signal decay of its cognate response regulator. *J Bacteriol* 186(9): 2655-2663.

[32] Cybulski LE, del Solar G, Craig PO, Espinosa M & de Mendoza D (2004) *Bacillus subtilis* DesR functions as a phosphorylation-activated switch to control membrane lipid fluidity. *J Biol Chem* 279(38): 39340-39347.

[33] Trajtenberg F, et al (2014) Allosteric activation of bacterial response regulators: The role of the cognate histidine kinase beyond phosphorylation. *Mbio* 5(6): e02105-14.

[34] Cybulski LE, et al (2002) Mechanism of membrane fluidity optimization: Isothermal control of the *bacillus subtilis* acyl-lipid desaturase. *Mol Microbiol* 45(5): 1379-1388.

[35] Martin N, Lombardia E, Altabe SG, de Mendoza D & Mansilla MC (2009) A lipA (yutB) mutant, encoding lipoic acid synthase, provides insight into the interplay between branched-chain and unsaturated fatty acid biosynthesis in *bacillus subtilis*. *J Bacteriol* 191(24): 7447-7455.

[36] Trajtenberg F, Grana M, Ruetalo N, Botti H & Buschiazzo A (2010) Structural and enzymatic insights into the ATP binding and autophosphorylation mechanism of a sensor histidine kinase. *J Biol Chem* 285(32): 24892-24903.

[37] Ottemann KM, Xiao W, Shin YK & Koshland DE,Jr (1999) A piston model for transmembrane signaling of the aspartate receptor. *Science* 285(5434): 1751-1754.

[38] Kwon O, Georgellis D, Lin EC (2003) Rotational on-off switching of a hybrid membrane sensor kinase Tar-ArcB in *Escherichia coli*. *J Biol Chem* 278:13192–13195.

[39] Gao R & Lynn DG (2007) Integration of rotation and piston motions in coiled-coil signal transduction. *J Bacteriol* 189:6048–6056.

[40] Hall BA, Armitage JP & Sansom MS (2011) Transmembrane helix dynamics of bacterial chemoreceptors supports a piston model of signalling. *PLoS Comput Biol* 7(10): e1002204.

[41] Cybulski LE, Martin M, Mansilla MC, Fernandez A & de Mendoza D (2010) Membrane thickness cue for cold sensing in a bacterium. *Curr Biol* 20(17): 1539-1544.

[42] Tristram-Nagle S, Liu Y, Legleiter J & Nagle JF (2002) Structure of gel phase DMPC determined by X-ray diffraction. *Biophys J* 83 3324–3335.

[43] Kucerka N, Liu Y, Chu N, Petrache HI, Tristram-Nagle S & Nagle JF (2005) Structure of fully hydrated fluid phase DMPC and DLPC lipid bilayers using X-ray scattering from oriented multilamellar arrays and from unilamellar vesicles. *Biophys J* 88 2626–2637.

[44] Killian JA (1998) Hydrophobic mismatch between proteins and lipids in membranes. *Biochim Biophys Acta* 1376(3): 401-415.

[45] Nyholm TK, Ozdirekcan S & Killian JA (2007) How protein transmembrane segments sense the lipid environment. *Biochemistry* 46(6): 1457-1465.

[46] Martin M & de Mendoza D (2013) Regulation of *bacillus subtilis* DesK thermosensor by lipids. *Biochem J* 451(2): 269-275.
[47] Porrini L, Cybulski LE, Altabe SG, Mansilla MC & de Mendoza D (2014) Cerulenin inhibits unsaturated fatty acids synthesis in *bacillus subtilis* by modifying the input signal of DesK thermosensor. *Microbiologyopen* 3(2): 213-224.
[48] Inda ME, et al (2014) A lipid-mediated conformational switch modulates the thermosensing activity of DesK. *Proc Natl Acad Sci U S A* 111(9): 3579-3584.
[49] Torchilin V, Weissig V, eds. (2003) Liposomes: A Practical Approach. (Oxford Univ. Press, Oxford/ New York)
[50] Basu SC & Basu ME (2002) Liposome Methods and Protocols. (Humana, Totowa NJ)
[51] Luisi PL & Walde P (1999) Giant Vesicles. (Wiley, New York)
[52] Bangham AD & Horne RW (1964) Negative staining of phospholipids and their structural modification by surface-active agents as observed in the electron microscope. *J Mol Biol* (8):660–668.
[53] Bangham AD, Standish MM & Watkins JC (1965) Diffusion of univalent ions across lamellae of swollen phospholipids. *J Mol Biol* (13):238–52
[54] Jesorka A & Orwar O (2008) Liposomes: Technologies and analytical applications. *Annu Rev Anal Chem (Palo Alto Calif)* (1): 801-832.
[55] Gurr MI, Frayn KN & Harwood J (2002) Lipid Biochemistry (Blackwell Science, Oxford)
[56] Killian JA (2003) Synthetic peptides as models for intrinsic membrane proteins. *FEBS Lett* 555(1): 134-138.
[57] Davis JH, Hodges RS & Bloom M (1982) The interaction between a synthetic amphiphilic polypeptide and lipids. *Biophys J* 37(1): 170-171.
[58] Zhang YP, Lewis RN, Hodges RS & McElhaney RN (1995) Interaction of a peptide model of a hydrophobic transmembrane alpha-helical segment of a membrane protein with phosphatidylethanolamine bilayers: Differential scanning calorimetric and fourier transform infrared spectroscopic studies. *Biophys J* 68(3): 847-857.
[59] de Planque MR, et al (1999) Different membrane anchoring positions of tryptophan and lysine in synthetic transmembrane alpha-helical peptides. *J Biol Chem* 274(30): 20839-20846.
[60] Ren J, Lew S, Wang J & London E (1999) Control of the transmembrane orientation and interhelical interactions within membranes by hydrophobic helix length. *Biochemistry* 38(18): 5905-5912.
[61] Demmers JA, Haverkamp J, Heck AJ, Koeppe RE,2nd & Killian JA (2000) Electrospray ionization mass spectrometry as a tool to analyze hydrogen/deuterium exchange kinetics of transmembrane peptides in lipid bilayers. *Proc Natl Acad Sci U S A* 97(7): 3189-3194.
[62] Lew S, Ren J & London E (2000) The effects of polar and/or ionizable residues in the core and flanking regions of hydrophobic helices on transmembrane conformation and oligomerization. *Biochemistry* 39(32): 9632-9640.
[63] Ganchev DN, Rijkers DT, Snel MM, Killian JA & de Kruijff B (2004) Strength of integration of transmembrane alpha-helical peptides in lipid bilayers as determined by atomic force spectroscopy. *Biochemistry* 43(47): 14987-14993.
[64] Holt A & Killian JA (2010) Orientation and dynamics of transmembrane peptides: The power of simple models. *Eur Biophys J* 39(4): 609-621.
[65] Sezgin E & Schwille P (2012) Model membrane platforms to study protein-membrane interactions. *Mol Membr Biol* 29(5): 144-154.
[66] Bayburt TH, Grinkova YV & Sligar SG (2002) Self-assembly of discoidal phospholipid bilayer nanoparticles with membrane scaffold proteins. *Nano Lett* 2(8): 853-856.
[67] Knowles TJ, et al (2009) Membrane proteins solubilized intact in lipid containing nanoparticles bounded by styrene maleic acid copolymer. *J Am Chem Soc* 131(22): 7484-7485.
[68] Bayburt TH & Sligar SG (2010) Membrane protein assembly into nanodiscs. *FEBS Lett* 584(9): 1721-1727.

[69] Dörr JM, et al (2016) The styrene-maleic acid copolymer: A versatile tool in membrane research. *Eur Biophys J* 45(1): 3-21.
[70] Denisov IG, McLean MA, Shaw AW, Grinkova YV & Sligar SG (2005) Thermotropic phase transition in soluble nanoscale lipid bilayers. *J Phys Chem B* 109(32): 15580-15588.
[71] Orwick-Rydmark M, et al (2012) Detergent-free incorporation of a seven-transmembrane receptor protein into nanosized bilayer lipodisq particles for functional and biophysical studies. *Nano Lett* 12(9): 4687-4692.
[72] Long AR, et al (2013) A detergent-free strategy for the reconstitution of active enzyme complexes from native biological membranes into nanoscale discs. *BMC Biotechnology* 13: 41-41.
[73] Marrink SJ & Berendsen HJC (1994) Simulation of water transport through a lipid membrane. *J Phys Chem* 98:4155–4168
[74] Tieleman DP, Marrink SJ & Berendsen HJC (1997) A computer perspective of membranes: molecular dynamics studies of lipid bilayer systems. *Biochim Biophys Acta* 1331:235–270
[75] Lindahl E & Edholm O (2000) Mesoscopic undulations and thickness fluctuations in lipid bilayers from molecular dynamics simulations. *Biophys J* 79:426–433
[76] Sum AK, Faller R & de Pablo JJ (2003) Molecular simulation study of phospholipid bilayers and insights of the interactions with disaccharides. *Biophys J* 85(5):2830–2844
[77] Spijker P, et al (2010) Coarse grained molecular dynamics simulations of transmembrane protein-lipid systems. *Int J Mol Sci* 11(6): 2393-2420.
[78] Stansfeld PJ & Sansom MS (2011) From coarse grained to atomistic: A serial multiscale approach to membrane protein simulations. *J Chem Theory Comput* 7(4): 1157-1166.
[79] Wassenaar TA, Pluhackova K, Bockmann RA, Marrink SJ & Tieleman DP (2014) Going backward: A flexible geometric approach to reverse transformation from coarse grained to atomistic models. *J Chem Theory Comput* 10(2): 676-690.
[80] Kar P & Feig M (2014) Recent advances in transferable coarse-grained modeling of proteins. *Adv Protein Chem Struct Biol* 96: 143-180.
[81] Wassenaar TA, et al (2015) High-throughput simulations of dimer and trimer assembly of membrane proteins: the DAFT approach. *J Chem Theory Comput* 11(5): 2278-2291.
[82] Greenfield NJ (2006) Using circular dichroism spectra to estimate protein secondary structure. *Nat Protoc* 1(6): 2876-2890.
[83] Sreerama N, Venyaminov SY & Woody RW (2000) Estimation of protein secondary structure from circular dichroism spectra: Inclusion of denatured proteins with native proteins in the analysis. *Anal Biochem* 287(2): 243-251.
[84] Lackowicz JR (2006) Principles of fluorescence spectroscopy (Springer, New York).
[85] Seppänen-Laakso T, Laakso I & Hiltunen R (2002) Analysis of fatty acids by gas chromatography, and its relevance to research on health and nutrition. *Anal Chim Acta* 465(1–2): 39-62.
[86] Fuchs B, Süß R, Teuber K, Eibisch M & Schiller J (2011) Lipid analysis by thin-layer chromatography—A review of the current state. *Journal of Chromatography A* 1218(19): 2754-2774.
[87] Lewis RAH, Mannock D & McElhaney R (2007) in Methods in membrane lipids, ed Dopico A (Humana Press, New York), pp 171-195.
[88] Suutari M & Laakso S (1992) Unsaturated and branched chain-fatty acids in temperature adaptation of *bacillus subtilis* and bacillus megaterium. *Biochim Biophys Acta* 1126(2): 119-124.

2

Activation of the bacterial thermosensor DesK involves a serine zipper dimerization motif that is modulated by bilayer thickness

Joost Ballering*, Larisa E. Cybulski*, Anastassiia Moussatova*, Maria E. Inda, Daniela B. Vazquez, Tsjerk A. Wassenaar, Diego de Mendoza, D. Peter Tieleman and J. Antoinette Killian

*Authors contributed equally

[Cybulski et al. (2015) Proc Natl Acad Sci U S A 112(20): 6353-6358]

Abstract

DesK is a bacterial thermosensor protein involved in maintaining membrane fluidity in response to changes in environmental temperature. Most likely, the protein is activated by changes in membrane thickness, but the molecular mechanism of sensing and signaling is still poorly understood. Here we aimed to elucidate the mode of action of DesK by studying the so-called minimal sensor DesK (MS-DesK), in which sensing and signaling are captured in a single transmembrane segment. This simplified version of the sensor allows investigation of membrane thickness-dependent protein-lipid interactions simply by using synthetic peptides, corresponding to the membrane-spanning parts of functional and non-functional mutants of MS-DesK incorporated in lipid bilayers with varying thickness. The lipid-dependent behavior of the peptides was investigated by circular dichroism, tryptophan fluorescence and molecular modeling. These experiments were complemented with *in vivo* functional studies on MS-DesK mutants. Based on the results we constructed a model that suggests a new mechanism for sensing in which the protein is present as a dimer and responds to an increase in bilayer thickness by membrane incorporation of a C-terminal hydrophilic motif. This results in exposure of three serines on the same side of the transmembrane helices of MS-DesK, triggering a switching of the dimerization interface to allow the formation of a serine zipper. The final result is activation of the kinase state of MS-DesK.

Introduction

All organisms have to be able to rapidly adapt to a vast variety of external stimuli to survive. In bacteria, two-component signal transduction systems are some of the most abundant mechanisms for sensing and adapting to changes in the extracellular environment. These systems mediate responses in chemotaxis and phototaxis, and regulate feedback to changes in osmolarity, redox state and temperature [1, 2]. However, despite the evident importance of two-component systems for bacterial survival, the molecular mechanisms of signal transduction via these systems has barely begun to be untangled.

The DesKR system is a two-component system first identified in the soil bacterium *Bacillus subtilis* [3]. Together with other regulatory systems, it is involved in maintaining membrane fluidity when the environmental temperature changes. The DesKR system works as follows. The actual thermosensor - i.e., the protein that senses the temperature change - is DesK. This protein consists of five transmembrane helices and an intracellular catalytic domain (DesKC) and is believed to function as a dimer [2, 4]. In response to decreased environmental temperature, DesKC phosphorylates the response regulator DesR, which in turn controls the expression levels of the effector enzyme, a desaturase. This desaturase is inserted into the membrane, where it can introduce double bonds into pre-existing lipids, allowing the recovery of membrane fluidity at this lower temperature [3].

In the present study we focused on the first step of the signaling pathway, examining how the sensor is able to sense and transmit a temperature-dependent signal. This challenge was recently simplified by the discovery that both the sensing and the signal transduction properties of the membrane-spanning part of DesK can be captured into a single transmembrane segment by fusing the N-terminal part of the first transmembrane segment to the C-terminal part of the fifth transmembrane segment [5]. The resulting protein is called the minimal sensor DesK (MS-DesK).

Importantly, MS-DesK shows a temperature-dependent switch in activity comparable to the full length DesK not only *in vivo*, but also when reconstituted in protein-free lipid bilayers made from bacterial lipids [5]. Therefore, no other membrane proteins are involved in sensing or signal transduction. Furthermore the activity of the catalytic domain DesKC itself, is not temperature-sensitive [5, 6], and thus it must be the transmembrane segment of MS-DesK that somehow reacts to changes in temperature, most likely by sensing corresponding changes in the physical properties of the lipids.

Which properties of the membrane could be sensed by DesK and MS-DesK? On a decrease in environmental temperature, membrane lipids become more ordered, and consequently the membrane becomes thicker [7]. Some evidence suggests that such changes in membrane thickness may be a key factor for regulation of DesK sensing and signaling. First, an MS-DesK length mutant (4V) containing 4 extra valines in the C-terminal region of its transmembrane segment was found to

be inactive and to remain locked in the phosphatase state on a decrease in temperature [5]. Second, reconstitution studies showed increasing activity of both DesK and MS-DesK with increasing acyl chain length of the lipids in which the protein is reconstituted [5, 8]. Third, increased incorporation of long-chain fatty acids into the membrane lipids was found to stimulate kinase activity of DesK *in vivo*, whereas increased levels of short-chain fatty acids result in loss of activity [9].

How can membrane thickness regulate activity of DesK? It has been shown that the N-terminus of MS-DesK at the exoplasmic side of the membrane contains a motif that may render the protein sensitive to membrane thickness and interfacial hydration. This motif contains two hydrophilic amino acids, K10 and N12, that are essential for activity [5] and that presumably are located within the transmembrane region just below the lipid-water interface. Because their side chains can snorkel to the hydrophilic membrane-water interface, these amino acids were proposed to act as a buoy, stabilizing the position of the transmembrane segment. For this reason, this has been called the sunken-buoy (SB) motif [5]. In addition to the SB-motif, a charged linker region at the intracellular membrane-water interface was found to be important for activity [10]. It has been proposed that both motifs act together as a molecular gauge that senses membrane thickness and thereby regulates the switching of activity of the intracellular catalytic domain of DesK [10]. The molecular details of the mode of action of this molecular gauge have remained elusive, however.

Because the activity of MS-DesK is most likely regulated by direct interactions of its single transmembrane segment with surrounding lipids, as discussed above, this system is ideally suited for studies on relatively simple model membranes. In such model systems the biological complexity of the host membrane is reduced to allow for systematic studies. Here, to gain insight into the molecular mode of action of the sensor, we studied the behavior of peptides mimicking the membrane-spanning parts of a functional mutant and a non-functional mutant of MS-DesK in synthetic lipid bilayers by spectroscopic techniques and molecular modeling. Combined with *in vivo* functional studies on MS-DesK mutants and cross-linking experiments, our results lead to a new model of thermo-sensing in which changes in bilayer thickness trigger a switch between distinct dimerization interfaces within the membrane, resulting in activation of the sensor.

Results

The MS-DesK transmembrane segment adopts a bilayer-thickness dependent α-helical structure

To study how membrane thickness may modulate the behavior of MS-DesK, we incorporated peptides corresponding to a functional and a non-functional MS-DesK transmembrane segment (Table 1) into model membranes of phosphatidylcholine (PC) lipids. These synthetic lipids were chosen because they allow the investigation of changes in membrane thickness by systematically varying the lipid acyl chain length. Furthermore, MS-DesK is active when incorporated into PC lipids and shows higher activity with longer acyl chains [5].

Peptide	Sequence
MS-TMS	MIKNHFTFQK LNGITPYVIT LISAILLPWS IKSRKERERL EEK
4V-TMS	MIKNHFTFQK LNGITPYVIT LISVVVVAIL LPWSIKSRKE RERLEEK

Table 1. Amino acid sequences of the peptides used in this study. The sequences of the synthetic peptides correspond to the transmembrane region of MS-DesK and the 4V extension (yellow) of MS-DesK (MS-TMS and 4V-TMS, respectively) with the SB motif (red) and the C-terminal charged linker (blue). A Trp (green) was incorporated instead of a Phe to allow for fluorescence measurements.

First, we used circular dichroism (CD) to investigate whether bilayer thickness affects secondary structure. Figure 1A shows the CD spectra of the transmembrane segment of MS-DesK (MS-TMS) in different bilayers. All spectra are characteristic for mainly α-helical structure; however, in thicker membranes, the negative peak at 208 nm has higher intensity, and the intersection with the x-axis is shifted to slightly lower wavelengths. Deconvolution of the spectra shows that helicity increases from ~55% in thin membranes to ~65% in thicker membranes (Table 2), which would correspond to approximately four amino acids and thus the folding of approximately one helix turn.

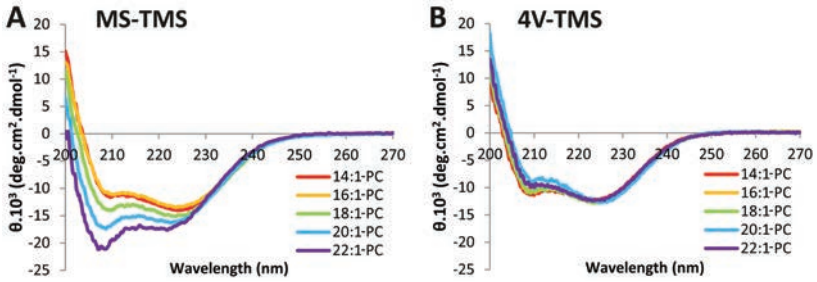

Figure 1. CD spectra of MS-TMS (A) and 4V-TMS (B) in lipid vesicles of 14:1-PC (red), 16:1-PC (yellow), 18:1-PC (green), 20:1-PC (blue) and 22:1-PC (purple). The peptide/lipid ratio used was 1:50. and measurements were performed at 25 °C. The data are a representative set of two independent experiments.

Figure 1B shows that the CD spectra of an elongated peptide corresponding to an inactive minimal sensor (4V-TMS) also exhibit mostly α-helical character. However, in contrast to MS-TMS, here no change in helicity is observed on increasing bilayer thickness, and the number of residues present as α -helix in 4V-TMS (~24 amino acids) is similar to that in MS-TMS in thinner membranes (Table 2). A regular helix of this length would correspond to ~36 Å, which in principle would suffice to span even membranes of 22:1-PC [11]. Why then are MS-TMS and 4V-TMS behaving in such a dissimilar manner? An important difference between the two helices is their hydrophobicity. For 4V-TMS, a helix of 24 amino acids between residues 11 and 35 will be hydrophobic and uncharged, whereas for MS-TMS, any helix with a length of 24 residues or more will contain at least one charged Lys residue and also will include more hydrophilic residues (Table 1). This will make it energetically less favorable for MS-TMS to incorporate in thicker membranes. Thus, MS-TMS will have to react to increases in bilayer thickness in a manner that possibly involves helix elongation and that allows for relief of the hydrophobic mismatch.

Lipids		MS-TMS				4V-TMS			
Fatty acid chain length	**Hydrophobic thickness (Å)**	**α-helix (%)**	**α-helix, no. of residues**	**Sheet (%)**	**Random coil (%)**	**α-helix (%)**	**α-helix, no. of residues**	**Sheet (%)**	**Random coil (%)**
14:1-PC	23	56±2	24±1	9±1	35±1	50±3	24±1	9±2	41±1
16:1-PC	26	55±3	24±1	9±1	36±3	52±3	24±1	8±2	40±1
18:1-PC	30	59±2	25±1	8±1	33±2	50±1	24±1	9±1	41±1
20:1-PC	33	63±1	27±1	6±2	31±1	52±2	24±1	10±2	38±1
22:1-PC	36	67±2	29±1	7±3	26±3	50±3	24±1	10±1	40±2

Table 2. Secondary structural elements in relation to membrane thickness of MS-TMS and 4V-TMS. Percentages of secondary structural elements are averages with SDs of the three deconvolution programs of CD-Pro based on two independent experiments. The number of residues in the α-helix is calculated from the percentage and the total number of residues in the peptide. In the case of a regular α-helix, one residue corresponds to 1.5 Å α-helix length. The hydrophobic thicknesses are carbonyl-carbonyl distances derived from previous work [11].

The MS-DesK transmembrane segment shows a bilayer-thickness dependent positioning in the membrane

Further insight into the interaction of MS-DesK with lipids was obtained by fluorescence spectroscopy. In the peptides used in this study, a phenylalanine residue near the C-terminal membrane-water interface was substituted for a tryptophan (Table 1). This allowed for further study of membrane-thickness dependent properties of the peptides by monitoring the Trp emission maximum, which depends on the polarity of the environment [12]. Mutagenesis and functional analysis showed that the corresponding MS-DesK mutant is active (Fig. S1).

Trp fluorescence spectra of MS-TMS in model membranes (Fig. 2A) show emission maxima at a lower wavelength (near 345 nm) than for a soluble tryptophan (near 356 nm), consistent with a position of the peptide inside the membrane with its Trp residues close to the lipid-water interface [12]. However, careful analysis of the emission maxima of MS-TMS as function of bilayer thickness shows a complex behavior (Fig. 2C, blue line). The maximum shifts to slightly lower wavelength when the acyl chain length increases from C14 to C18, suggesting a more hydrophobic environment, but on a further increase in chain length from C18 to C22, the maximum shifts back to a somewhat higher wavelength. This behavior clearly differs from that of 4V-TMS (Fig. 2B and C, red line), which is more straightforward. In thinner membranes, the emission maximum of 4V-TMS is shifted to a higher wavelength, in line with positioning of Trp closer to the aqueous phase owing to the longer transmembrane segment of 4V-TMS. More importantly, the spectrum shows a blue shift of the emission maximum with increasing chain length, as expected for a Trp residue that simply becomes located in a more hydrophobic environment on thickening of the bilayer. Qualitatively comparable results for MS-TMS and 4V-TMS were obtained with quenching experiments using the aqueous quencher acrylamide (Fig. S2, Table S1).

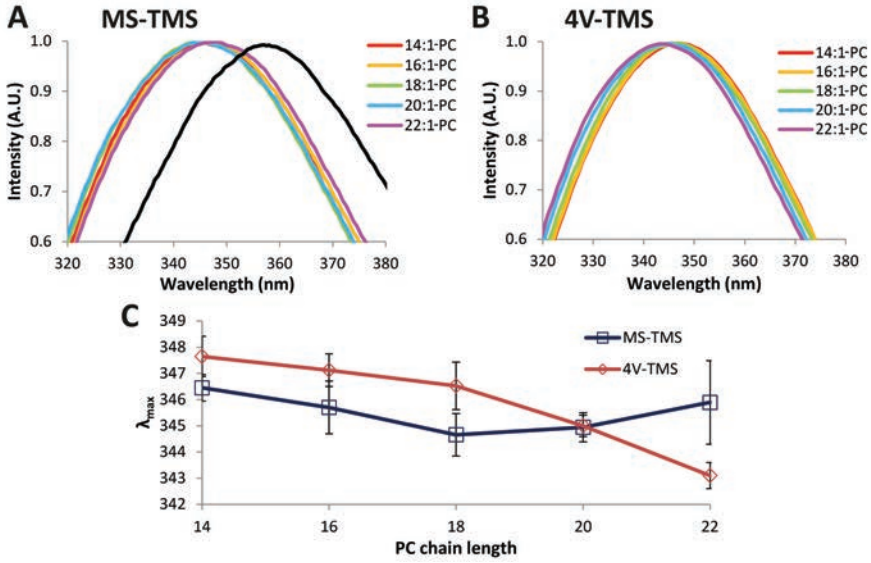

Figure 2. Comparison of MS-TMS and 4V-TMS emission spectra in lipid vesicles with varying acyl chain length. (A and B) Emission spectra of soluble Trp (black), MS-TMS (A) and 4V-TMS (B) in lipid vesicles of 14:1-PC (red), 16:1-PC (orange), 18:1-PC (green), 20:1-PC (cyan) and 22:1-PC (magenta). (C) Emission maxima for MS-TMS (blue squares) and 4V-TMS (red diamonds) as a function of acyl chain length. The peptide/lipid ratio used was 1:50 and measurements were performed at 25 °C. The error bars indicate the standard deviation for three independent experiments.

How can we understand the complex behavior of MS-TMS? A tentative interpretation is that two events are involved with opposite outcomes. The first event could be a localization of Trp deeper into the membrane on increasing bilayer thickness, leading to a more hydrophobic environment. This event would then be dominant from 14:1-PC to 18:1-PC, whereas in thicker membranes a second event would become dominant, which places Trp in a more hydrophilic environment. What could this second event be? One possibility is that the elongation of the helix, as suggested by CD experiments, results in a change of the polarity of the environment of the tryptophan residue. Alternatively, it is possible that the increase in membrane thickness, perhaps in combination with helix elongation, leads to additional events, such as dimerization of the peptide or reorientation of helices within a dimer, which then might result in a more hydrophilic environment of the Trp residue. This latter possibility seems realistic, give that all histidine kinases of two-component systems studied to date have been seen to function as a dimer [2] and that the crystal structure of the intracellular domain of DesK was found to be a dimer in both its functional state and a non-functional state [4]. Taken together, these results raise the immediate question of whether MS-TMS indeed does prefer to form dimers and, if so, what the conformations of these dimers would be. We addressed these questions next.

Molecular dynamics simulations

To gain insight into the dimerization behavior of the transmembrane region of MS-DesK, we carried out large-scale coarse-grained (CG) molecular dynamics (MD) simulations on the MS-TMS sequence. In the absence of structural data, we chose the CG approach because it enables efficient screening of a large number of different dimer conformations; however, the nature of the CG model does not support changes in the secondary structure of the proteins, and thus it must be decided beforehand. As a first approximation, we modeled the MS-DesK sequence as a canonical α-helix for the transmembrane segment. Our goal here was not only to identify TMS dimer conformations, but also to establish shifts as a function of temperature. Specifically, we expected that the most populated dimer configuration at low temperature should become less populated at the higher temperature, and vice versa. With this goal in mind, we carried out MD simulations in a fully solvated 18:1-PC lipid bilayer as a function of temperature. We selected this bilayer because it has been well characterized with CG-MD simulations [13], and because it allowed us to detect possible shifts in dimer populations simply by varying temperature, while keeping the composition constant.

The data was collected at three different temperatures from 1000 simulations for each temperature, providing a large pool of potential dimer conformations. The results thus obtained were interpreted by applying cluster analysis without using any experimental input, to avoid bias. To gain insight into the shifts between different cluster populations, we performed cluster analysis using all dimers found across all

temperatures (Fig. S3). Overall, our cluster analysis suggests that MS-TMS behaves as a dimer, and that two distinct dimer conformations dominate at different temperatures. These two dimer conformations are shown in the corresponding lipid bilayer at 310K and 290K in Figure 3. The dominating dimer conformation found at 300K is similar to the conformation at 310K with an RMSD value of 0.28 nm between the central structures, and thus is not shown here. At high temperature, the residues S23 and S30 are found facing the lipid environment. At low temperature, the opposite situation is found, with residues S23 and S30 facing toward the dimer interface (Fig. S4). In this case, S33 also faces the interface and may contribute to helix-helix interactions (Fig. S4, S5). The opposite is observed for W29. At high temperature, W29 is distributed around the dimer interface, whereas at low temperature it is oriented toward the lipid-water interface in most of the cluster members. Unfortunately, owing to the different setups and the fixed helix constraint, the MD simulations do not allow straightforward comparison with the fluorescence results on MS-TMS. Residue T20 does not appear to contribute to helix-helix interactions in either orientation.

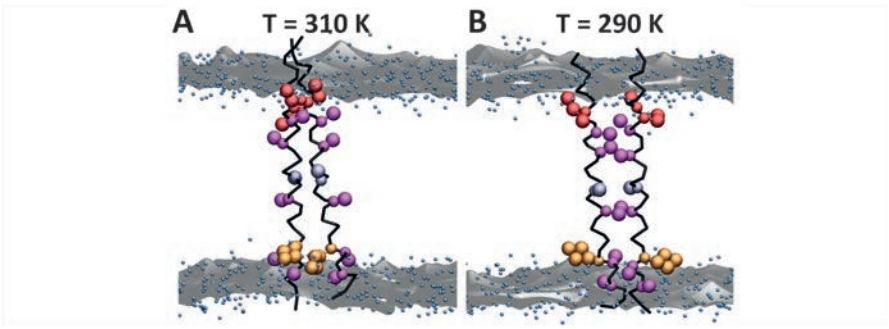

Figure 3. Interfaces formed by MS-DesK dimer as found in MD simulations at 310K (A) and at 290K (B). The central structures of the major clusters are shown as representative conformations for each temperature. The peptide backbone is shown in black and key amino acids are highlighted as spheres. The amino acid residues are color-coded as follows: W29 in orange; T20 in light blue; T15, S23, S30, S33, and N12 in magenta as the residues forming the signal dimer interface; and Q9 and K10 in red. The location of lipid PO4 groups is shown as a grey surface to indicate the position of the dimer in the bilayer. Water at the interface is shown in blue spheres.

Our simulations also suggest changes in dimer interface structure at the N-terminal end. Residues Q9 face the dimer interface at 310K, whereas N12 faces the dimer interface at 290K, suggesting opposite rotations. The position of K10 remains the same at both temperatures, always facing the lipids and located close to the lipid-water interface, which supports its role as sunken buoy.

Thus, we can observe that at low temperature, MS-TMS is capable of forming an energetically favorable dimer interface defined by three serine residues located at the same face of the helix, which would form a serine zipper. Structural motifs formed by small residues such as serine have been previously suggested to promote strong and specific transmembrane helix-helix association [14]. In particular, the spatial arrangement of repeating serine residues recognized through analysis of interhelical H-bonds has been termed "serine zipper", in analogy to the coiled-coil leucine zipper heptad motif [15]. The structural arrangement of three serine residues (S23, S30, S33) in MS-TMS dimer forms a similar serine zipper motif and could be capable of driving helix-helix associations at low temperature. Our results suggest a model of reorientation of the dimer as possible mechanism for activation of the thermosensor, which would be consistent with the fluorescence data.

Mutational studies confirm an essential zipper motif

To directly test the importance of the serine zipper dimerization motif for activation of MS-DesK *in vivo*, we introduced a series of point mutations that would either weaken or favor the putative dimerization interface. According to the MD model, mutations which eliminate serine residues at the C-terminus would destabilize the serine zipper dimerization motif and thereby weaken the driving force for rotation, resulting in stabilization of the phosphatase state. Indeed, we found that the mutations S23A, S30A and S33A all result in decreased kinase activity at 25 °C, favoring the phosphatase state of the sensor regardless of the temperature signal (Fig. 4 and Fig. S6). In accordance with the molecular modeling data, T20A seems not to have an effect on MS-DesK signaling (Fig. 4).

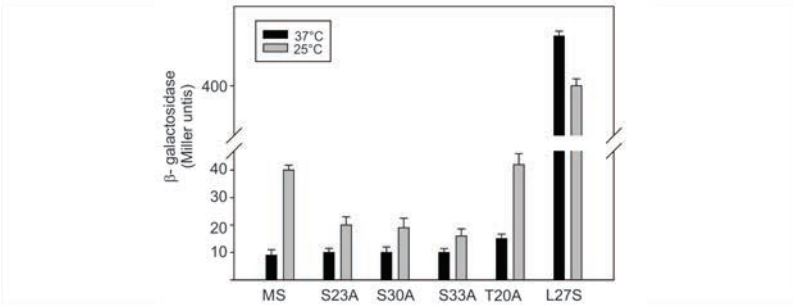

Figure 4. Activity of MS-DesK variants with an altered hydrophilic motif at the C-terminus of the TM segment. *B. subtilis* desK- cells harboring each of the MS-DesK point mutants were grown at 37 °C to an OD of 0.3 at 525 nm and divided into two samples. One sample was transferred to 25 °C (grey) and the other was kept at 37 °C (black). Aliquots were taken every hour, and β-galactosidase activities were determined. The values are representative of three independent experiments and correspond to 4 h after the shift.

As an additional control we analyzed the effect of introducing an extra serine at position 27 of the postulated helix-helix interface. This would favor the kinase state owing to stabilization of the dimerization interface now constituted by four serines localized one turn apart in the helix: S23, S27, S30 and S33. We found that this construct indeed strongly stabilizes the kinase conformation (Fig. 4). We noted the same effects when these mutations were introduced in full-length DesK (Fig. S7), supporting the importance of a specific dimer interface for functional activity.

If a serine zipper connects the two helices at the C-terminus of the transmembrane segment at low temperature, then the helices should be close enough to allow capture by cysteine cross-linking. The presence of a cysteine residue in the dimerization interface can serve as a label to detect the proximity of the monomers by formation of a disulfide bond [16]. Cultures of *B. subtilis* strains carrying MS-DesK or MS-DesK with the mutation S30C were incubated at 25 °C with diamide (a membrane-permeable oxidant). Western blot analyses were performed to analyze the presence of monomers and dimers. As shown in Figure 5, in MS-DesK S30C, cysteine residues are cross-linked leading mainly to dimer formation, whereas MS-DesK without cysteine residues in the transmembrane region forms monomers. We obtained similar results when using variant MS-DesK S23C, S33C or L27C (Fig. S8). As a control, we introduced a cysteine at position 31 (I31C). In this mutant, cysteine is located on the other side of the helix, and the ratio dimer to monomer is decreased, as expected. Taken together, these results confirm that the interface delineated by the serine zipper motif at the C-terminus of the transmembrane segment is responsible for dimer stabilization, a requirement for stabilizing the kinase conformation.

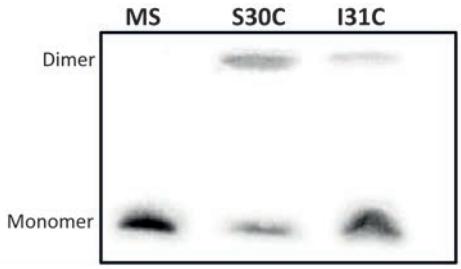

Figure 5. Disulfide cross-linking of cysteine reporters. Cells expressing MS-DesK, MS-DesK S30C or MS-DesK I31C were treated with diamide at 25 °C, and disulfide-cross-linked molecules were analyzed by Western blot analysis, as detailed in Materials & Methods.

Discussion

The model: a serine zipper as a kinase-regulatory motif

In this work, our specific aim was to decipher in molecular detail how the thermosensor DesK reacts to temperature changes by alternating between two opposite activities, kinase and phosphatase. By making use of a fully active but minimal version of DesK with only one membrane-spanning segment, and using complementary approaches, we obtained a detailed picture that allows us to propose a novel mechanism for thermo-sensing as illustrated schematically in Figure 6.

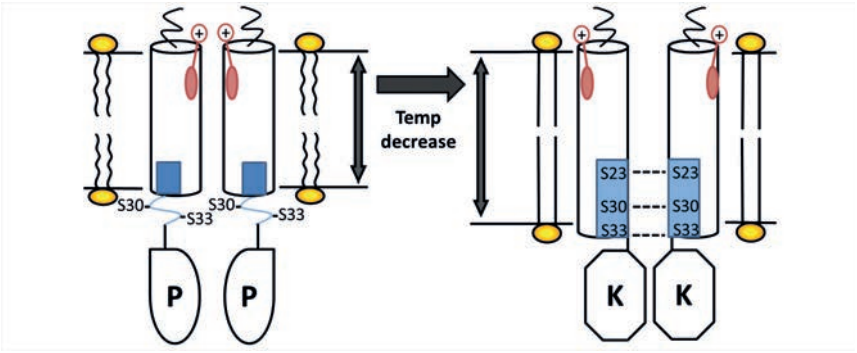

Figure 6: Schematic representation of the mode of action of MS-DesK. Its transmembrane segment (MS-TMS) contains an N-terminal charged hydrophilic motif (K10, N12; red), the so-called sunken-buoy (SB) motif. The sidechains of these residues can snorkel to the hydrophilic membrane interface and limit the further downward vertical movement of the MS-TMS. The C-terminus of the transmembrane part contains a hydrophilic motif of three serine residues (S23, S30, S33; blue). Under standard conditions in a fluid membrane, these serines interact with the hydrophilic interface (left). With decreasing temperature, the membrane thickens, and an extra turn of the helix folds inside the membrane, resulting in the formation of a serine zipper motif (right). This motif can form intrahelical hydrogen bonds that shield the hydroxyl groups from the hydrophobic core of the membrane. The reorientation, necessary for this interaction, will lead to a change in the C-terminal domain (DesKC) from the phosphatase to the kinase state.

This model suggests that MS-DesK acts as a dimer both at high and low temperatures, but that it switches between two different conformations according to the physical state of the lipid bilayer. In response to decreasing temperature, the lipid acyl chains become more ordered, leading to an increase of bilayer thickness and decreases in fluidity and hydration [7]. MS-DesK reacts to these physical changes by elongation of its transmembrane helix, resulting in location of three serine residues (S23, S30 and S33) at the same face of the helix. This serine zipper motif, located at the C-terminal region of the transmembrane segment, now becomes the dominant

dimerization motif at low temperature, so that the helices will reorient to achieve the new lowest energy state of the dimer. *In vivo*, such a reorientation could be a mechanism by which a signal is transmitted to the cytoplasmic domain, resulting in a switch in the activity of DesK.

Our model is fully consistent with the results reported herein, as well as with data in literature. The CD data suggest elongation of the transmembrane helix in thicker membranes for MS-TMS. This elongation most likely occurs at the C-terminus, because the N-terminal sunken-buoy (SB) motif can be pulled into the membrane with the lysine residue (K10) snorkeling towards the interface [5], but this same motif will prevent the N-terminal part from being pulled further into the membrane on further increases in bilayer thickness. On elongation of the C-terminal part of the helix, three hydrophilic serine residues (S23, S30 and S33) cluster together on one side of this helix, thereby constituting a potential serine zipper dimerization motif [15, 17, 18]. These serines would be able to form inter-helical H-bonds when located inside the membrane. Furthermore, dimerization of the transmembrane region of MS-DesK is consistent with the fluorescence data, and molecular dynamics simulation data confirm that MS-TMS is prone to form dimers inside the membrane, showing two dominant dimer interfaces. Moreover, the interface that includes the serine zipper motif is formed at low temperature, indicating that the serine zipper is associated with the active MS-DesK. Finally, our mutational and cross-linking studies confirm that the transmembrane part of MS-DesK forms mainly dimers in its active form with the serine zipper at the interface.

The model is also consistent with the data obtained for the 4V length mutant. The straightforward behavior of this mutant in model membranes may be related to its longer hydrophobic length, which takes away the driving force for reorientation of the helices upon increasing bilayer thickness. In addition, it should be noted that the 4V extension interrupts the serine zipper motif. Consequently, S23 is spatially separated from S30 and S33 and also is not located on the same face of the helix. This would inhibit formation of the active dimer conformation.

Finally, in our model studies, the length of the acyl chains of PC varied from 14:1 to 22:1, corresponding to hydrophobic thicknesses of 23-36 Å [11]. This does not necessarily mean that such large differences in thickness are required for the actual temperature switch of DesK *in vivo*, however. Indeed, changes in membrane thickness as function of temperature are likely to be quite small, particularly when lipids remain in a fluid phase. However, it was recently suggested that the fluid-to-gel phase transition may contribute to the switch in activity of DesK *in vivo* [19]. If the lipids approach their fluid-to-gel transition temperature on cooling, this could result in a greater increase in bilayer thickness. Thus, it is possible that other changes in membrane physical properties related to the phase transition might contribute to the activity switch of DesK. Nevertheless, regardless of whether exclusively thickness is sensed or is a combination of physical properties, our model remains valid: a mo-

lecular gauge consisting of the sunken buoy motif on one side of the membrane, and the serine zipper motif on the other side, with the serine zipper acting as a reversible helix-helix association motif that is ultimately responsible for triggering the switch in DesK activity in response to temperature-induced changes in bilayer properties.

Perspective

It has been shown that serine zippers represent a structural motif that tightly connects TM helices in several membrane proteins, including halorhodopsin, Ca-transporting ATPase and cytochrome c oxidase [15]. Here we present data on the reversible formation of an intramembrane serine zipper motif subjected to regulation by physical properties of membrane lipids. Based on the level of conservation between TCS [1], and on the notion that our general model of switching between two different interfaces is consistent with other models for TCS [20, 21], we suggest that the reversible formation of a serine zipper represents a possibly more general mechanism by which membrane-embedded sensors may detect and transmit signals.

Materials and methods

Materials

1,2-dimyristoleoyl-*sn*-glycero-3-phosphocholine [14:1 (Δ9-Cis) PC], 1,2-dipalmitoleoyl-*sn*-glycero-3-phosphocholine [16:1 (Δ9-Cis) PC], 1,2-dioleoyl-*sn*-glycero-3-phosphocholine [18:1 (Δ9-Cis) PC], 1,2-dieicosenoyl-*sn*-glycero-3-phosphocholine [20:1 (Δ11-Cis) PC] and 1,2-dierucoyl-*sn*-glycero-3-phosphocholine [22:1 (Δ13-Cis) PC] were obtained from Avanti Polar Lipids (Alabaster, AL). Routine quality controls of the lipid stocks by thin layer chromatography confirmed the purity of the lipids and the absence of degradation products. Synthetic peptides were obtained from Eurogentec (Seraing, Belgium) as > 95% pure peptides. Identity and purity were confirmed with mass spectrometry and analytical HPLC. Water was deionized and purified with a Milli-Q gradient water purification system from Millipore Corp. (Billerica, MA). All chemicals used were analytical grade.

Sample preparation

Samples were prepared as previously described [22]. Briefly, peptides, dissolved in 0.5 mL trifluoroethanol were added to 0.5 mL of the desired phospholipid dispersion. Excess water was added and subsequently the samples were lyophilized after rapid freezing in liquid nitrogen. Vesicles were prepared by rehydrating the dry film at room temperature in buffer [10 mM PIPES, 150 mM NaCl, 1 mM EDTA (pH 7.4)] for the fluorescence experiments and [10 mM Phosphate (pH 7.4)] for circular dichroism (CD) measurements. After 10 freeze–thawing cycles, the vesicles were extruded 10 times through 0.2 μm filters (Avanti hand-held extrusion device). The final peptide concentration was 25 μM for fluorescence experiments and 15 μM for CD measurements, with a molar peptide/lipid ratio of 1:50 for all samples. Peptide concentrations were quantified by the average absorbance of tryptophan at 280 nm using a molar extinction coefficient of ε = 5600 [23]. Lipid concentrations were determined by a phosphorus titration according to the method of Rouser [24].

Fluorescence measurements

Tryptophan fluorescence was measured on a Varian Cary Eclipse fluorescence spectrophotometer, using a 10 mm quartz cuvette, 5 mm excitation slit, 5.0 mm emission slit, 0.5 nm resolution, 1 s averaging time, and a scan speed of 30 nm/min. Temperature was controlled with a Peltier device at 25 °C. The tryptophan residues were excited at 295 nm, and the emission in the 300-500 nm region was recorded. The contribution of pure lipid samples was subtracted from the obtained signal. Because optical densities of the samples were below 0.05, correction for the inner filter effect was unnecessary [25]. The recorded spectra were fitted to a Log-normal distribution using SigmaPlot software as described in [12], normalized and smoothed using a

moving average filter with a window size of 5. Acrylamide quenching of tryptophan fluorescence was performed by adding acrylamide in aliquots from a 3 M stock solution to each sample up to a concentration of ~180 mM. The results were analyzed using Stern-Volmer plots [25].

Circular Dichroism

Measurements were carried out on a JASCO J-810 spectropolarimeter (Jasco Inc., Easton, MD), using a 1 mm path length quartz cuvette, 1 nm bandwidth, 0.2 nm resolution, 4 s response time, and a scan speed of 20 nm/min. Temperature was controlled with a Peltier device at 25 °C. For each measurement 10 scans were recorded over a wavelength range of 200 – 270 nm. These spectra were averaged and normalized to molar ellipticity per residue. The spectra were deconvoluted with CD-pro software [26].

Molecular modeling

We carried out large scale coarse-grained (CG) molecular dynamics (MD) simulations on the MS-DesK sequence with the Martini 2.2 force field [27] and standard Martini settings in GROMACS 4.5.x [28]. Martini is a widely used CG force field [29] and this type of approach has been proven successful in modeling helix-helix interactions in membrane environments [21, 30-34]. Here, we used a recently developed high-throughput method called Docking Assay For Transmembrane components (DAFT) [35] to screen MS-TMS dimers. For modeling, a sequence was used that corresponded to MS-TMS in Table 1, but in which the 6 C-terminal residues were left out to reduce the size of the system. Further details are provided in SI Materials & Methods.

Plasmid and strain constructions

The *MS-DesK* gene and its variants were PCR-amplified from plasmid TM1/5-DesKC-pHPKS or from DesK-pHPKS for full-length DesK [5, 6]. Site-directed mutagenesis was performed to introduce the mutations (T20A, S23A, S30A and L27S for MS-DesK and T140A, S143A, S150A and L147S for full length DesK). The resulting plasmids were used to transform CM21 or AKP20 *B. subtilis* cells [3, 6]. These strains are $desK^-$ and contain a transcriptional fusion between the reporter gene β-galactosidase and the promoter of the desaturase (gene upregulated by DesK-DesR at low temperature), which allows monitoring DesK activity. To induce the expression of DesK variants, 0.1% xylose was added to the growth medium. All mutations were confirmed by DNA sequence analysis.

Bacterial strains and growth conditions

B. subtilis JH642 strains were grown at 37 °C or 25 °C, with 250 r.p.m. gyration in Spizizen salts supplemented with 0.1% glycerol, 50 μg/ml each tryptophan and phenylalanine, 0.05% cas amino acids and trace elements [36, 37]. β-galactosidase activity was assayed in independent triplicates The results shown are the average of three independent experiments and correspond to 4 hours after the cold shock. For the disulfide cross-linking experiments a *B. subtilis* strain CM21 (desK) [6] carrying plasmid pHPKS with MS-DesK cysteine variants was grown at 37 °C in SPI medium supplemented with 0.8% xylose to induce MS-DesK expression. At OD_{600} = 0.5, cells were shifted to 25 °C and treated with 1 mM diamide (Sigma) for 30 minutes. Reactions were quenched by the addition of 10 mM N-ethylmaleimide (NEM). Cells were pelleted, and then lysed by lysozyme treatment and sonication. After ultracentrifugation, the membrane proteins were analyzed by non-reducing SDS-PAGE and visualized by immunoblotting with the specific antiserum anti-DesK.

References

[1] Stock AM, Robinson VL & Goudreau PN (2000) Two-component signal transduction. *Annu Rev Biochem* 69: 183-215.

[2] Gao R & Stock AM (2009) Biological insights from structures of two-component proteins. *Annu Rev Microbiol* 63: 133-154.

[3] Aguilar PS, Hernandez-Arriaga AM, Cybulski LE, Erazo AC & de Mendoza D (2001) Molecular basis of thermosensing: A two-component signal transduction thermometer in *bacillus subtilis*. *Embo J* 20(7): 1681-1691.

[4] Albanesi D, et al (2009) Structural plasticity and catalysis regulation of a thermosensor histidine kinase. *Proc Natl Acad Sci U S A* 106(38): 16185-16190.

[5] Cybulski LE, Martin M, Mansilla MC, Fernandez A & de Mendoza D (2010) Membrane thickness cue for cold sensing in a bacterium. *Curr Biol* 20(17): 1539-1544.

[6] Albanesi D, Mansilla MC & de Mendoza D (2004) The membrane fluidity sensor DesK of *bacillus subtilis* controls the signal decay of its cognate response regulator. *J Bacteriol* 186(9): 2655-2663.

[7] Pan J, Tristram-Nagle S, Kucerka N & Nagle JF (2008) Temperature dependence of structure, bending rigidity, and bilayer interactions of dioleoylphosphatidylcholine bilayers. *Biophys J* 94(1): 117-124.

[8] Martin M & de Mendoza D (2013) Regulation of *bacillus subtilis* DesK thermosensor by lipids. *Biochem J* 451(2): 269-275.

[9] Porrini L, Cybulski LE, Altabe SG, Mansilla MC & de Mendoza D (2014) Cerulenin inhibits unsaturated fatty acids synthesis in *bacillus subtilis* by modifying the input signal of DesK thermosensor. *Microbiologyopen* 3(2): 213-224.

[10] Inda ME, et al (2014) A lipid-mediated conformational switch modulates the thermosensing activity of DesK. *Proc Natl Acad Sci U S A* 111(9): 3579-3584.

[11] Nagle JF & Tristram-Nagle S (2000) Structure of lipid bilayers. *Biochimica Et Biophysica Acta (BBA) - Reviews on Biomembranes* 1469(3): 159-195.

[12] Ladokhin AS, Jayasinghe S & White SH (2000) How to measure and analyze tryptophan fluorescence in membranes properly, and why bother? *Anal Biochem* 285(2): 235-245.

[13] Schäfer LV, et al (2011) Lipid packing drives the segregation of transmembrane helices into disordered lipid domains in model membranes. *Proc Natl Acad Sci U S A* 108(4): 1343-1348.

[14] Dawson JP, Weinger JS & Engelman DM (2002) Motifs of serine and threonine can drive association of transmembrane helices. *J Mol Biol* 316(3): 799-805.

[15] Adamian L & Liang J (2002) Interhelical hydrogen bonds and spatial motifs in membrane proteins: Polar clamps and serine zippers. *Proteins: Structure, Function, and Bioinformatics* 47(2): 209-218.

[16] Studdert CA & Parkinson JS (2007) *In vivo* crosslinking methods for analyzing the assembly and architecture of chemoreceptor arrays. *Methods Enzymol* 423: 414-431.

[17] Zhou FX, Merianos HJ, Brunger AT & Engelman DM (2001) Polar residues drive association of polyleucine transmembrane helices. *Proc Natl Acad Sci U S A* 98(5): 2250-2255.

[18] Gratkowski H, Lear JD & DeGrado WF (2001) Polar side chains drive the association of model transmembrane peptides. *Proc Natl Acad Sci U S A* 98(3): 880-885.

[19] de Mendoza D (2014) Temperature sensing by membranes. *Annu Rev Microbiol* 68: 101-116.

[20] Ottemann KM, Xiao W, Shin YK & Koshland DE,Jr (1999) A piston model for transmembrane signaling of the aspartate receptor. *Science* 285(5434): 1751-1754.

[21] Hall BA, Armitage JP & Sansom MS (2011) Transmembrane helix dynamics of bacterial chemoreceptors supports a piston model of signalling. *PLoS Comput Biol* 7(10): e1002204.

[22] Killian JA, et al (1996) Induction of nonbilayer structures in diacylphosphatidylcholine model membranes by transmembrane alpha-helical peptides: Importance of hydrophobic mismatch and proposed role of tryptophans. *Biochemistry* 35(3): 1037-1045.
[23] Pace CN, Vajdos F, Fee L, Grimsley G & Gray T (1995) How to measure and predict the molar absorption coefficient of a protein. *Protein Sci* 4(11): 2411-2423.
[24] Rouser G, Fleischer S & Yamamoto A (1970) Two dimensional thin layer chromatographic separation of polar lipids and determination of phospholipids by phosphorus analysis of spots. *Lipids* 5(5): 494-496.
[25] Lackowicz JR (2006) Principles of fluorescence spectroscopy (Springer, New York).
[26] Sreerama N, Venyaminov SY & Woody RW (2000) Estimation of protein secondary structure from circular dichroism spectra: Inclusion of denatured proteins with native proteins in the analysis. *Anal Biochem* 287(2): 243-251.
[27] de Jong DH, et al (2013) Improved parameters for the martini coarse-grained protein force field. *J Chem Theory Comput* 9(1): 687-697.
[28] Pronk S, et al (2013) GROMACS 4.5: A high-throughput and highly parallel open source molecular simulation toolkit. *Bioinformatics* 29(7): 845-854.
[29] Marrink SJ & Tieleman DP (2013) Perspective on the martini model. *Chem Soc Rev* 42(16): 6801-6822.
[30] Castillo N, Monticelli L, Barnoud J & Tieleman DP (2013) Free energy of WALP23 dimer association in DMPC, DPPC, and DOPC bilayers. *Chem Phys Lipids* (169): 95-105.
[31] Psachoulia E, Fowler PW, Bond PJ & Sansom MS (2008) Helix-helix interactions in membrane proteins: Coarse-grained simulations of glycophorin a helix dimerization. *Biochemistry* 47(40): 10503-10512.
[32] Kalli AC, Hall BA, Campbell ID & Sansom MS (2011) A helix heterodimer in a lipid bilayer: Prediction of the structure of an integrin transmembrane domain via multiscale simulations. *Structure* 19(10): 1477-1484.
[33] Chavent M, Chetwynd AP, Stansfeld PJ & Sansom MS (2014) Dimerization of the EphA1 receptor tyrosine kinase transmembrane domain: Insights into the mechanism of receptor activation. *Biochemistry* 53(42): 6641-6652.
[34] Reddy T, et al (2014) Primary and secondary dimer interfaces of the fibroblast growth factor receptor 3 transmembrane domain: Characterization via multiscale molecular dynamics simulations. *Biochemistry* 53(2): 323-332.
[35] Wassenaar TA, et al (2015) High-throughput simulations of dimer and trimer assembly of membrane proteins. the DAFT approach. *J Chem Theory Comput*, 11(5): 2278-2291.
[36] Spizizen J (1958) Transformation of biochemically deficient strains of *bacillus subtilis* by deoxyribonucleate. *Proc Natl Acad Sci U S A* 44(10): 1072-1078.
[37] Harwood CR & Cutting SM (1990) Molecular biological methods for Bacillus. (Wiley, Chichester).

Supporting Information

SI Materials & Methods

The peptide was initially built atomistically as a canonical TM helix and then converted to a coarse-grained (CG) representation without applying elastic network constraints. Two copies of the TM helix were placed in a simulation box at a distance of 6.5 nm from each other, roughly corresponding to five or six lipids apart, after which they were randomly rotated around their helical axes to generate different starting structures. Then, DOPC lipids with Martini 2.0 lipid parameters [1, 2] and Martini water were added using the INSANE procedure (http://cgmartini.nl/cgmartini/index.php/tools2/proteins-and-bilayers, version June 12, 2014) and subsequently energy-minimized for 500 steps. Each starting system was equilibrated for 10 ps of NVT MD, using a 2 fs integration time step, followed by a production run with an NPT ensemble, using a 20 fs time step. Simulations were performed at three different temperatures: 310K, 300K and 290K. At each temperature, a total of 1000 simulations from different starting structures (as described above) were carried out for a length of 1.5 μs each. The temperature was maintained at the reference value using the V-rescale [3] thermostat with a coupling constant of 1 ps. The pressure was coupled semi-isotropically to a reference value of 1 bar using the Berendsen barostat [4] with a coupling constant of 3 ps and a compressibility of 3×10^{-4} bar^{-1}. Lennard-Jones and electrostatic interactions were shifted to zero in the range between 0.9-1.2 nm and 0.0-1.2 nm, respectively. The relative dielectric constant utilized for electrostatic interactions was 15. The neighbor list was updated every 10 steps, with the non-bonded cutoff set to 1.2 nm.

The final structures from each simulation in which a dimer was formed were analyzed based on clustering by rmsd using the Daura algorithm [5] and a cutoff of 0.5 nm for the whole protein rmsd. This procedure identifies the most-populated dimer conformations at each temperature and their respective central structure within each cluster. To gain additional insight into the shifts between different cluster populations, we also performed cluster analysis using all dimers found across all temperatures to identify the most populated clusters and the contributions from each temperature to these clusters. The cluster analysis was first carried out on the last frames collected from the simulations at all temperatures together. The results of this global cluster analysis are shown in Figure S3. The top ten clusters together (Fig. S3B) account for 75% of all the dimer conformation and were considered for further analysis of population shifts between the temperatures.

To observe the shifts, we calculated the contributions from each temperature per cluster, as seen in Figure S3C. It can be seen that the main cluster (C1) contains

the most significant contribution resulting from 310K, and that its population is decreasing by roughly 5% with decreasing temperature. This cluster also presents the highest population at 310K among the top-10 clusters at 18% and is considered to be the dominant conformation at this temperature. The opposite trend is observed for the second-largest cluster (C2) as its population increases by 4% with decreasing temperature. The C2 population size is 14% of the total at the 290K, and it also appears to be the predominant cluster at this temperature. Thus, the C1 and C2 clusters not only represent the dominant structures at high and low temperatures, respectively, but also demonstrate a conformational switch as a function of temperature.

Structurally, clusters C1 and C2 show two distinct dimer interfaces based on the orientation of the key amino acid residues (Fig. S3D), whereas the rest of the clusters represent intermediate conformational states. The main difference, however, corresponds to the locations of the serine residues lining up the dimer interface at the low-temperature cluster C2. Figure S4 shows distribution of the serine side chains throughout both clusters C1 and C2, further confirming that S23 and S30 have a very clear preference to orient toward the dimer interface. In case of S33, the changes are more subtle, with no preferred orientation seen at the high temperature (C1 in Fig. S4C); however, the distance distribution between the S33 pair (Fig. S5) clearly shows that at the low-temperature cluster C2, the majority of cluster members are at closer distances, indicative of its location at the interface, similar to the other serine residues. These changes indicate that the dimer formation at the low temperature involves formation of the serine-interacting pairs.

[1] Marrink SJ, de Vries AH & Mark AE (2004) Coarse grained model for semiquantitative lipid simulations. *J Phys Chem B* 108(2): 750-760.

[2] Marrink SJ, Risselada HJ, Yefimov S, Tieleman DP & de Vries AH (2007) The MARTINI force field: Coarse grained model for biomolecular simulations. *J Phys Chem B* 111(27): 7812-7824.

[3] Bussi G, Donadio D & Parrinello M (2007) Canonical sampling through velocity rescaling. *J Chem Phys* 126(1): 014101.

[4] Berendsen HJC, Postma JPM, van Gunsteren WF, DiNola A & Haak JR (1984) Molecular dynamics with coupling to an external bath. *J Chem Phys* 81(8): 3684-3690.

[5] Daura X, et al (1999) Peptide folding: When simulation meets experiment. *Angewandte Chemie International Edition* 38(1-2): 236-240.

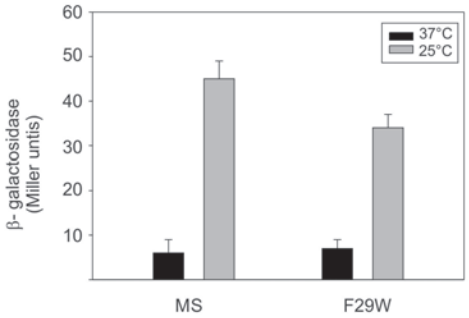

Figure S1. Activity of MS-DesK and the F29W mutant. *B. subtilis* strain desK- cells (CM21) allow measurement of the kinase activity of DesK [1, 2]. In a desK-null background, the expression of a des-lacZ fusion is null regardless temperature. If strain CM21 is complemented with DesK variants exhibiting kinase activity, then β-galactosidase activity increases at 25 °C, when DesK activates. CM21 cells were transformed with plasmids expressing MS-DesK or the MS-DesK F29W mutant under the control of the xylose-inducible Pxyl promoter. The two strains were grown at 37 °C to an OD of 0.3 at 525 nm and then divided into two samples. One sample was transferred to 25 °C (grey bars) and the other was kept at 37 °C (black bars). Aliquots were taken every hour and β-galactosidase activities were determined. The values are representative of three independent experiments and correspond to 4h after the shift.

[1] Albanesi D, Mansilla MC & de Mendoza D (2004) The membrane fluidity sensor DesK of *bacillus subtilis* controls the signal decay of its cognate response regulator. *J Bacteriol* 186(9): 2655-2663.

[2] Cybulski LE, Martin M, Mansilla MC, Fernandez A & de Mendoza D (2010) Membrane thickness cue for cold sensing in a bacterium. *Curr Biol* 20(17): 1539-1544.

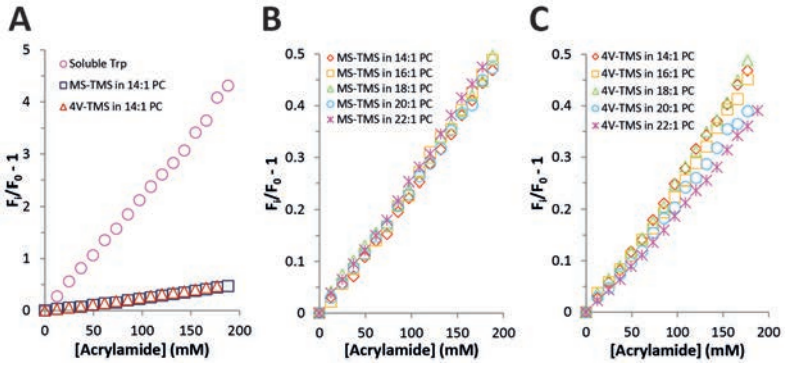

Figure S2. Ster-Volmer plots. (A) Soluble Trp (magenta) and the peptides MS-TMS (black) and 4V-TMS (red) incorporated in lipid vesicles of 14:1-PC. (B) MS-TMS in vesicles with 14:1-PC (red, diamonds), 16:1-PC (orange, squares), 18:1-PC (green, triangles), 20:1-PC (cyan, circles) and 22:1-PC (magenta, stars). (C) 4V-TMS in vesicles with 14:1-PC (red, diamonds), 16:1-PC (orange, squares), 18:1-PC (green, triangles), 20:1-PC (cyan, circles) and 22:1-PC (magenta, stars). The peptide/lipid ratio used was 1:50 and measurements were performed at a temperature of 25 °C. All data are representative sets of two independent experiments. Compared with a soluble tryptophan, both MS-TMS and 4V TMS show significantly decreased quenching (A), consistent with incorporation into the membrane. However, the quenching behavior of MS-TMS clearly differs from that of 4V-TMS (compare B, C and Table S1). For 4V-TMS, quenching decreases in the longer lipids, consistent with a location deeper in the membrane, but for MS-TMS, quenching does not show a systematic dependence on fatty acid chain length, validating the differences in behavior observed by the Trp-fluorescence experiments. Unfortunately, the differences in the specific bimodal behavior seen for MS-TMS in the fluorescence maximum experiments are too small to be

reproduced with quenching experiments.

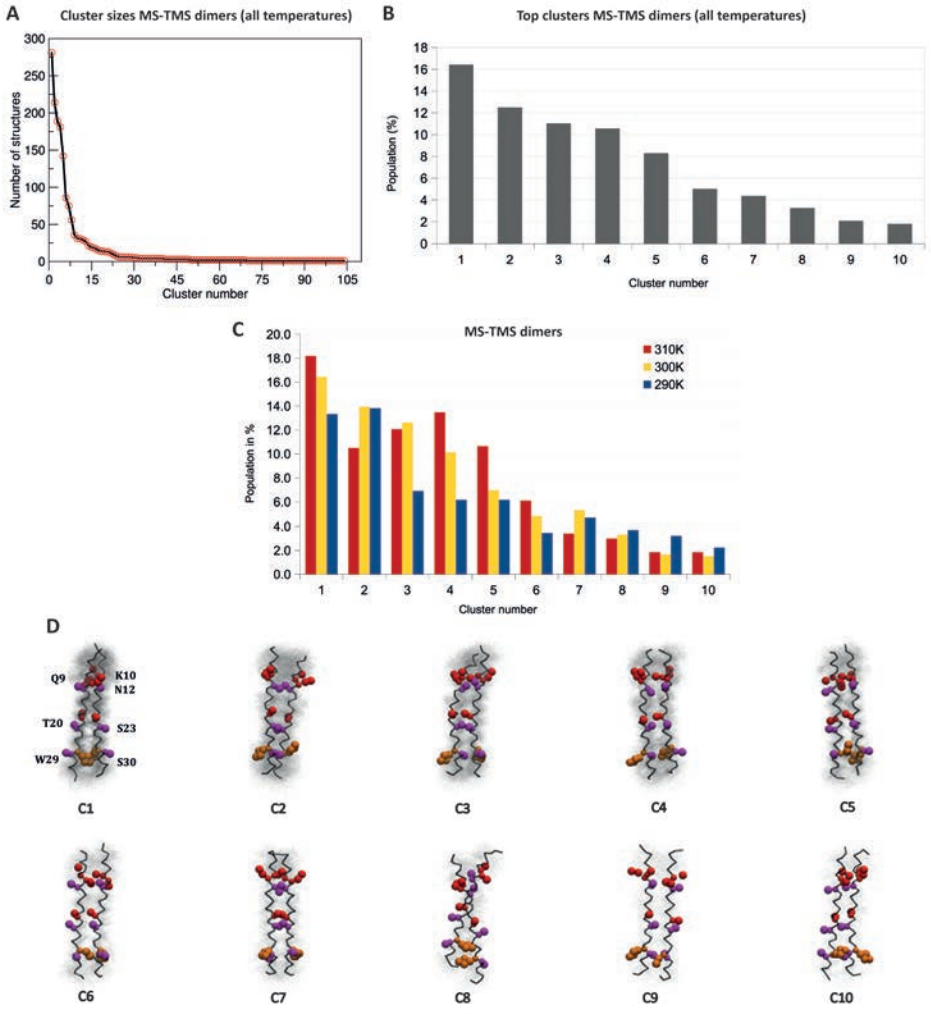

Figure S3. Cluster analysis. (A) Global cluster analysis of MS-TMS dimers for conformations from all the temperatures taken together. (B) Population sizes of the top-10 clusters from global cluster analysis. (C) Contributions from each temperature to the population size of the top-10 clusters of MS-TMS dimers. (D) Dimer conformations for the top-10 clusters of MS-TMS over all the temperatures clustered together. For each cluster, all the members were aligned to the corresponding central structure, shown as a backbone in black. Only specific amino acid residues of the central structures are shown for reference as VDW spheres. The amino acid residues shown here were selected to illustrate how the dimer interfaces change between different clusters. The residues are color-coded as follows: W29 in orange; N12, S23, and S30 in magenta; Q9, K10, and T20 in red. The T20 residue is located approximately in the middle of the helix.

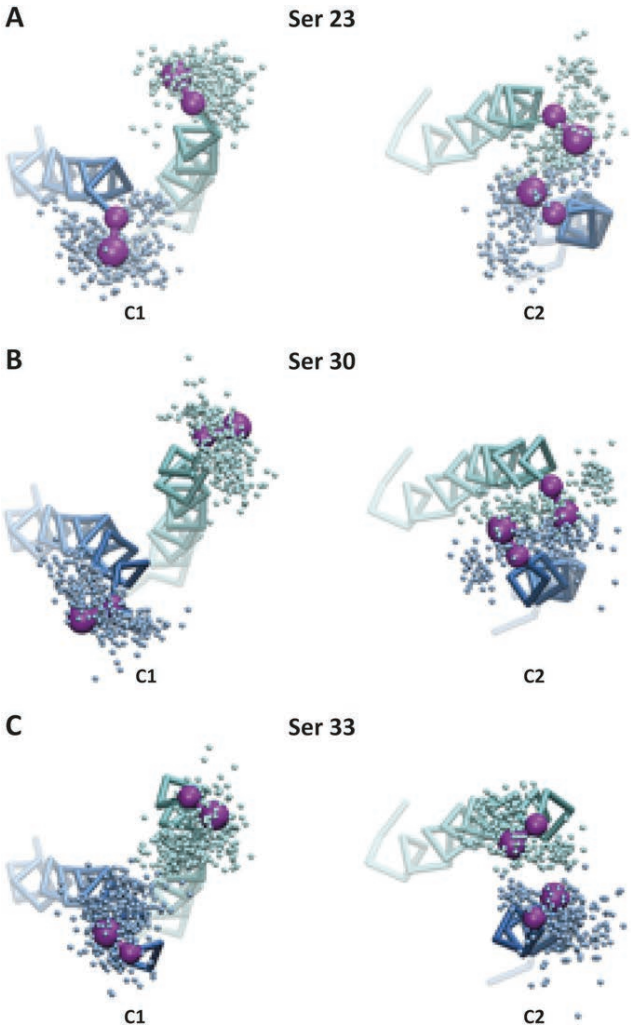

Figure S4. Distribution of serine side chains in clusters C1 and C2 in MS-TMS dimers. The bottom view from the C-terminus is shown. The residues corresponding to the position in the central structures are shown in magenta for reference. Only the side chain positions of each serine residue are shown for all the members in the cluster. Side chains belonging to different helical chains are shown in the corresponding colors (chain A in cyan; chain B in blue).

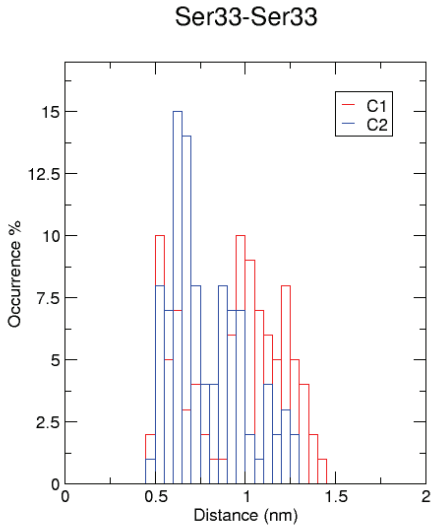

Figure S5. Distance distribution for Ser33-Ser33 pair measured between their centers of mass in clusters C1 and C2 from global cluster analysis.

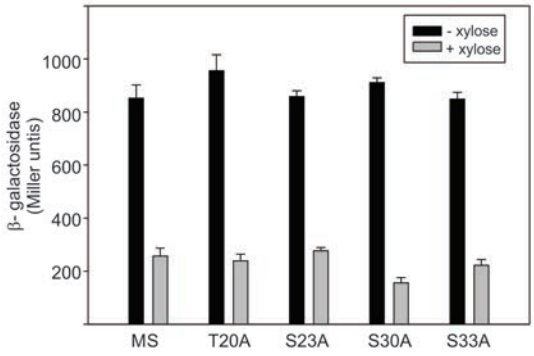

Figure S6. *In vivo* phosphatase activity of MS-DesK variants. *B. subtilis* strain AKP20 allows measurement of phosphatase activity of DesK [1, 2]. It is based on overexpression of phospho-DesR, in a desK-null background, leading to constitutive expression of a des-lacZ fusion at 37 °C. If strain AKP20 is complemented with DesK variants exhibiting phosphatase activity, then phospho-DesR is decreased, resulting in reduced β-galactosidase activity. AKP20 cells were transformed with plasmids expressing MS-DesK or its point mutants (T20A, S23A, S30A, S33A) under the control of the xylose-inducible Pxyl promoter. β-galactosidase activity was measured in the reporter strain growing at 37 °C in the presence (gray bars) or in the absence (black bars) of xylose.

[1] Cybulski LE, Martin M, Mansilla MC, Fernandez A & de Mendoza D (2010) Membrane thickness cue for cold sensing in a bacterium. Curr Biol 20(17): 1539-1544.

[2] Aguilar PS, Hernandez-Arriaga AM, Cybulski LE, Erazo AC & de Mendoza D (2001) Molecular basis of thermosensing: A two-component signal transduction thermometer in *bacillus subtilis*. Embo J 20(7): 1681-1691.

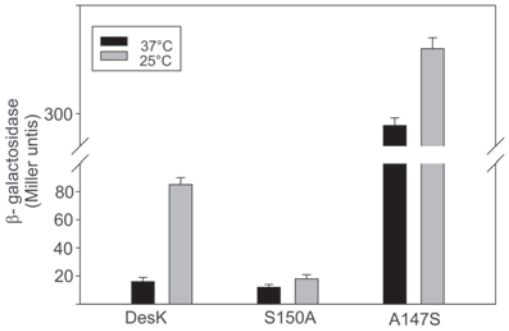

Figure S7. *In vivo* β-galactosidase activities of DesK variants. *B. subtilis* desK- cells harboring full-length DesK or its point mutants (S150A and L147S) were processed as in Figure S1.

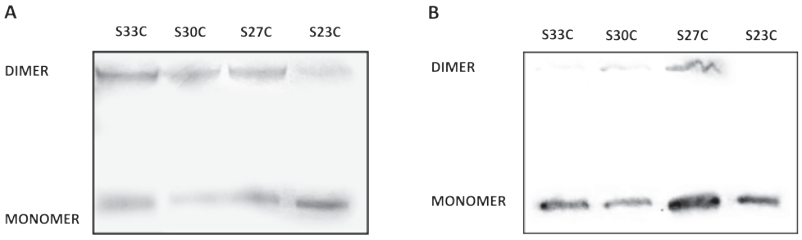

Figure S8. Disulfide cross-linking of cysteine reporters. Cells expressing MS-DesK with the independent substitutions S33C, S30C, L27C or S23C were treated with diamide (A) or without diamide (B), and analyzed by Western blot analysis, as detailed in Materials & Methods. In the presence of diamide, Cys-labelled MS-DesK molecules mainly form dimers, whereas in the absence of the oxidant, the construct mainly forms monomers. It is interesting to note that variant L27C, which is locked in the kinase state, can still form dimers in the absence of diamide, although only at low levels.

Lipid chain length	MS-TMS	4V-TMS
14:1-PC	2.5 ± 0.1	2.7 ± 0.2
16:1-PC	2.6 ± 0.2	2.6 ± 0.3
18:1-PC	2.5 ± 0.1	2.6 ± 0.1
20:1-PC	2.6 ± 0.2	2.3 ± 0.1
22:1-PC	2.6 ± 0.1	2.1 ± 0.1

Table S1. Stern-Volmer constants (M-1) for MS-TMS and 4V-TMS peptides incorporated in PC lipid vesicles with different acyl chain length. The values are averages of two independent quenching experiments with errors.

3

Structural properties of the transmembrane helices of the thermosensor DesK are regulated by both length and phase state of the surrounding lipids

Joost Ballering, Thomas E. Rijpma, Mariëtte E. van Eck
and J. Antoinette Killian

[Manuscript in preparation]

Abstract

The bacterial thermosensor DesK reacts to changes in ambient temperature, ultimately resulting in membrane fluidity maintenance. The minimal sensor DesK (MS-DesK) is an elegant model of DesK, preserving the sensing and signaling properties in only one transmembrane segment, allowing for studies in model membrane systems. Here we used a model of MS-DesK in synthetic lipid bilayers to investigate whether thickness and phase transition are sensed in a similar fashion, and how the sensing is influenced by the charge of the membrane lipids. To this end peptides corresponding to the transmembrane segment of MS-DesK and mutants studied in the previous chapter were incorporated in model systems with varying lipid composition. The influence of the lipid phase transition on the conformation of these peptides was investigated and the results were compared with the conformations in membranes with varying thickness. We found that changes in thickness and phase state induce a similar structural change in the transmembrane segment of MS-DesK. These structural changes were found to be independent of the charge of the membrane lipids. Our findings resulted in a model in which sensing and signal transduction of MS-DesK can occur through both the thickness and the phase state of the membrane lipids.

Introduction

The DesKR system is a two-component system in the soil bacterium *Bacillus subtilis* involved in maintaining membrane fluidity on a decrease in the environmental temperature [1-4]. The membrane-embedded component of this system is the protein DesK, which acts as a thermosensor that is able to detect a temperature decrease through corresponding changes in biophysical properties of the lipid environment. Here we focus on a simplified version of DesK, the so-called minimal sensor (MS-DesK), in which the five original transmembrane helices are replaced by a single transmembrane segment. This simplification facilitates studies on how the lipid environment allows for switching of the sensor from the off-state (phosphatase state) to the on-state (kinase state) on a temperature decrease. MS-DesK proved to be fully functional and the length and composition of its transmembrane segment was found to be crucial for the temperature dependence of sensing and signaling [4, 5].

What exactly is the membrane property that is detected by the thermosensor? Evidence exists that an increase in membrane thickness as a result of a temperature decrease is an important factor in DesK function [6]. This is supported by the observation that the activity of MS-DesK can be regulated by altering the membrane thickness without changing the temperature [4, 5, 7]. On the other hand, temperature-induced changes in membrane thickness are generally only substantial when accompanied by a change in phase state of the lipids, i.e. a change from a liquid-crystalline phase to a gel phase. This raises the question whether a change in phase state may be the actual trigger for activation of DesK at lower temperature and hence whether changes in phase state may have similar effects on the structure of DesK as changes in thickness of fluid bilayers.

Previous studies showed that a further simplified system of a peptide corresponding to the transmembrane segment of MS-DesK incorporated into model membranes of synthetic lipids can provide useful information on the mode of action of MS-DesK [4]. Indeed, a model could be proposed for the molecular mode of action of MS-DesK by using model membranes of lipids with varying acyl chain length and studying the behavior of the peptides with a combination of circular dichroism, tryptophan fluorescence spectroscopy and molecular dynamics simulations [4]. In this model, thicker bilayers induce elongation of the C-terminal region, resulting in the formation of a more favorable dimerization motif, a serine zipper, which then induces the helices to reorient. *In vivo* such reorientation could result in a conformational change of the cytoplasmic domain, allowing it to switch from the phosphatase state to the kinase state at low temperature. This model was supported by mutational studies in which the serine zipper motif was either strengthened or weakened.

Here we used model membrane systems to explore how the sensor reacts to its natural stimulus of temperature-dependent changes in lipid physical properties. By using CD and fluorescence on the MS-DesK transmembrane peptide in synthetic lipid bilayers we show that similar structural changes occur on inducing a lipid phase transition, as on varying lipid acyl chain length. Experiments using peptide analogs with either a strengthened or weakened serine zipper motif further indicate that these changes correspond to the kinase-on and kinase-off state of the protein [4]. Our findings thus suggest that *in vivo* the increase in thickness accompanying the phase change is the dominant feature causing the switch to kinase activity on a decrease in temperature.

Results & Discussion

The MS-DesK transmembrane segment conformation is sensitive to the lipid phase

Model membrane systems of synthetic lipids and peptides have been used successfully as a tool to study the temperature sensing mechanism of DesK [4]. In these studies a peptide, corresponding to the transmembrane segment of MS-DesK (MS-TMS, Table 1) was incorporated into bilayers of lipids with varying acyl chain length. Circular dichroism (CD) and fluorescence studies showed a conformational change of the peptide on increasing bilayer thickness that was associated to a switch in activity of the protein *in vivo* [4]. Here we aimed to use a comparable approach to investigate whether a temperature-induced change in phase state of the lipids has similar effects as changing bilayer thickness.

		Kinase state [a]	
Peptide	**Sequence**	**25 °C**	**37 °C**
MS-TMS wt	**MIKNHFTFQK LNGITPYVIT LISAILLPWS IKSRKERERL EEK**	On	Off
L27S-TMS	**MIKNHFTFQK LNGITPYVIT LISAILSPWS IKSRKERERL EEK**	On	On
ΔSerZip-TMS	**MIKNHFTFQK LNGITPYVIA LIAAILLPWA IKSRKERERL EEK**	Off	Off
ΔP-TMS	**MIKNHFTFQK LNGITAYVIT LISAILLAWS IKSRKERERL EEK**	Off	Off

Table 1. Sequences of the synthetic peptides corresponding to the transmembrane region of MS-DesK (MS-TMS) and mutants of MS-DesK. The sunken-buoy motif is marked orange and the C-terminal charged linker colored blue. Mutations are shown in red, underlined. L27S-TMS has a strengthened serine zipper. ΔSerZip-TMS is unable to form the serine zipper because of the T20A, S23A and S30A mutations. ΔP-TMS has an altered backbone structure because of two proline mutations (P16A and P27A). A Trp (green) was incorporated instead of a Phe to allow for fluorescence measurements. As shown previously [4], CD spectra of MS-TMS in bilayers of unsaturated lipids have two minima at around 222 nm and 208 nm (Fig.1A), indicative for a mainly α-helical character of the peptide. However, the shape of the spectra is clearly dependent on bilayer thickness, with a decrease in ellipticity ratio of the minima (222/208 nm) in thicker bilayers, as quantified in Fig. 1B. This decrease has been correlated with a lengthening of the α-helix [4] (see also the fits in Table S1), and with a switch in activity from off-state in the thinner bilayers to on-state in the thicker ones.

[a] Expected state of the corresponding protein based on mutation studies.

To compare this behavior with the effect of a temperature-induced change in phase state of the lipids, we selected dipalmitoylphosphatidylcholine (16:0-PC) lipids as model systems because the gel to liquid-crystalline phase transition (Tm) occurs at an experimentally convenient temperature of 41 °C [8] and because the change in thickness on the phase transition approaches the thickness range of unsaturated PC lipids where the switch behavior of MS-TMS was observed (Table 2). As in unsatu-

rated lipids, the spectra show mainly α-helical character (Figure 1C, Table S1), but with a decrease in ellipticity ratio when the temperature drops from around T_m to lower temperatures (Fig. 1G blue diamonds), indicating an elongation of the α-helix when the gel-phase character of the membrane increases. The temperature-dependent effect of MS-TMS is absent in dioleoylphosphatidylcholine (18:1-PC), which has a T_m at -17 °C [10], demonstrating that the temperature change itself has no effect on the structure of the peptide (Fig. 1D, Fig. 1G red triangles). Experiments on MS-TMS in dimyristoylphosphatidylcholine (14:0-PC) show a similar change in structure as for 16:0-PC, but now around the T_m of 23 °C (Fig. 1E, Fig. 1G green diamonds), confirming that a phase transition is indeed responsible for the observed structural changes.

Acyl chain composition	Transition temperature (°C)	Hydrophobic thickness (Å) [a]	
		Fluid phase	Gel phase
di-14:1		23.4	
di-16:1	-36	26.2	
di-18:1	-17	29.6	
di-20:1	-4	32.5	
di-22:1	13	36.3	
di-14:0	24	25.4	30.3
di-16:0	41	28.5	34.4

Table 2. Phosphatidylglycerol transition temperatures and hydrophobic thicknesses as function of acyl chain composition. Hydrophobic thicknesses are defined as carbonyl-carbonyl distance, derived from Marsh [9].

a) Hydrophobic thicknesses at 30 °C, except for the gel phase of di-14:0-PC (10 °C) and the fluid phase of di-16:0-PC (50 °C)

Because negatively charged lipids could influence the activation mechanism of MS-DesK [11], we also studied the conformational behavior of MS-TMS in the anionic lipids dipalmitoylphosphatidylglycerol (16:0-PG) and dioleoylphosphatidylglycerol (18:1-PG), which have similar phase transition temperatures as the corresponding PC lipids [12]. The spectra showed a similar trend for MS-TMS in PG lipids (Fig. 1F, 1H), suggesting that the switch is not affected by the charge of the lipid head groups.

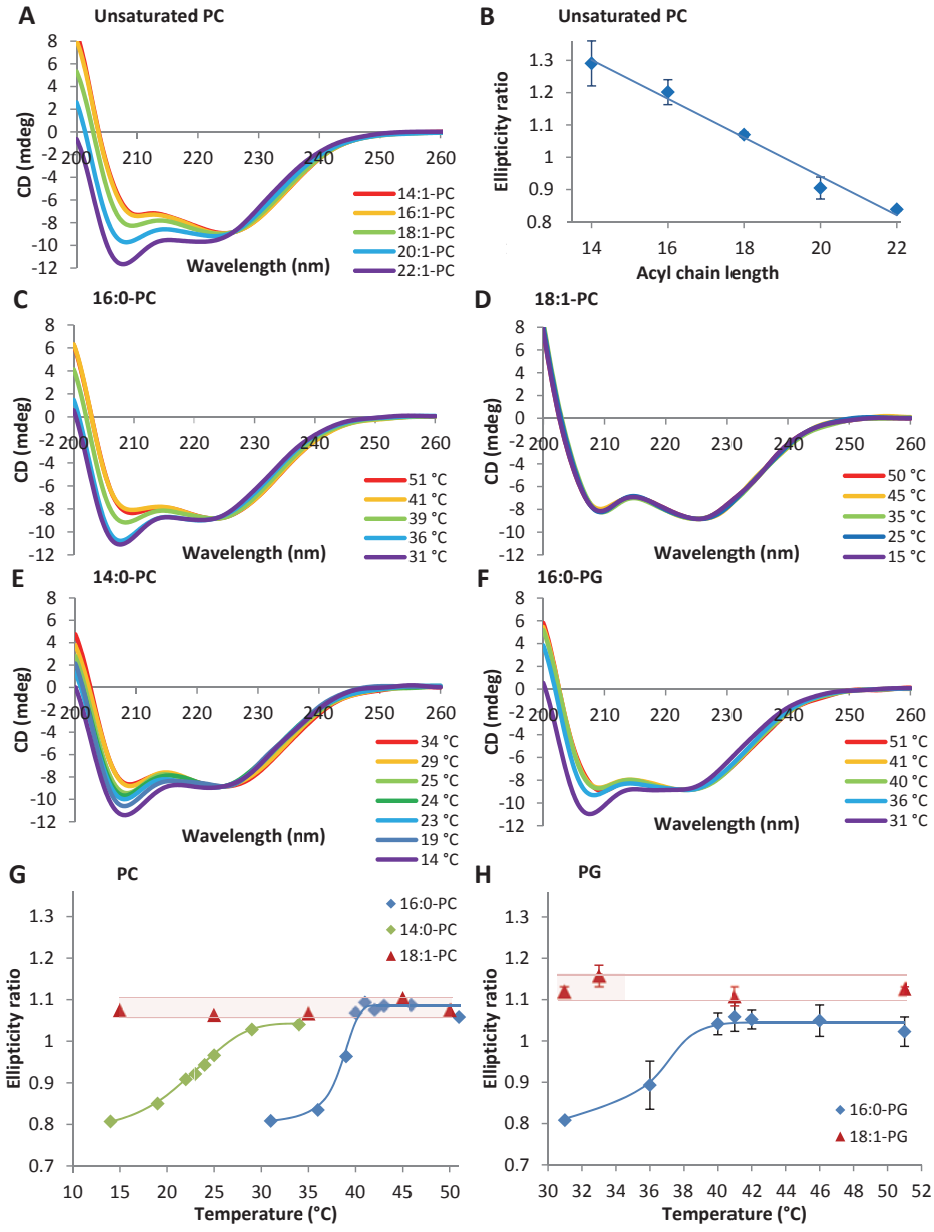

Figure 1. Structural behavior of MS-TMS characterized by CD in various model membrane systems. A) CD spectra of MS-TMS in lipid vesicles of 14:1-PC (red), 16:1-PC (yellow), 18:1-PC (green), 20:1-PC (blue) and 22:1-PC (purple) and B) the ellipticity ratios depending on acyl chain length. C) CD spectra of MS-TMS in model membrane systems with 18:0-PC, 18:1-PC (D), 14:0-PC (E) and 18:1-PG (F). G) The ellipticity ratios of model membrane systems with PC and PG (H). The peptide lipid ratio used was 1:50. All emission spectra are a representative set of two independent experiments except for the temperature-dependent PC experiments.

Next, Trp-fluorescence experiments were performed to obtain complimentary data on the conformational change of MS-TMS. Previously, fluorescence spectra of MS-TMS in model membranes of varying thickness demonstrated a complex, non-linear behavior of the emission maxima (Fig. 2A, B), with an initial decrease in wavelength of the emission maximum on increasing bilayer thickness from 14:1-PC to 18:1-PC and a small increase of the wavelength on further increasing bilayer thickness from 18:1-PC to 20:1-PC. This behavior was thought to reflect the re-orientation between the two dimerization interfaces of MS-TMS [4] during transition from the off-state to the on-state on increasing bilayer thickness.

When the fluorescence spectra are measured in 16:0-PC as function of temperature (Fig. 2C), a different behavior is observed. A relatively large change in wavelength of the emission maximum occurs when going through the phase transition temperature (Fig. 2G blue diamonds). A similar behavior is observed around T_m for 14:0-PC (Fig. 2E, 2G green diamonds), and to a lesser extent for 16:0-PG (Fig. 2F, Fig 2H blue diamonds). No such transition is observed for the unsaturated lipids as function of temperature, demonstrating that this behavior is indeed connected to the phase transition. Nevertheless, the results are much less straightforward than the CD measurements. Most importantly, the fluorescence signal is highly sensitive to interfacial hydration, and hence will be dominated by the fluid-to-gel phase transition. This makes it very difficult to visualize subtle biphasic behavior owing to helix reorientation, if present. Second, some of the spectra show broadening, e.g. in 16:0-PC, which may suggest the presence of different environments for the Trp residue. Taken together, these results show that Trp-fluorescence is less valuable for the study of MS-DesK in lipid phase dependent experiments and therefore in the remainder of this study we will focus mainly on CD analysis for these experiments.

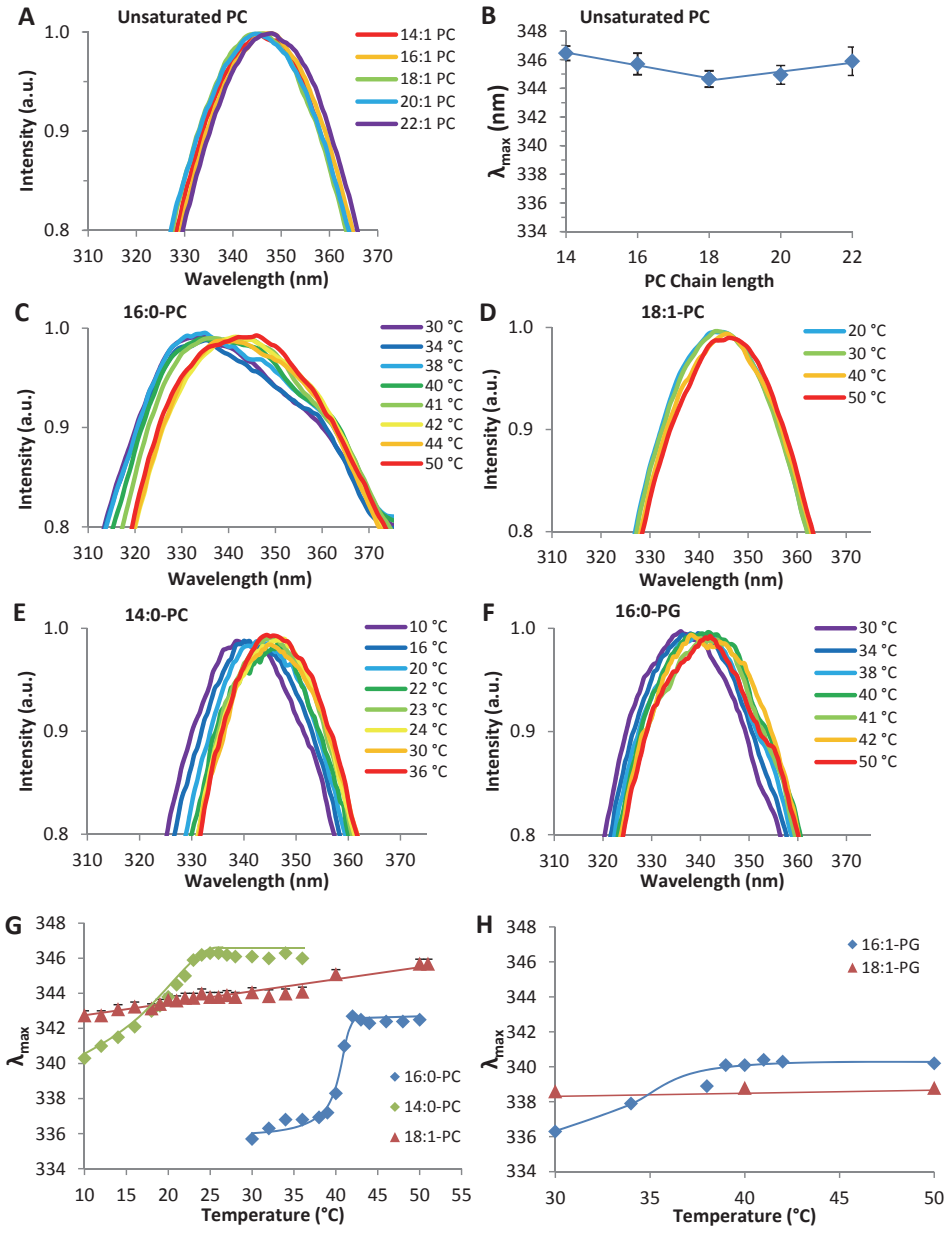

Figure 2. Structural behavior of MS-TMS characterized by Trp-fluorescence in various model membrane systems. A) Emission spectra of MS-TMS in lipid vesicles of 14:1-PC (red), 16:1-PC (yellow), 18:1-PC (green), 20:1-PC (blue) and 22:1-PC (purple) and B) the emission maxima depending on acyl chain length. C) Emission spectra of MS-TMS in model membrane systems with 16:0-PC, 18:1-PC (D), 14:0-PC (E) and 16:0-PG (F). G) The ellipticity ratios of model membrane systems with PC and PG (H). The peptide lipid ratio used was 1:50. All emission spectra are a representative set of two independent experiments.

The conformational behavior of MS-DesK transmembrane segments with strengthened or weakened serine zippers reflects the *in vivo* kinase activity of the corresponding proteins

The results so far using CD on model membrane systems suggest that changes in conformation of the MS-DesK transmembrane segment as function of bilayer thickness are similar to changes resulting from a temperature-induced phase change of the lipids. To further investigate whether this conformational behavior is related to functional properties, we next made use of peptides corresponding to functional and non-functional mutants of DesK. The serine zipper of MS-DesK is an excellent target for such mutations, because mutants with strengthened or weakened serine zipper motifs showed permanent kinase-on and kinase-off activity respectively [4]. The amino acid sequences of the peptides are shown in Table 1. In L27S-TMS the zipper is strengthened by an extra serine residue at the zipper interface and the corresponding MS-DesK mutant is active at all temperatures. In ΔSerZip-TMS the zipper motif is completely removed by replacing all three serines by alanines. Note that in MS-DesK replacement of only one serine is already sufficient to cause inactivity at all temperatures [4]. Finally, in ΔP-TMS the serine zipper is disrupted in an indirect way by mutating the two proline residues to alanines. In the corresponding MS-DesK it was observed that replacement of only one of either proline is sufficient to cause inactivity at all temperatures (Cybulski, unpublished). It seems most likely that these prolines disrupt the backbone structure in a way that allows for favorable positioning of the dimer interface in its active state.

The peptides were first incorporated into model membranes of unsaturated phosphatidylcholine (PC) lipids with varying acyl chain length. The CD spectra in Figure 3A-C show that all peptides exhibit mainly α-helical character, albeit with striking differences in their behavior. Importantly, for all three mutants the CD spectra appear to be independent of acyl chain length (Fig. 3A-C). However, the ellipticity ratios of L27S-TMS are similar to those for MS-TMS in thicker membranes (Fig. 3D), while ΔSerZip-TMS and ΔP-TMS show ellipticity ratios, which resemble those of MS-TMS in thinner membranes (Fig. 3E, F). Deconvolution of the CD spectra (Table S1) indicates that the helix of L27S-TMS is somewhat elongated in all bilayers, while both ΔSerZip-TMS and ΔP-TMS contain shorter α-helices. Thus, these results suggest that the two different states previously proposed for MS-DesK [4] in thick and in thin bilayers are similar to the states of the corresponding active and inactive mutants.

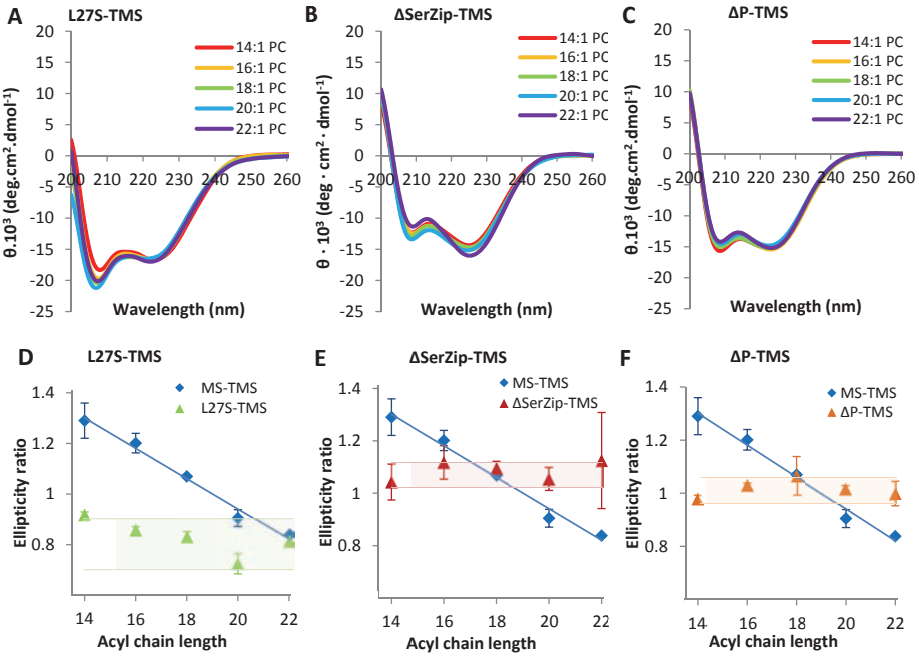

Figure 3. Behavior of mutants with strengthened or weakened serine zipper motif in model membrane systems with varying bilayer thickness. CD spectra of A) L27S-TMS, B) ΔSerZip-TMS and C) ΔP-TMS in lipid vesicles of 14:1-PC (red), 16:1 PC (yellow), 18:1-PC (green), 20:1-PC (blue) and 22:1-PC (purple). D) Bilayer thickness dependent change in ellipticity ratio for L27S-TMS (green triangles), ΔSerZip-TMS (E, red triangles) and ΔP-TMS (F, orange triangles) as compared to MS-TMS (D-F, blue diamonds). The CD spectra are a representative set of two independent experiments and the ellipticity ratios are averages of two independent experiments with errors. The linear trendline for MS-TMS is shown to guide the eye. The transparent areas with solid borders indicate the minimum and maximum value for the mutants for straightforward comparison with MS-TMS.

The CD results were further supported by Trp-fluorescence measurements (Fig. 4). The behavior of the three mutants clearly differs from that of MS-TMS. One difference is that the spectra of these mutants are slightly blue-shifted with respect to MS-TMS (Fig. 4D-F). The reason for this is not clear, but it is most likely related to a change in the chemical environment of the Trp in these mutants, for example owing to the substitutions themselves, to a change in dimer interface, or to a change in localization with respect to the lipid/water interface. A more relevant difference in the context of this study is that for all three mutants the wavelength of the emission maximum decreases with increasing chain length, albeit less pronounced in the case of L27S-TMS. This would correspond to a Trp residue simply becoming located in a more hydrophobic environment on thickening of the bilayer. Therefore, the trends in the fluorescence spectra are consistent with mutants, which lack a bilayer thickness-dependent activity switch.

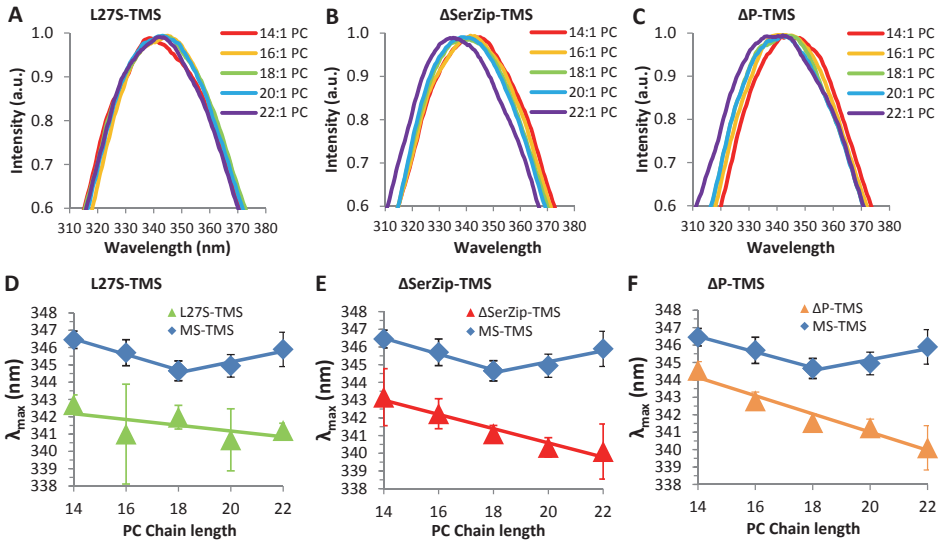

Figure 4. Trp-fluorescence behavior of mutants with strengthened or weakened serine zipper motif in model membrane systems with varying bilayer thickness. Emission spectra of A) L27S-TMS, B) ΔSerZip-TMS and C) ΔP-TMS in lipid vesicles of 14:1-PC (red), 16:1-PC (orange), 18:1-PC (green), 20:1-PC (cyan) and 22:1-PC (magenta). D) Emission maxima as a function of acyl chain length for L27S-TMS (green triangles), ΔSerZip-TMS (E, red triangles) and ΔP-TMS (F, orange triangles) of as compared to MS-TMS (D-F blue diamonds). The emission spectra are a representative set of two independent experiments. The emission maxima are averages of two independent experiments. The errors are relative to the previous measurement.

Next, the behavior of peptides with altered serine zipper motifs (Table 1) was investigated as function of temperature-induced changes in the phase state of the lipids, using bilayers of 16:0-PC. The CD spectra in Figure 5A-C show that the conformational behavior of the peptides is much less dependent on the phase state as compared to that of MS-TMS. The ellipticity ratios observed for L27S-TMS are in the range of the values found for MS-TMS at temperatures in the gel phase, while for ΔSerZip-TMS and ΔP-TMS the ellipticity ratios are more similar to those of MS-TMS in the fluid phase (Fig. 5D-F). However, the situation is somewhat complex, because in all cases significant variations are observed around T_m. The CD spectra of L27S-TMS show a slightly lower ellipticity ratio in the gel phase, indicating that ordered acyl chains could induce slightly more helicity. In contrast, both ΔSerZip-TMS and ΔP-TMS show a slightly higher value in the gel phase as compared to the fluid phase. This trend is opposite to the switch from MS-TMS, suggesting that it may be an artifact caused by the ordered acyl chains of the gel phase. However, the differences are small as compared to the changes for MS-TMS and well within the fluctuations observed for the unsaturated lipids (Fig. 1, 3). Thus, the results are generally consistent with the phase transition inducing similar transitions for MS-TMS as changes in bilayer thickness in fluid bilayers.

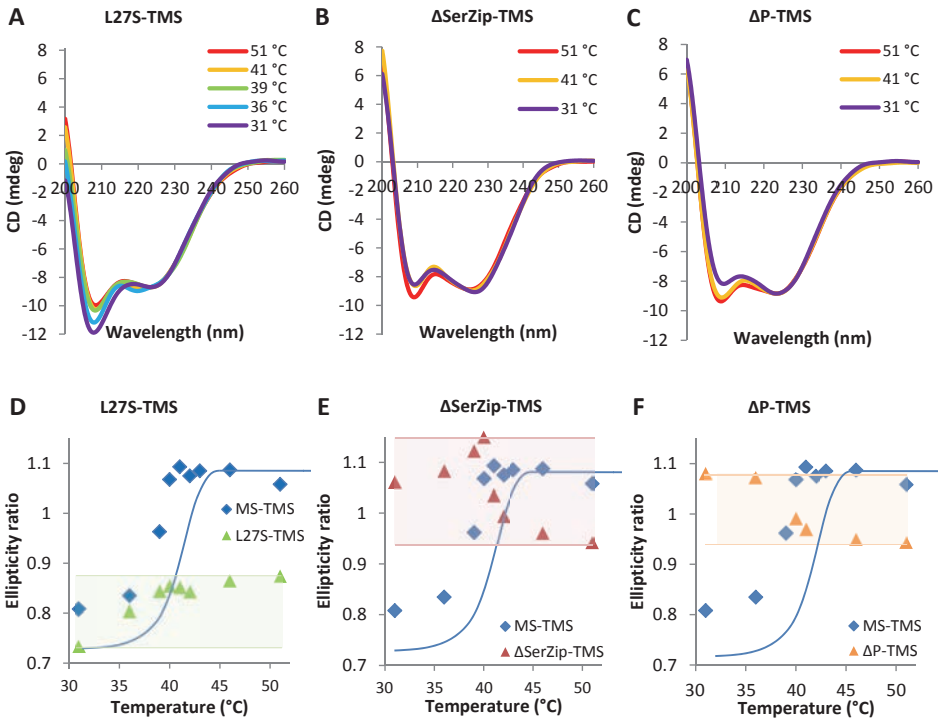

Figure 5. Behavior of mutants with strengthened or weakened serine zipper motif in response to the lipid phase transition. CD spectra of A) L27S-TMS, B) ΔSerZip-TMS and C) ΔP-TMS in lipid vesicles of DPPC at different temperatures. C) Temperature-dependent change in ellipticity ratios of L27S-TMS (green triangles), ΔSerZip-TMS (E, red triangles) and ΔP-TMS (F, orange triangles) as compared to MS-TMS (D-F, blue diamonds). The trendlines for MS-TMS and L27S-TMS are shown to guide the eye. The transparent areas with solid borders indicate the minimum and maximum value for the mutants for straightforward comparison with MS-TMS.

The extended model of the mode of action of MS-DesK thermo-sensing

In this study we identified CD as a powerful tool to gain insight into the activity of MS-DesK by using synthetic peptides corresponding to active and non-active forms of the transmembrane segment of DesK in model membrane systems. The ellipticity ratios of MS-TMS and the mutants in systems of saturated lipids as a function of temperature compared well to the values for the model systems with unsaturated lipids as function of bilayer thickness. Based on the results we extend the previous model of the mode of action of MS-DesK sensing and signaling as presented in Figure 6. We propose that activity can be triggered by thickening of the membrane either by a temperature-induced phase transition to a gel phase or by a lengthening of the acyl chains. The mechanism is most likely similar, with a reorientation of the helices combined with lengthening of the helices to form a serine zipper. This model links

the activity switch of MS-DesK to both phase transition and membrane-thickness change. Furthermore, the proposition that phase transition is a trigger for MS-DesK is in accordance with the situation *in vivo*, where this mechanism protects the membranes from the liquid-to-gel transition.

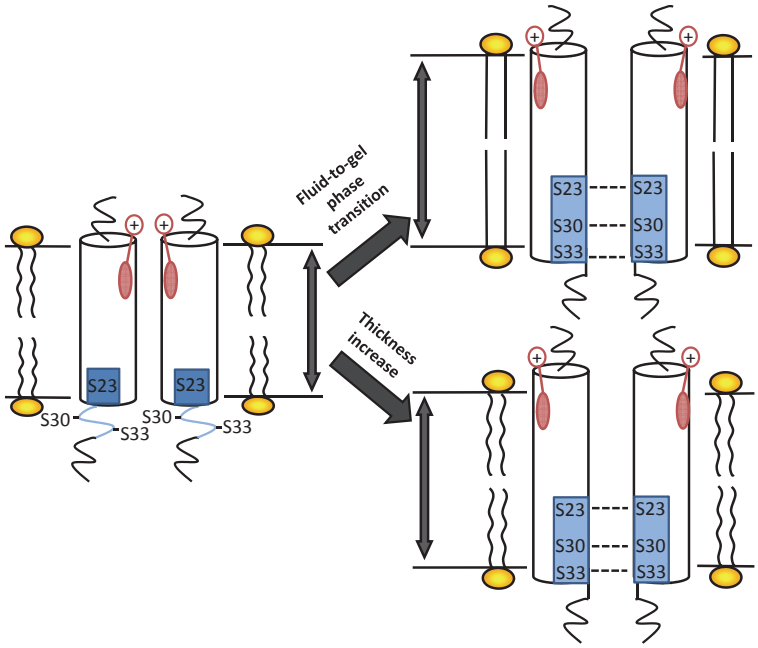

Figure 6. Schematic representation of the mode of action of MS-DesK. Its transmembrane segment (MS-TMS) contains a charged hydrophilic N-terminal sunken-buoy motif (K10, N12; red). Their sidechains can snorkel to the hydrophilic membrane interface and limit the further downward lateral movement of MS-TMS. The C-terminus contains a serine zipper motif of three serine residues (S23, S30, S33; blue). In a fluid, thin membrane these serines interact with the hydrophilic interface (left). When the temperature decreases the lipids undergo a fluid-to-gel transition and the membrane becomes thicker. Thereupon, an extra turn of the helix folds inside the membrane resulting in the formation of a serine zipper motif (upper right). This motif can form intrahelical hydrogen bonds that shield the hydroxyl groups from the hydrophobic core of the membrane. This mechanism is similar when the membrane becomes thicker by increasing the acyl chain length. Mutants without a serine-zipper or with a disrupted one will not form the serine zipper and when the serine zipper is strengthened by an extra serine residue, it will always form the serine zipper, regardless of the physical state of the lipids.

Summarizing conclusion

The results in this manuscript suggest that both fluidity and thickness influence MS-DesK structure and activity. However, these properties are not independent of each other: a decrease in membrane fluidity results in significant thickening of the membrane. Thus, it is likely that the phase transition is sensed as an increase in membrane thickness. However, there are also other possibilities. For example, it is possible that *in vivo*, a phase separation is sensed by DesK [6]. Around the phase transition temperature of the membrane, fluid-phase and gel-phase domains coexist [13]. DesK might be able to sense and react to these coexisting domains by reorientation of its transmembrane segments by partitioning at the interfaces of these domains and reorient to have the most favorable interaction with both types of domains.

Still another possibility would be that MS-DesK senses the hydration of the membrane. Membranes in the gel phase are less hydrated than fluid membranes [13]. The depletion of water inside the membrane could induce the kinase active conformation of MS-DesK, until the hydration level is so low that it starts to aggregate. However, to investigate the hydration or phase separation in the membrane without changing other properties is experimentally very challenging. An option would be to use molecular dynamics simulation as was previously described [4] to further explore the MS-DesK dimer conformation dependence on hydration levels and phase separation induced phenomena.

Materials & Methods

Materials

1,2-dimyristoyl-*sn*-glycero-3-phosphocholine (DMPC), 1,2-dipalmitoyl-*sn*-glycero-3-phosphocholine (DPPC), 1,2-dipalmitoyl-*sn*-glycero-3-phospho-(1'-*rac*-glycerol) (sodium salt) 1,2-dimyristoleoyl-*sn*-glycero-3-phosphocholine [14:1 (Δ9-Cis) PC], 1,2-dipalmitoleoyl-*sn*-glycero-3-phosphocholine [16:1 (Δ9-Cis) PC], 1,2-dioleoyl-*sn*-glycero-3-phosphocholine [18:1 (Δ9-Cis) PC], 1,2-dieicosenoyl-*sn*-glycero-3-phosphocholine [20:1 (Δ11-Cis) PC], and 1,2-dierucoyl-*sn*-glycero-3-phosphocholine [22:1 (Δ13-Cis) PC] were obtained from Avanti Polar Lipids (Alabaster, AL). Routine quality controls of the lipid stocks by thin layer chromatography confirmed the purity of the lipids and the absence of degradation products. Synthetic peptides were obtained from Eurogentec (Seraing, Belgium) as > 95 % pure peptides. Identity and purity were confirmed with mass spectrometry and analytical HPLC. Water was deionized and purified with a Milli-Q gradient water purification system from Millipore Corp. (Billerica, MA). All chemicals used were analytical grade.

Sample preparation

Samples were prepared as previously described [4]. Briefly, peptides (10/15 μM), dissolved in 0.5 mL trifluoroethanol were added to 0.5 mL of the desired phospholipid dispersion acquiring a final molar peptide/lipid ratio of 1/50 with the lipid concentrations determined by a phosphorus titration according to the method of Rouser [14]. Excess water was added and subsequently the samples were lyophilized after rapid freezing in liquid nitrogen. Vesicles were prepared by rehydrating the dry film at room temperature in buffer [10 mM PIPES, 150 mM NaCl, 1 mM EDTA (pH 7.4)] for the fluorescence experiments and [10 mM Phosphate, 10 mM NaCl (pH 7.4)] for circular dichroism (CD) measurements. After 10 freeze–thawing cycles, the vesicles were extruded 10 times through 0.2 μm filters (Avanti hand-held extrusion device). The final peptide concentrations in these samples were quantified by the average absorbance of tryptophan at 280 nm using a molar extinction coefficient of ε = 5600 [15]. The final yield ranged from 85 – 50 %.

Fluorescence measurements

Tryptophan fluorescence was measured on a Varian Cary Eclipse fluorescence spectrophotometer, using a 10 mm quartz cuvette, 5 mm excitation slit, 5.0 mm emission slit, 0.5 nm resolution, 1 s averaging time, and a scan speed of 30 nm/min. Temperature was controlled with a Peltier device. The tryptophan residues were excited at 295 nm, and the emission in the 300-500 nm region was recorded. The contribution of pure lipid samples was subtracted from the obtained signal. Because optical densities of the samples were below 0.05, correction for the inner filter effect

was unnecessary [16]. The recorded spectra were fitted to a Log-normal distribution as described in [17], normalized and smoothed using a moving average filter with a window size of 5.

Circular dichroism

Measurements were carried out on a JASCO J-810 spectropolarimeter (Jasco Inc., Easton, MD), using a 1 mm path length quartz cuvette, 1 nm bandwidth, 0.2 nm resolution, 4 s response time, and a scan speed of 20 nm/min. Temperature was controlled with a Peltier device. For each measurement 10 to 20 scans were recorded over a wavelength range of 200 – 260 nm. These spectra were averaged and Fourier filtered to reduce the high frequency noise. The spectra for the bilayer thickness dependence experiments were normalized to molar ellipticity per residue (Fig. 5). These spectra were deconvoluted with CD-pro software [18]. The temperature-dependent measurements in the saturated lipids showed slight precipitation at temperatures below the lipid phase transition. Therefore the peptide concentration in the cuvet could not be determined accurately and the ellipticity is shown in mdeg. The spectra were normalized to the minimum around 222 nm because of the high α-helix content. When precipitation was observed after a measurement, the cuvet was vortexed until the solution was clear.

References

[1] Aguilar PS, Hernandez-Arriaga AM, Cybulski LE, Erazo AC & de Mendoza D (2001) Molecular basis of thermosensing: A two-component signal transduction thermometer in *bacillus subtilis*. *Embo J* 20(7): 1681-1691.

[2] Gao R & Stock AM (2009) Biological insights from structures of two-component proteins. *Annu Rev Microbiol* 63: 133-154.

[3] Albanesi D, et al (2009) Structural plasticity and catalysis regulation of a thermosensor histidine kinase. *Proc Natl Acad Sci U S A* 106(38): 16185-16190.

[4] Cybulski LE, et al (2015) Activation of the bacterial thermosensor DesK involves a serine zipper dimerization motif that is modulated by bilayer thickness. *Proc Natl Acad Sci U S A* 112(20): 6353-6358.

[5] Cybulski LE, Martin M, Mansilla MC, Fernandez A & de Mendoza D (2010) Membrane thickness cue for cold sensing in a bacterium. Curr Biol 20(17): 1539-1544.

[6] Martin M & de Mendoza D (2013) Regulation of *bacillus subtilis* DesK thermosensor by lipids. *Biochem J* 451(2): 269-275.

[7] Porrini L, Cybulski LE, Altabe SG, Mansilla MC & de Mendoza D (2014) Cerulenin inhibits unsaturated fatty acids synthesis in *bacillus subtilis* by modifying the input signal of DesK thermosensor. *Microbiologyopen* 3(2): 213-224.

[8] Lewis RN, Mak N & McElhaney RN (1987) A differential scanning calorimetric study of the thermotropic phase behavior of model membranes composed of phosphatidylcholines containing linear saturated fatty acyl chains. *Biochemistry* 26(19): 6118-6126.

[9] Marsh D (2013) Handbook of lipid bilayers (CRC Press, Boca Raton)

[10] Lewis RN, Sykes BD & McElhaney RN (1988) Thermotropic phase behavior of model membranes composed of phosphatidylcholines containing cis-monounsaturated acyl chain homologues of oleic acid: Differential scanning calorimetric and 31P NMR spectroscopic studies. *Biochemistry* 27(3): 880-887.

[11] Inda ME, et al (2014) A lipid-mediated conformational switch modulates the thermosensing activity of DesK. *Proc Natl Acad Sci U S A* 111(9): 3579-3584.

[12] Zhang YP, Lewis RN & McElhaney RN (1997) Calorimetric and spectroscopic studies of the thermotropic phase behavior of the n-saturated 1,2-diacylphosphatidylglycerols. *Biophys J* 72(2 Pt 1): 779-793.

[13] Cevc G & Marsh D (1987) Phospholipid Bilayers: Physical Principles and Models (Wiley-Interscience, New York)

[14] Rouser G, Fleischer S & Yamamoto A (1970) Two dimensional thin layer chromatographic separation of polar lipids and determination of phospholipids by phosphorus analysis of spots. *Lipids* 5(5): 494-496.

[15] Pace CN, Vajdos F, Fee L, Grimsley G & Gray T (1995) How to measure and predict the molar absorption coefficient of a protein. *Protein Sci* 4(11): 2411-2423.

[16] Lackowicz JR (2006) Principles of fluorescence spectroscopy (Springer, New York).

[17] Ladokhin AS, Jayasinghe S & White SH (2000) How to measure and analyze tryptophan fluorescence in membranes properly, and why bother? *Anal Biochem* 285(2): 235-245.

[18] Sreerama N, Venyaminov SY & Woody RW (2000) Estimation of protein secondary structure from circular dichroism spectra: Inclusion of denatured proteins with native proteins in the analysis. *Anal Biochem* 287(2): 243-251.

Supporting Information

A **MS-TMS**

	α-helix (%)	α-helix, no. of residues	Hydrophobic thickness (Å)	Sheet (%)	Random coil (%)
14:1 PC	56±2	24±1	23	9±1	35±1
16:1 PC	55±3	24±1	26	9±1	36±3
18:1 PC	59±2	25±1	30	8±1	33±2
20:1 PC	63±1	27±1	33	6±2	31±1
22:1 PC	67±2	29±1	36	7±3	26±3

B **L27S-TMS**

	α-helix (%)	α-helix, no. of residues	Hydrophobic thickness (Å)	Sheet (%)	Random coil (%)
14:1 PC	60±1	26±1	23	6±1	34±1
16:1 PC	59±1	25±1	26	6±1	35±1
18:1 PC	59±1	25±1	30	7±1	34±1
20:1 PC	60±1	26±1	33	10±2	30±1
22:1 PC	61±2	26±1	36	9±3	30±1

C **ΔSerZip-TMS**

	α-helix (%)	α-helix, no. of residues	Hydrophobic thickness (Å)	Sheet (%)	Random coil (%)
14:1 PC	54±1	23±1	23	9±1	40±1
16:1 PC	57±2	24±1	26	9±1	34±2
18:1 PC	56±3	24±1	30	9±1	34±2
20:1 PC	57±2	24±1	33	9±1	33±2
22:1 PC	58±1	25±1	36	8±2	34±1

D **ΔP-TMS**

	α-helix (%)	α-helix, no. of residues	Hydrophobic thickness (Å)	Sheet (%)	Random coil (%)
14:1 PC	57±1	24±1	23	7±1	36±1
16:1 PC	57±1	24±1	26	7±1	36±1
18:1 PC	57±1	24±1	30	7±1	36±1
20:1 PC	56±2	24±1	33	7±1	37±1
22:1 PC	55±1	24±1	36	7±1	38±1

Table S1. Secondary structural elements in relation to membrane thickness of MS-TMS and mutants. Percentages of secondary structural elements are averages with standard deviations of the three deconvolution programs of CD-Pro based on two independent experiments. The number of residues in the α-helix is calculated from the percentage and the total number of residues in the peptide. In the case of a regular α-helix one residue corresponds to 1.5 Å α-helix length. The hydrophobic thicknesses are carbonyl-carbonyl distances derived from [9].

4

Cold adaptation of *Bacillus subtilis* by regulation of lipid composition

Joost Ballering, Thomas E. Rijpma, Antoine Deschamps, Ineke Kool, Larisa E. Cybulski and J. Antoinette Killian

Abstract

Several regulation systems are involved in membrane fluidity maintenance of *Bacillus subtilis*. Two well-known fluidity regulatory mechanisms are the iso-anteiso switch of branched-chain fatty acids and the DesKR two-component system, regulating expression of a desaturase. To investigate the regulation of fluidity in *B. subtilis*, here the fatty acid and head group composition of membranes of *B. subtilis* grown at relevant conditions was analyzed. At a growth temperature of 25 °C more anteiso branched fatty acids were observed than at a growth temperature of 37 °C, consistent with the expected effect of the iso-anteiso switch. Within hours after a cold shock from 37 °C to 25 °C, unsaturated acyl chains were detected, showing the effect of the DesK fluidity regulation mechanism. For the head groups non-systematic differences in composition were observed between individual samples and there was no clear effect of regulation. However, differential scanning experiments on membrane lipid extracts of *B. subtilis* cultures grown under different conditions all showed a transition temperature of ~10 °C below the growth temperature. To gain more insight into the mechanism of regulation by the thermosensor DesK, the extracted *B. subtilis* lipids were next used in model membrane studies with an incorporated synthetic peptide corresponding to the transmembrane segment of MS-DesK. The behavior of the peptide in these model systems was studied with circular dichroism and tryptophan fluorescence spectroscopy. Rather surprisingly, the results indicate the absence of a switch from the active to the inactive conformation and vice versa upon phase transition of the lipids. These results imply that the *B. subtilis* lipids may stabilize both the active and the inactive conformation, and that the energetic barrier for switching from one state to the other may be relatively high in these more native-like membrane systems.

Introduction

Surviving the cold is a clear necessity for countless species, since most habitats are subject to substantial daily temperature fluctuations. Unlike larger organisms, microorganisms are unable to maintain a constant cytoplasmic temperature. Therefore specific adaptations have evolved to cope with temperature fluctuations. Some species can form endospores to survive harsh conditions. However, endospore formation is a long-term process, which can take from several hours up to few days, depending on the conditions [1, 2]. Therefore bacteria have complementary mechanisms to adapt to cold-induced problems on a shorter timescale. Immediate cold leads to problems at the level of proteins, DNA and RNA, such as increase of the super helical density of the DNA, decreased ribosomal and enzyme activity, inefficient protein folding and stabilization of secondary structures of mRNA. These problems are dealt with by expression of cold-induced stabilizing proteins [3, 4]. In addition, changes in temperature will affect properties of membranes with potentially dramatic consequences. Therefore the composition of the membrane must be extensively regulated [5, 6].

An important bacterial membrane property that is regulated is membrane fluidity, because reduced membrane fluidity compromises membrane protein activity [7, 8]. The fluidity of bacterial membranes can drop significantly mainly as a result of the temperature-dependent lipid phase transition from a liquid-crystalline state to a more rigid gel-like state. Recovery of membrane fluidity requires adaptation of the lipid composition, which can be achieved by alteration of the lipid head groups or acyl chains [9, 10]. The adjustment of membrane fluidity is mainly achieved by the incorporation of fatty acids of lower melting points. Lipid head groups are less affected, possibly because of the consequences for membrane charge and curvature [11-13]. As illustrated in Figure 1, the bacteria generally use three types of acyl chain modifications: shortening, branching or unsaturation. Since both shortening and branching of acyl chain require *de novo* fatty acid synthesis, unsaturation is the short-term alternative for membrane fluidity maintenance [4, 10].

Bacillus subtilis, a widely distributed soil bacterium is genetically easily accessible and is generally accepted as a model organism for gram-positive bacteria and is widely used in industry [15, 16]. This bacterium has a distinct membrane lipid profile, with a significantly variable composition under different conditions [6, 17-24]. *B. subtilis* maintains its membrane fluidity on a longer timescale by varying the incorporation of branched-chain fatty acids [21]. The biosynthesis pathway of fatty acids determines the straight/branched-chain character of the lipid acyl chains [25]. *B. subtilis* produces mainly branched-chain fatty acids owing to the specificity of the fatty acid synthase system, which is responsible for the production of fatty acid structures [26]. Initiation of the fatty acid elongation cycle by acetyl-CoA derived from intermediary metabolism results in straight chain fatty acids. However, in *B. subtilis* the elongation cycle is preferentially initiated using bulkier substrates derived from valine, leucine and isoleucine precursors, which results in iso-branched and

anteiso-branched fatty acids [27]. Temperature-dependent specificity of this system is likely to be a key factor to membrane fluidity maintenance through this pathway [28]. Next to this long-term adaptation, *B. subtilis* has an immediate response to decreased membrane fluidity by desaturation of existing membrane lipids. Desaturation is performed by a Δ5-desaturase [29] that is expressed under the control of the DesKR two component system [30-33]. DesK is the thermosensor of this system, and it is able to detect a temperature decrease through corresponding changes in biophysical properties of the lipid environment.

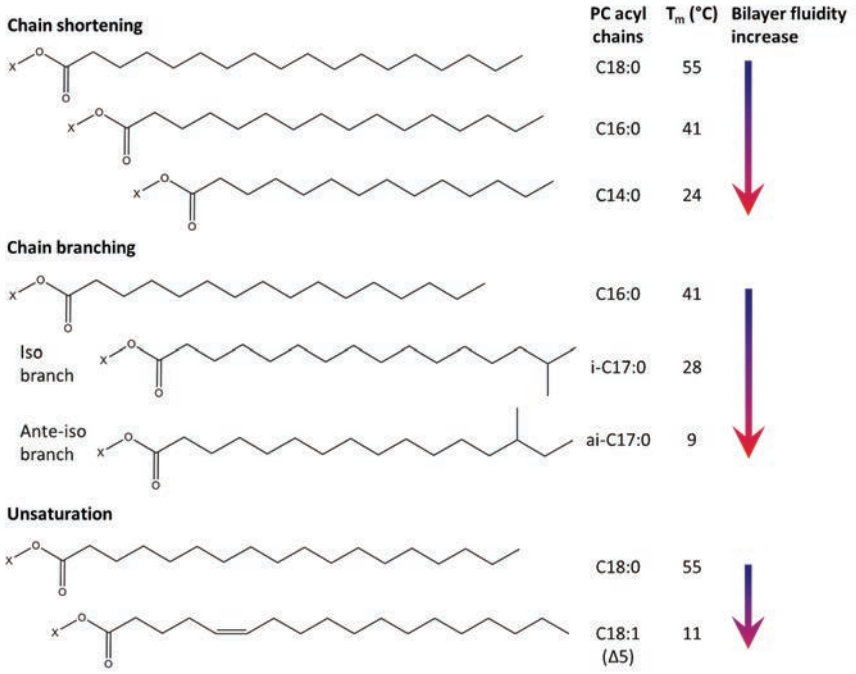

Figure 1. Bacterial acyl chain modifications that influence bilayer fluidity. To compare the influence of these modifications on the membrane fluidity, transition temperatures (T_m) are given for the phosphatidylcholines with symmetrical acyl chains. Values are derived from Marsh [14].

Here we focus on the mechanism of thermo-sensing of DesK. Changes in the physical properties of the membrane lipids are directly responsible for activation of DesK [33, chapter 3]. Therefore the lipid composition of the membrane and temperature-dependent variations therein are crucial to understanding the activation mechanism of DesK. To investigate the role of DesK in membrane fluidity regulation, here we analyzed the membrane lipids of *B. subtilis* grown at optimal (37 °C) and cold (25 °C) temperatures as well as several hours after cold shock (instant cooling from 37 °C to 25 °C). Changes in lipid composition were characterized with gas chromatography, thin-layer chromatography and differential scanning calorimetry. Furthermore the *B. subtilis* lipids grown at 37 °C and 25 °C were used in model membrane systems with an MS-DesK-derived transmembrane peptide. These model systems were studied with circular dichroism and Trp-fluorescence to investigate conformational changes of MS-DesK in its native lipid environment. The results will be discussed in the light of the fluidity regulation and how the model systems compare to the *in vivo* situation.

Results & Discussion

When *Bacillus subtilis* experiences cold shock, membrane fluidity is maintained by altering the membrane lipid fatty acid profile. Various cold adaptations can occur that cause the membrane fluidity to increase and hence the transition temperature (T_m) of the membrane lipids to decrease. To investigate these time dependent effects of cold adaptation, membrane lipids were extracted from *B. subtilis* with different culturing temperatures (T_c). The cultures were either grown at both 37 °C and 25 °C, or they were grown at 37 °C and submitted to a cold shock by cooling instantly to 25 °C, subsequently growing further at this temperature for 1, 2 or 3 hours. These lipid extracts were analyzed with gas chromatography (GC), thin-layer chromatography (TLC) and differential scanning calorimetry (DSC).

Figure 2A shows the fatty acid profile of the lipid extracts from *B. subtilis* cultures grown at 37 °C and 25 °C as determined by GC. At T_c = 37 °C, the main fatty acids are iso- and anteiso branched species with 15-17 carbon atoms. Next to the branched fatty acids, small amounts of straight chain fatty acids with 12-18 carbon atoms are present. This profile is in agreement with published data [6, 17-24]. At T_c = 25 °C, an increased amount of anteiso-branched fatty acids is observed, whereas the amount of iso branched fatty acids is reduced. Figure 2B shows the time-dependent changes in branching pattern of the fatty acids. After cold shock, over time, more anteiso-branched acyl chains are incorporated at the expense of iso-branched acyl chains, whereas the amount of straight chains remains unaffected. A substantial shift of branching acyl chains is required for the bacteria to adapt from a T_c = 37 °C to T_c = 25 °C. After three hours ~¼ of the total shift has occurred, indicating that the replacement of the acyl chains is a longer-term process. Figure 2C shows the time-dependent change in unsaturation of the fatty acids. Small amounts of unsaturated acyl chains can be detected upon cold shock and in several batches at T_c = 25 °C, but not at T_c = 37 °C (Fig. 2C). The unsaturation of the acyl chains within three hours of cold shock can be as much as twice the amount observed at T_c = 25 °C. These findings indicate that the DesKR-controlled desaturase of *B. subtilis* acts immediately upon cold shock. In the longer term, when DesKR is switched off, the unsaturated acyl chains are no longer synthesized and will decrease over time.

The lipid-head group composition at T_c = 25 °C and T_c = 37 was examined by thin-layer chromatography. The results of four independent experiments with lipid extracts of *B. subtilis* at these culturing temperatures are shown in Figure 3. The main constituents were assigned as cardiolipin, phosphatidylethanolamine (PE), phosphatidylglycerol (PG), lysyl-phosphatidylglycerol (lysyl-PG) and phosphatidic acid (PA). These lipids are also observed in earlier published data [6, 17-24]. However, relatively large quantitative fluctuations are found between the experiments. Especially the amount of PA and lysyl-PG differs significantly, and smaller fluctuations in the amount of PG and PE are observed as well. Unfortunately, these fluctuations in the head group composition make it difficult to detect systematic changes owing to

temperature dependent regulation. Therefore we next explored whether regulation of fluidity occurs by investigating the melting behavior of the lipid extracts of cultures grown at 37 °C and 25 °C.

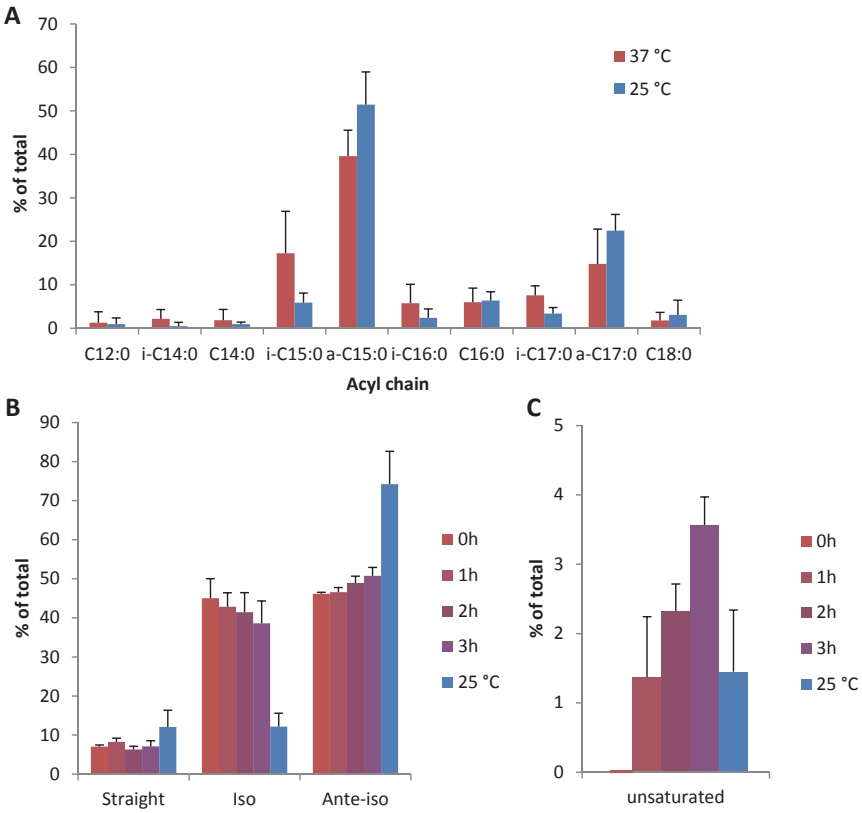

Figure 2. Growth temperature dependent lipid acyl chain composition of *B. subtilis*. A) Acyl chain composition of *B. subtilis* lipids grown at 25 °C or 37 °C. B) Acyl chain branching and C) unsaturation of *B. subtilis* extracts under various growth conditions. *B. subtilis* was grown at 37 °C, submitted to a cold shock by cooling instantly to 25 °C and further grown at this temperature for 0, 1, 2 or 3 hours. The fatty acid profile under these conditions is compared to the lipid extract from *B. subtilis* grown at 25 °C (blue). The values are averages of at least two independent experiments.

The melting behavior of the extracted lipids was investigated by using differential scanning calorimetry. Despite the considerable variations in lipid composition, the lipid extracts show consistent phase behavior. Figure 4 shows the thermograms of representative lipid samples derived from cultures grown at 37 °C and 25 °C. Both samples show a broad transition with the average T_m ~10 °C below the growth temperature (Table 1), clearly showing that the membrane fluidity of these samples is actively regulated. Such regulation was also observed for other bacteria including *E. coli* [5, 7].

Growth temperature	Transition temperature
37 °C	25.3 ± 0.8
25 °C	15.0 ± 1.9

Table 1. Average transition temperatures of *B. subtilis* lipids grown at 25 °C or 37 °C as determined from four independent measurements, of which the maximum heat capacity is determined as the transition temperature.

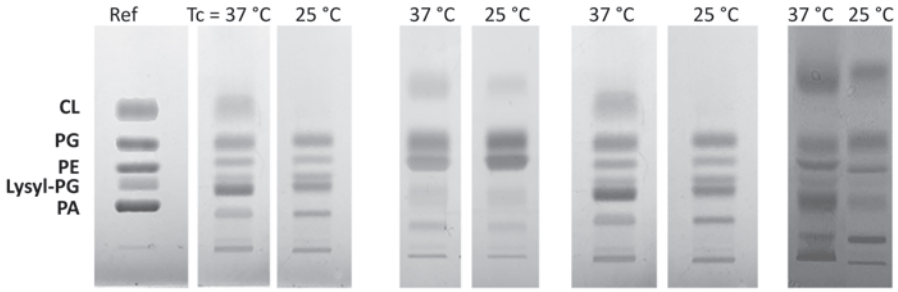

Figure 3. Thin-layer chromatograms of four independent experiments with lipid extracts of *B. subtilis* grown at 25 °C and 37 °C. The reference lipids of the first experiment are included.

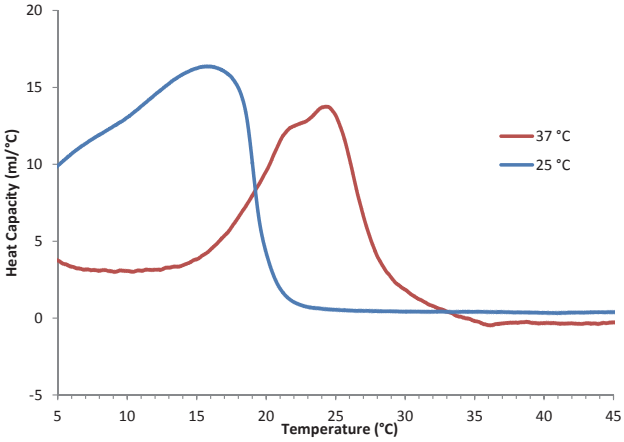

Figure 4. Thermogram of lipid extracts from *B. subtilis*, grown at 25 °C and 37 °C. Representative set of four independent measurements.

Next these lipids were used in model membrane systems with synthetic peptides, which proved to be a successful tool to study the temperature sensing mechanism of DesK [33, chapter 3]. To this end the MS-DesK derived transmembrane peptide MS-TMS was incorporated in vesicles consisting of the native *B. subtilis* lipids from cultures grown at 37 °C or 25 °C. The CD spectra from these two model membrane systems were recorded at several temperatures above and below T_m (Fig. 5A, B). All spectral shapes show mainly α-helical character for the peptide. Interestingly, the shape of the spectrum is clearly dependent on the culturing temperature, with a significantly lower ellipticity ratio for the model system with T_c = 25 °C as compared to T_c = 37 °C (Fig. 5C). When this trend is compared to the behavior of MS-TMS in DPPC lipids, the conformation of MS-TMS in lipids grown at 25 °C corresponds to the kinase active structure, and the conformation of MS-TMS in lipids grown at 37 °C corresponds to the kinase inactive structure. Furthermore, for both model membrane systems the shape of the spectrum is independent of temperature, indicating no change of secondary structure for MS-TMS upon going through the fluid-to-gel transition. Therefore the native *B. subtilis* lipids seem to force the peptide in either the kinase-on or the kinase-off structure. These findings clearly differ from the results with synthetic lipid systems [chapter 3], and therefore complementary experiments were performed using fluorescence spectroscopy to monitor corresponding changes in environment of the Trp residues.

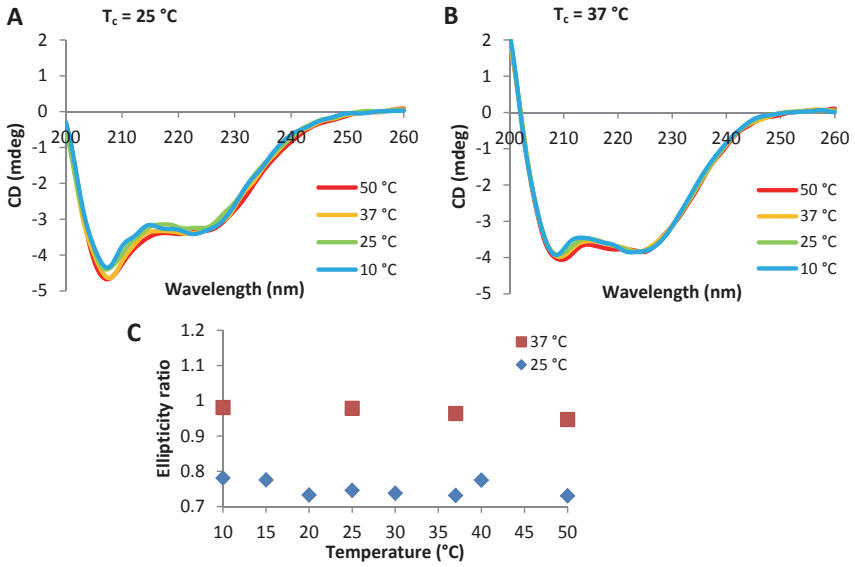

Figure 5. Circular dichroism analysis of two model membrane systems with MS-DesK-derived transmembrane peptide (MS-TMS) in *B. subtilis* lipids grown at 25 °C (T_c = 25 °C) or 37 °C (T_c = 37 °C), with the spectra of model membrane system with (A) T_c = 25 °C lipids or (B) T_c = 37 °C lipids at temperatures around the phase transition and (C) the ellipticity ratios of the two model systems plotted versus temperature.

Figure 6 shows the results of the fluorescence experiments. The spectra, represented in Figure 6A and B, show emission maxima below 450 nm, characteristic for a peptide incorporated in the membrane. The somewhat increased spectral width for T_c = 37 °C could indicate a slight aggregation of the peptide. Comparison of the emission maxima of the two model systems (Fig. 6C) shows a more hydrophobic environment for MS-TMS in T_c = 25 °C lipids as compared to T_c = 37 °C lipids. However, the emission maxima show no significant temperature dependence. This result indicates no change in hydrophobicity of the MS-TMS environment upon the fluid-to-gel transition, therefore no change in conformational state of the peptide, consistent with the CD results.

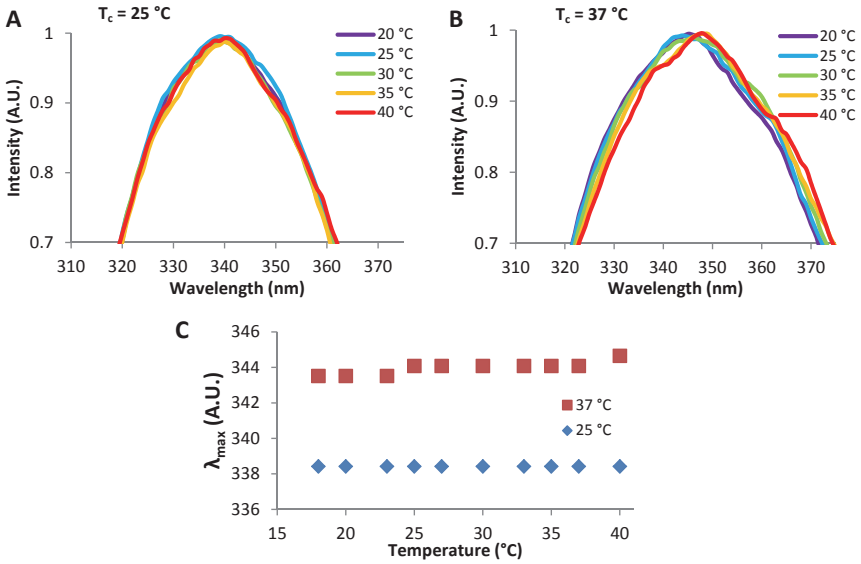

Figure 6. Trp-fluorescence analysis of two model membrane systems with MS-DesK derived transmembrane peptide (MS-TMS) in *B. subtilis* lipids grown at 25 °C (T_c = 25 °C) or 37 °C (T_c = 37 °C), with the spectra of model membrane system with (A) T_c = 25 °C lipids or (B) T_c = 37 °C lipids at temperatures around the phase transition and (C) the emission maxima of the two model systems plotted versus temperature.

Why would the conformational switch, observed previously upon fluid-to-gel transition of the membrane [chapter 3] not occur in the native *B. subtilis* lipids? Since the membrane composition of the model systems used here is closer to the *in vivo* situation, there is no obvious explanation. We note however that the acyl chain composition is very different than in the model systems of synthetic lipids. A possible explanation may be that the presence of branched side chains increases the energetic barrier for reorientation of the helices. *In vivo* the energetics of this barrier may be slightly different and thereby perhaps easier to overcome. For example, the attached cytosolic domain could lower the energetic barrier of the switch by stabilizing the linker region. Alternatively, the presence of many other proteins in the lipid bilayer could affect properties of the membrane, thereby lowering the barrier for reorientation.

Perspectives

Here we showed that *B. subtilis* regulates the membrane lipid acyl chain composition in a temperature-dependent fashion, indicating that the fluidity of the membrane is maintained. For the head group composition large variations were observed between different batches, but no significant temperature dependence was found. This observation would be consistent with the idea that remodeling the head group composition would be a less favorable way of adjusting to temperature composition, because it would also affect other, temperature-independent membrane properties. For example, the composition of the lipid head groups of cell membranes is known to affect the charge and curvature of the membrane. These properties are crucial for correct membrane-protein topology [34, 35] and they are maintained via biochemical regulation of the regulatory enzymes within a window that ensures proper flexibility of the membrane and correct folding of membrane proteins [36]. Our results show the flexibility of the head group composition, but it is not clear which are the underlying properties for the regulation mechanisms of charge and curvature maintenance. To further investigate these mechanisms, more advanced quantitative lipidomics would be required as well as biophysical studies on model systems, and this is beyond the topic of this research.

Nevertheless, the lipid extracts of *B. subtilis*, which contain a large amount of branched-chain fatty acids, were useful to investigate the effects of temperature and growth temperature on the mechanism of sensing and signal transduction of MS-DesK. Surprisingly, these *B. subtilis* lipids failed to induce the temperature dependent conformational switch in the transmembrane segment of MS-DesK, which was found in other lipids [33, chapter 3]. To further investigate the influence of branched-chain fatty acids on the transmembrane segment of MS-DesK it is possible to use synthetic lipids. However, iso- and anteiso-branched lipids are unavailable commercially and should therefore be synthesized. Another possibility is the incorporation of full-length MS-DesK into the native *B. subtilis* lipids. However the biochemical and biophysical analysis of such model system would be highly challenging owing to the increased size of the protein. Solid state NMR on labeled full-length MS-DesK could then be an attractive method to obtain detailed information on structural changes at different temperatures.

Materials & Methods

Materials

All chemicals and enzymes were purchased from Sigma-Aldrich unless otherwise indicated. The reference lipids were obtained from Avanti Polar Lipids (Alabaster, AL). Te synthetic peptide was obtained from Eurogentec (Seraing, Belgium) as a > 95% pure peptide. The amino acid sequence of the peptide is: MIKNHFTFQK LNGITPYVIT LISAILLPWS IKSRKERERL EEK. Identity and purity were confirmed with mass spectrometry and analytical HPLC. Water was deionized and purified with a Milli-Q gradient water purification system from Millipore Corp. (Billerica, MA). All chemicals used were analytical grade.

Strains and growth conditions

B. subtilis JH642 strains were grown until mid-log phase (OD_{600} = 0.7) at 25 °C and 37 °C with 250 r.p.m. gyration in Spizizen salts supplemented with 0.57% glycerol, 100 μg/ml each tryptophan and phenylalanine, 0.05% cas amino acids and trace elements [37, 38]. Cooling of the cultures from 37 °C to 25 °C was achieved by applying running water for 5 minutes. These cultures were grown further for 1, 2 or 3 hours at 25 °C. Cells were harvested by centrifugation and lysed by lysozyme treatment. Four independent cultures at 25 °C and 37 °C were obtained and the cold shock experiments were performed in duplicate.

Lipid extraction and analysis

Total cellular lipids were chloroform/methanol extracted [39, 40]. The phase transition of the total lipid extract was measured by differential scanning calorimetry. The lipids were lyophilized and redispersed in 50 mM TRIS pH 7.4, 1mM EDTA. For all analysis methods lipid concentrations were determined by a phosphorus titration according to the method of Rouser [41]. The acyl chain composition of the total lipid extract was characterized by gas chromatography (GC). Isolated lipids were transesterified in 2.5% (vol/vol) H_2SO_4 in methanol for 2 h at 70 °C. Fatty acid methyl esters were extracted by three washing steps with hexane. Analysis was performed with a Trace GC ultra (Interscience, Louvain-la-Neuve, Belgium) using a 30 m, 0,32 mm i.d., 0,25 μm f.t. Stabilwax column (Restek, Bellefonte, PA) and a temperature gradient from 180 °C to 220 °C. Peaks were assigned by calibration with the standard "Bacterial Acid Methyl Ester Mix" (Sigma-Aldrich). The Δ5 unsaturated lipids were assigned by determining the peak shift caused by mono unsaturation in the standard GLC 63b (Nu-Chek Prep). The lipid head group composition of the total lipid extract was characterized by thin-layer chromatography. Lipids were applied using a Linomat 5 setup (CAMAG, Muttenz, Switzerland) on Nano-ADAMANT plates (Macherey-Nagel), impregnated with 1.2% (wt/vol) boric acid in

ethanol:water (1:1) and dried for 1.5 h at 160 °C. The plates were developed in an automated development chamber (ACD 2; CAMAG, Muttenz, Switzerland) at 50% relative humidity, using a solvent mixture of chloroform:methanol:water:ammonia [60:38:3:1 (vol/vol/vol/vol)]. Chromatograms were exposed to iodine vapor and sprayed with ninhydrin to localize the lipids and the amino-positive lipids. The phospholipids were assigned with the appropriate standards.

Differential scanning calorimetry

Calorimetry was performed on a Q2000 differential scanning calorimeter (TA Instruments, New Castle, DE) with a scan speed of 0.5 °C/min. For equilibration a scan was performed and thereafter the sample was kept at 0 °C for 30 min. A linear baseline was substracted to obtain the final thermogram.

Model membrane system experiments

Samples were prepared as previously described [33]. Briefly, peptides (15 μM), dissolved in 0.5 mL trifluoroethanol were added to 0.5 mL of the desired phospholipid dispersion at temperatures around the growth temperature of the culture from which the lipids were extracted. A final molar peptide/lipid ratio of 1/50 was acquired with the lipid concentrations determined by a phosphorus titration according to the method of Rouser [41]. Excess water was added and subsequently the samples were lyophilized after rapid freezing in liquid nitrogen. Vesicles were prepared by rehydrating the dry film in buffer at temperatures around the growth temperature of the culture from which the lipids were extracted. For the fluorescence experiments [10 mM PIPES, 150 mM NaCl, 1 mM EDTA (pH 7.4)] buffer was used and for circular dichroism measurements [10 mM Phosphate, 10 mM NaCl (pH 7.4)] buffer was used. After 10 freeze–thawing cycles, the vesicles were extruded with a hand-held extrusion device (Avanti, Alabaster, AL) passing a 0.2 μm filter at least 10 times. The final peptide concentrations in these samples were quantified by their absorbance at 280 nm, using the molar extinction coefficient of Trp [42]. The final yield was ~85%.

Circular dichroism measurements

Measurements were carried out on a JASCO J-810 spectropolarimeter (Jasco Inc., Easton, MD), using a 1 mm path length quartz cuvette, 1 nm bandwidth, 0.2 nm resolution, 4 s response time, and a scan speed of 10 nm/min. Temperature was controlled with a Peltier device. For each measurement 10 scans were recorded over a wavelength range of 200 – 260 nm. These spectra were averaged and normalized to molar ellipticity per residue.

Fluorescence measurements

Tryptophan fluorescence was measured on a Varian Cary Eclipse fluorescence spectrophotometer, using a 10 mm quartz cuvette, 5 mm excitation slit, 5.0 mm emission slit, 0.5 nm resolution, 1 s averaging time, and a scan speed of 30 nm/min. Temperature was controlled with a Peltier device. The tryptophan residues were excited at 295 nm, and the emission in the 300-500 nm region was recorded. The contribution of pure lipid samples was subtracted from the obtained signal. Because optical densities of the samples were below 0.05, correction for the inner filter effect was unnecessary [43]. The recorded spectra were fitted to a Log-normal distribution as described in [44], normalized and smoothed using a moving average filter with a window size of 5.

References

[1] Fritze D (2004) Taxonomy of the genus bacillus and related genera: The aerobic endospore-forming bacteria. *Phytopathology* 94(11): 1245-1248.

[2] McKenney PT, Driks A & Eichenberger P (2013) The *bacillus subtilis* endospore: Assembly and functions of the multilayered coat. *Nat Rev Microbiol* 11(1): 33-44.

[3] Graumann PL & Marahiel MA (1999) Cold shock response in *bacillus subtilis*. *J Mol Microbiol Biotechnol* 1(2): 203-209.

[4] Weber MH & Marahiel MA (2002) Coping with the cold: The cold shock response in the gram-positive soil bacterium *bacillus subtilis*. *Philos Trans R Soc Lond B Biol Sci* 357(1423): 895-907.

[5] Sinensky M (1974) Homeoviscous adaptation--a homeostatic process that regulates the viscosity of membrane lipids in *escherichia coli*. *Proc Natl Acad Sci U S A* 71(2): 522-525.

[6] Van de Vossenberg JLCM, Driessen AJM, da Costa MS & Konings WN (1999) Homeostasis of the membrane proton permeability in *bacillus subtilis* grown at different temperatures. *Biochimica Et Biophysica Acta (BBA) - Biomembranes* 1419(1): 97-104.

[7] Suutari M & Laakso S (1994) Microbial fatty acids and thermal adaptation. *Crit Rev Microbiol* 20(4): 285-328.

[8] de Mendoza D (2014) Temperature sensing by membranes. *Annu Rev Microbiol* 68: 101-116.

[9] Dowhan W (1997) Molecular basis for membrane phospholipid diversity: Why are there so many lipids? *Annu Rev Biochem* 66: 199-232.

[10] Zhang YM & Rock CO (2008) Membrane lipid homeostasis in bacteria. *Nat Rev Microbiol* 6(3): 222-233.

[11] Grau R & de Mendoza D (1993) Regulation of the synthesis of unsaturated fatty acids by growth temperature in *bacillus subtilis*. *Mol Microbiol* 8(3): 535-542.

[12] Shaw MK & Ingraham JL (1965) Fatty acid composition of *escherichia coli* as a possible controlling factor of the minimal growth temperature. *J Bacteriol* 90(1): 141-146.

[13] Svobodova J, Julak J, Pilar J & Svoboda P (1988) Membrane fluidity in *bacillus subtilis*; validity of homeoviscous adaptation. *Folia Microbiol (Praha)* 33(3): 170-177.

[14] Marsh D (2013) Handbook of lipid bilayers (CRC Press, Boca Raton)

[15] Schallmey M, Singh A & Ward OP (2004) Developments in the use of bacillus species for industrial production. *Can J Microbiol* 50(1): 1-17.

[16] Harwood CR (2013) Bacillus (Springer, New York)

[17] Bishop DG, Rutberg L & Samuelsson B (1967) The chemical composition of the cytoplasmic membrane of *bacillus subtilis*. *Eur J Biochem* 2(4): 448-453.

[18] Op den Kamp JA, Redai I & van Deenen LL (1969) Phospholipid composition of *bacillus subtilis*. *J Bacteriol* 99(1): 298-303.

[19] Minnikin DE, Abdolrahimzadeh H & Baddiley J (1972) Variation of polar lipid composition of *bacillus subtilis* (marburg) with different growth conditions. *FEBS Lett* 27(1): 16-18.

[20] Svobodova J, Julak J, Pilar J & Svoboda P (1988) Membrane fluidity in *bacillus subtilis*. validity of homeoviscous adaptation. *Folia Microbiol (Praha)* 33(3): 170-177.

[21] Suutari M & Laakso S (1992) Unsaturated and branched chain-fatty acids in temperature adaptation of *bacillus subtilis* and bacillus megaterium. *Biochim Biophys Acta* 1126(2): 119-124.

[22] Klein W, Weber MH & Marahiel MA (1999) Cold shock response of *bacillus subtilis*: Isoleucine-dependent switch in the fatty acid branching pattern for membrane adaptation to low temperatures. *J Bacteriol* 181(17): 5341-5349.

[23] Altabe SG, Aguilar P, Caballero GM & de Mendoza D (2003) The *bacillus subtilis* acyl lipid desaturase is a delta5 desaturase. *J Bacteriol* 185(10): 3228-3231.

[24] Gidden J, Denson J, Liyanage R, Ivey DM & Lay JO (2009) Lipid compositions in *escherichia coli* and *bacillus subtilis* during growth as determined by MALDI-TOF and TOF/TOF mass spectrometry. *Int J Mass Spectrom* 283(1-3): 178-184.

[25] Choi KH, Heath RJ & Rock CO (2000) Beta-ketoacyl-acyl carrier protein synthase III (FabH) is a determining factor in branched-chain fatty acid biosynthesis. *J Bacteriol* 182(2): 365-370.
[26] Schujman GE & de Mendoza D (2008) Regulation of type II fatty acid synthase in gram-positive bacteria. *Curr Opin Microbiol* 11(2): 148-152.
[27] Parsons JB & Rock CO (2013) Bacterial lipids: Metabolism and membrane homeostasis. *Prog Lipid Res* 52(3): 249-276.
[28] Beranova J, Jemiola-Rzeminska M, Elhottova D, Strzalka K & Konopasek I (2008) Metabolic control of the membrane fluidity in *bacillus subtilis* during cold adaptation. *Biochim Biophys Acta* 1778(2): 445-453.
[29] Altabe SG, Aguilar P, Caballero GM & de Mendoza D (2003) The *bacillus subtilis* acyl lipid desaturase is a delta5 desaturase. *J Bacteriol* 185(10): 3228-3231.
[30] Aguilar PS, Hernandez-Arriaga AM, Cybulski LE, Erazo AC & de Mendoza D (2001) Molecular basis of thermosensing: A two-component signal transduction thermometer in *bacillus subtilis*. *Embo J* 20(7): 1681-1691.
[31] Gao R & Stock AM (2009) Biological insights from structures of two-component proteins. *Annu Rev Microbiol* 63: 133-154.
[32] Albanesi D, et al (2009) Structural plasticity and catalysis regulation of a thermosensor histidine kinase. *Proc Natl AcadSci U S A* 106(38): 16185-16190.
[33] Cybulski LE, et al (2015) Activation of the bacterial thermosensor DesK involves a serine zipper dimerization motif that is modulated by bilayer thickness. *Proc Natl Acad Sci U S A* 112(20): 6353-6358.
[34] Zhang W, Campbell HA, King SC & Dowhan W (2005) Phospholipids as determinants of membrane protein topology. phosphatidylethanolamine is required for the proper topological organization of the gamma-aminobutyric acid permease (GabP) of *escherichia coli*. *J Biol Chem* 280(28): 26032-26038.
[35] Xie J, Bogdanov M, Heacock P & Dowhan W (2006) Phosphatidylethanolamine and monoglucosyldiacylglycerol are interchangeable in supporting topogenesis and function of the polytopic membrane protein lactose permease. *J Biol Chem* 281(28): 19172-19178.
[36] Dowhan W (1997) Molecular basis for membrane phospholipid diversity: Why are there so many lipids? *Annu Rev Biochem* 66: 199-232.
[37] Spizizen J (1958) Transformation of biochemically deficient strains of *bacillus subtilis* by deoxyribonucleate. *Proc Natl Acad Sci U S A* 44(10): 1072-1078.
[38] Harwood CR & Cutting SM (1991) Molecular biological methods for Bacillus. (Wiley, Chichester).
[39] Bligh EG & Dyer WJ (1959) A rapid method of total lipid extraction and purification. *Can J Biochem Physiol* 37(8): 911–917.
[40] Dörr JM, et al (2014) Detergent-free isolation, characterization, and functional reconstitution of a tetrameric K+ channel: The power of native nanodiscs. *Proc Natl Acad Sci U S A* 111(52): 18607-18612.
[41] Rouser G, Fleischer S & Yamamoto A (1970) Two dimensional thin layer chromatographic separation of polar lipids and determination of phospholipids by phosphorus analysis of spots. *Lipids* 5(5): 494-496.
[42] Pace CN, Vajdos F, Fee L, Grimsley G & Gray T (1995) How to measure and predict the molar absorption coefficient of a protein. *Protein Sci* 4(11): 2411-2423.
[43] Lackowicz JR (2006) Principles of fluorescence spectroscopy (Springer, New York).
[44] Ladokhin AS, Jayasinghe S & White SH (2000) How to measure and analyze tryptophan fluorescence in membranes properly, and why bother? *Anal Biochem* 285(2): 235-245.

5

Exploring the use of a styrene-maleic acid polymer to determine the oligomerization state of MS-DesK

Joost Ballering, Mariëtte E. van Eck, Larisa E. Cybulski, Jonas M. Dörr, Martijn C. Koorengevel, Stefan Scheidelaar and J. Antoinette Killian

Abstract

The oligomerization state of the transmembrane segments of sensory proteins is often crucial for their mechanism of sensing and signal transduction. Here, to develop new, relatively simple experimental approaches to determine the oligomerization state within the membrane, we investigated the use of a styrene-maleic acid polymer (SMA), which spontaneously solubilizes membranes into nanodiscs. Two approaches using these nanodiscs including synthetic peptides of the transmembrane segments of interest were explored. In the first approach, the oligomerization state of the peptides is investigated by determination of the peptide/lipid ratio within purified nanodiscs. In the second approach, the oligomerization state is fixed by chemical cross-linking of the peptides within nanodiscs. The results show that both of these approaches are promising tools for the characterization of oligomerization states. However, both methods require further optimization.

Introduction

DesK is a membrane-embedded thermosensor protein that is involved in maintaining membrane fluidity when environmental temperature decreases [1-4]. Recently, a simplified version of DesK, the minimal sensor DesK (MS-DesK), was created, in which five original transmembrane helices are replaced by a single transmembrane segment, facilitating studies on the influence of the lipid environment on the activation mechanism of the sensor. MS-DesK was found to be fully functional and the temperature sensitivity proved to be dependent on the length and composition of its transmembrane segment [4, 5]. The results indicated a mechanism of sensing, in which a temperature decrease leads to changes in the physical properties of the lipid environment, which allows for switching of the sensor from the off-state (phosphatase state) to the on-state (kinase state).

Based on the crystal structure of the intracellular domain of DesK, molecular dynamics simulations and biophysical experiments a model was proposed for the activation mechanism of MS-DesK [3, 4]. In this model MS-DesK functions as a dimer and a change in physical properties of the membrane results in reorientation of the transmembrane segments to form an alternative dimerization interface. Since no direct evidence exists for the dimerization of the transmembrane segment, we here aimed to investigate the oligomerization state experimentally. To this end the use of a styrene-maleic acid polymer (SMA) was explored.

When SMA is added to membranes, this amphipathic polymer cuts out disc-like structures with a diameter in the order of 10 nm. The hydrophobic part of the lipids in these nanodiscs is protected from the aqueous environment by the SMA polymer [6]. Furthermore, this polymer can be used to extract membrane proteins from cell membranes. When SMA is added to biological membranes, so-called "native nanodiscs" will form, containing these proteins in their native lipid environment [7, 8]. These nanodiscs could provide valuable information on the oligomerization state of the embedded proteins, because it is expected that not only protein-lipid interactions would be conserved but also protein-protein interactions, and hence, that oligomers would be conserved in their native state [8]. Here we explored two complimentary approaches, both based on the SMA technology, to investigate the oligomerization state of the transmembrane segment of MS-DesK.

The first approach comprises the determination of the peptide/lipid ratio within nanodiscs by chemical analysis. This approach was explored using model membrane systems containing a His-tagged model peptide, which was solubilized by addition of SMA and purified by nickel-affinity chromatography. Based on the assumption that the formation of 10 nm sized discs will result in particles that contain about 140 lipids [9], determination of the peptide/lipid ratio of purified, peptide-containing discs would reveal whether the peptide is present in these discs as monomer or as oligomer. Variation of the initial peptide/lipid ratio would then allow for further characterization and validation of the oligomerization behavior.

The second approach is based on determination of the oligomeric state of peptides or proteins in the nanodiscs by chemical cross-linking and gel-electrophoresis, which is a widely used method to examine protein-protein interactions [10]. This latter approach has the advantage that no purification is required. The results showed that, owing to various possible reasons, neither one of these approaches was successful. These reasons will be discussed and improvements will be suggested for both approaches to analyze the oligomeric state of proteins using SMA-based techniques.

Results & Discussion

The intracellular domain of DesK crystallizes as a dimer [3]. Additionally, molecular dynamics simulations predicted that MS-DesK forms a dimer in the hydrophobic core of the membrane [4]. Here we experimentally explored the oligomerization state of the MS-DesK transmembrane segment. Styrene-Maleic Acid (SMA) solubilization of model membrane systems into nanodiscs was used as a tool to study the interactions of transmembrane helices. SMA (Table 1) was selected for solubilization because it has been shown to solubilize membrane proteins in their native oligomerization state [11]. We used two complementary approaches that will be discussed below.

	Name	Structure
Styrene-maleic acid polymer	SMA2000	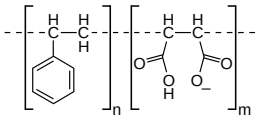
Cross-linker	Dithiobis [succinimidylpropionate]	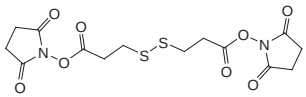

Table 1. Chemical structures of the polymer and the cross-linker used in this study. The specific styrene-maleic acid polymer used in this study is SMA2000, which has a n:m ratio of 2:1 and a Mw of 7.5 kD. The cross-linker is membrane permeable and thiol-cleavable.

Investigation of the MS-DesK oligomerization state by characterization of the peptide/lipid ratio in purified peptide-containing nanodiscs

For the first approach, we hypothesized that the native oligomerization state is retained in the nanodiscs, independent of the initial peptide/lipid ratio. Furthermore, it was observed that lipid containing nanodiscs are constant in size with approximately 140 lipids [6, 9], and we further assume that peptide-containing nanodiscs are similar in size and structure but that some of the lipids are simply replaced by the peptides. In that case, it should be possible to establish the number of peptides per disc by analysis of the peptide/lipid ratio in purified peptide-containing nanodiscs, thus allowing for the determination of the oligomerization state of the peptide.

We decided to first test the proof of principle of this approach using model membrane systems with a His-tagged WALP peptide (His-WALP, Table 2). This has several advantages. First WALP peptides are a family of well-studied model peptides that are not expected to form aggregates [12]. Furthermore it is available with a cleavable His-tag, allowing for purification by using nickel-affinity chromatography, which has proven to be successful in purifying protein-containing nanodiscs [8]. Additionally, it has 4 tryptophan residues, facilitating quantification of the peptide content by UV absorbance at 280 nm.

Peptide	Sequence
MS-TMS	MIKNHFTFQK LNGITPYVIT LISAILLPWS IKSRKERERL EEK
His-WALP	HHHHHHENLY FQGAGAGAGW WLALALALAL ALALALALWW A-NH_2

Table 2. Sequences of the synthetic peptides used in this study. MS-TMS corresponds to the transmembrane region of MS-DesK. His-WALP was synthesized with a TEV cleavable His-tag. The TEV cleavage site is represented in red and the His-tag in blue.

Thus, model membrane systems of dioleoylphosphatidylcholine (DOPC), containing a His-WALP were solubilized with SMA. Free SMA was removed by size exclusion chromatography, because it could interfere with the His-tag binding to the nickel-affinity column. Figure 1A illustrates the separation between the nanodiscs containing His-WALP and some smaller impurities, presumably containing free SMA. Subsequently the fractions containing His-WALP nanodiscs were pooled and subjected to nickel-affinity chromatography. The concentration of His-WALP in each step of the purification was quantified by UV-VIS spectroscopy. As shown in Figure 1B, the His-WALP peptide in DOPC clearly absorbs in the region above 280 nm. Unfortunately most of the His-WALP was observed in the column wash, and only ~4% was retrieved in the elution fraction. This yield was too low for further analysis. As discussed in Dörr et al. [8], one possible explanation is that SMA interferes with the His-tag binding to the nickel affinity column because the negative charges of the SMA chelate the nickel, thereby competing with the His-tag. Alternatively, the His-tag, even though separated from the hydrophobic membrane core by 12 residues, might be unavailable for binding to the nickel because it somehow folds back on the membrane or interacts with the polymer. Because this method of analyzing the peptide oligomerization state relies on purification of intact nanodiscs, the SMA associated to these nanodiscs will always remain in the sample, possibly interfering with the purification. Therefore it may be useful to investigate an alternative purification method, using other tags (Strep tag, FLAG tag, etc.) to separate the peptide. However, also in those systems inhibitory effects on binding might occur. For these reasons we decided to first explore a second approach to determine the oligomerization state of MS-DesK employing SMA.

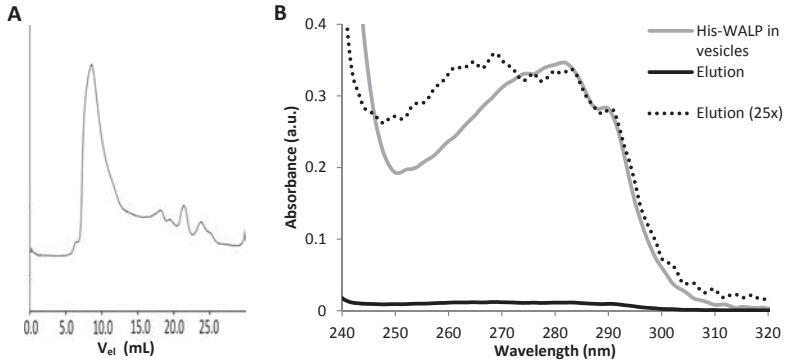

Figure 1. Purification of nanodiscs containing the model peptide His-WALP. A) Size exclusion chromatogram with the nanodiscs eluting from 8 to 12 ml. and smaller impurities, probably containing free SMA eluting from 17 ml. B) Absorption spectra of 20 μM His-WALP in 1 mM DOPC vesicles (gray) and the elution fraction from the nickel affinity purification (black). When the elution fraction is 25 x enlarged (dotted line), it has similar intensity as the His-WALP spectrum, indicating that the elution fraction contains only ~4% of the His-WALP. The remaining His-WALP was observed in the wash steps prior to elution.

Cross-linking within nanodiscs for investigation of MS-DesK oligomerization state

A second approach to investigate the oligomerization state of the MS-DesK transmembrane segment involves chemical cross-linking of the oligomers in model membrane systems. This approach is visualized in Figure 2. When peptides in model membrane systems are subjected to chemical cross-linking, the native oligomers will be covalently attached to each other. However, when using vesicular lipid systems, different oligomers can be cross-linked as well because they diffuse within the vesicles. Solubilizing the model membrane systems with SMA would yield nanodiscs with native oligomers [7, 8] which then can be cross-linked in their native state. Subsequently, these cross-linked systems can be visualized with SDS-PAGE, and from the size of the cross-linked peptides the native oligomerization state can be determined.

For this second approach, dithiobis[succinimidylpropionate] (DSP, Table 1) was selected as a cross-linker. DSP is a primary amine selective cross-linker, which covalently binds peptides via their lysine residues and N-termini. Thus, the introduction of labels, which could interfere with the oligomerization site, is unnecessary. DSP is suitable for cross-linking transmembrane oligomers because it is membrane permeable and its spacer arm length of 1.2 nm is sufficient to bridge typical inter-oligomer distances. For these experiments, it is possible to use the MS-DesK transmembrane segment as used in previous chapters (MS-TMS, table 2), since a His-tag labeling is not necessary for this approach. Furthermore, MS-TMS contains various lysines for cross-linking and they are located at both ends of the peptide.

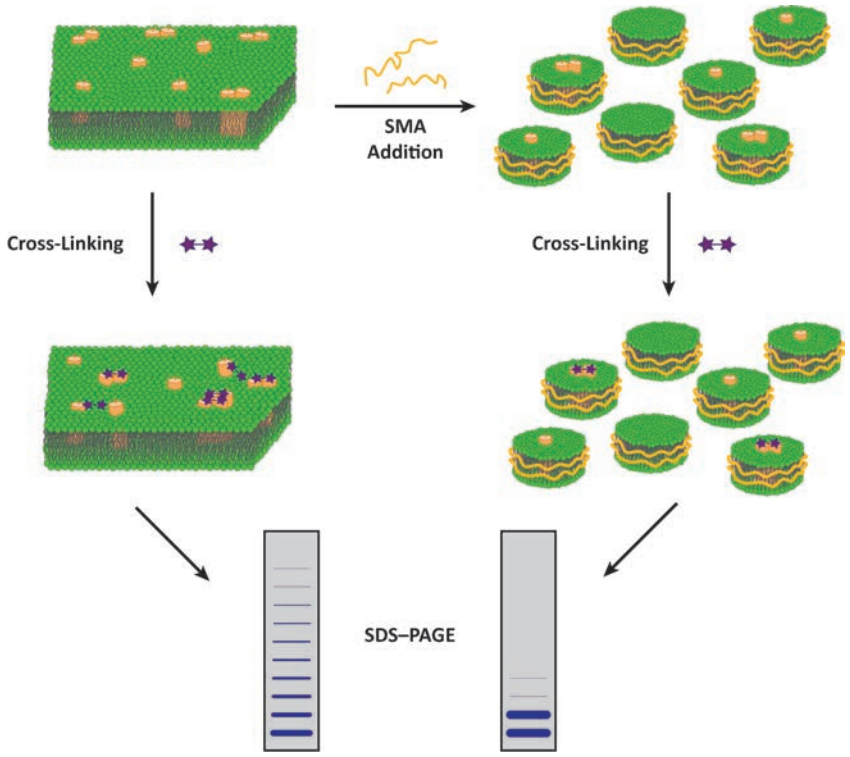

Figure 2. Schematic representation of the cross-linking experiments. Cross-linking in liposomes results in large aggregates because peptides diffuse freely. When liposomes are solubilized with SMA prior to cross-linking, it is hypothesized that only oligomers within nanodiscs will cross-link.

Model membrane systems consisting of MS-TMS in DOPC lipids were solubilized with SMA and exposed to DSP and cross-linked products were visualized by SDS-PAGE. Figure 3A shows that without the addition of SMA, i.e. when no nanodiscs are formed, oligomers of MS-TMS of different sizes are formed, indicating that the cross-linking is not limited to linking residues within the oligomers. Increasing the molar excess of DSP yields larger aggregates (Fig 3A) and shorter cross-link times yield no cross-linked products (data not shown). With the formation of nanodiscs, cross-links were hypothesized to be exclusive to peptides within the nanodiscs. However, SMA is also detected by SDS-PAGE, making it impossible to distinguish the MS-TMS cross-linked products (Fig 3B). To reduce the amount of free SMA, the nanodiscs were purified with size exclusion chromatography prior to cross-linking. Figure 3C shows that the amount of SMA is significantly reduced by this purification step and no large aggregates of the peptide are visible. However, the SMA still interferes with detection of the lower molecular weight oligomers that are expected

to be present in the nanodiscs. Next to size exclusion chromatography, removing free SMA with selective centrifugal filters was explored. However, after 10 times filtering of the sample, the SMA contribution was still higher than after size exclusion (data not shown). In principle, only the cross-linked peptides are necessary for analysis of the native oligomerization state. Therefore purification of the cross-linked products from the nanodiscs with more harsh methods is feasible. Protein precipitation with acetone was explored but did not yield promising results. Possibly, this method could be further optimized or alternative methods could be investigated to separate the SMA from the peptides and the lipids, for example the use of detergents and subsequent precipitation of the polymer. However, we first tried to circumvent the problem of the SMA signal by changing the model system.

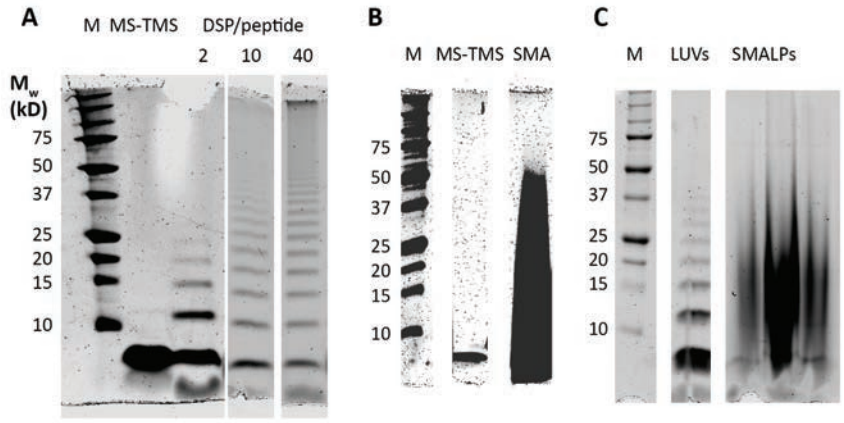

Figure 3. Visualization by SDS-PAGE of cross-linked MS-DesK transmembrane segment (MS-TMS) in various model systems. A) Cross-linked products of MS-TMS in LUVs with varying concentrations of cross-linker. B) The signal of MS-TMS compared to the signal of a 0.1 % (v/w) styrene-maleic acid polymer (SMA). The SMA is visible up to 50 kD, interfering with the detection of MS-TMS and cross-linked products. C) Cross-linked MS-TMS in LUVs compared to cross-linked MS-TMS in SMALPS after size exclusion chromatography. The three main fractions of the purification step are shown, with SMA interfering with the signals of the cross-linked products of MS-TMS.

The presence of SMA would no longer be problematic if the peptide had a molecular weight larger than 25 kD, where the SMA is no longer visible on gel after size exclusion chromatography. Therefore we explored solubilizing the entire MS-DesK protein. Oligomeric membrane proteins have been solubilized successfully by treating cell-lysates with SMA [8]. For example, KcsA was recently purified with this procedure [11]. Here we explored this approach for MS-DesK. *E. coli* cells expressing

KcsA were mixed with cells expressing MS-DesK. Both KcsA and MS-DesK were expressed in high quantities (Fig 4A). DesK is visible as monomer and KcsA runs as a tetramer on gel [13]. The mixture of whole cells was incubated at room temperature overnight with SMA. Figure 4A shows that the solubilization of KcsA is successful, with only a small part of the protein remaining in the pellet. However, MS-DesK is not solubilized and all the protein remains in the pellet. Increasing the SMA concentration did not result in MS-DesK solubilization. From this we conclude that no nanodiscs containing the MS are being formed. Therefore, further analysis of the oligomerization state of MS-DesK by the cross-linking approach is not possible at this moment.

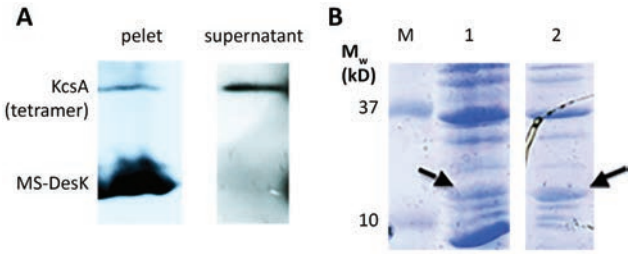

Figure 4. Analysis of MS-DesK and KcsA expression. A) Western blot analysis of the solubilization of MS-DesK and KcsA. Proteins were solubilized by SMA after cell lysis and subjected to centrifugation, yielding SMA soluble components in the supernatant and insoluble components in the pellet. B) SDS-PAGE analysis of total cell lysate (lane 1) and the recovered pellet fraction after washing with Triton X-100 (lane2). MS-DesK (indicated with an arrow) is present in the total cell lysate and after washing with Triton X-100, indicating that it is expressed in inclusion bodies.

What could cause the resistance of MS-DesK to solubilization by SMA? Possibly MS-DesK is not properly inserted into the membrane and expressed in inclusion bodies. In that case SMA is unlikely to solubilize MS-DesK because it is not present in a membrane. In contrast to inclusion bodies, membrane proteins properly incorporated in the membrane are soluble in mild detergents such as Triton X-100, provided they are non-raft associated [14]. Therefore the insoluble fraction of the cell lysate was isolated, washed with Triton X-100 and visualized on SDS-PAGE. Figure 4B shows that MS-DesK is observed in the total cell extract and that it is still present after the detergent wash steps, indicating that MS-DesK was expressed in inclusion bodies. Several attempts were made to prevent the formation of inclusion bodies, including optimizing MS-DesK expression, using different strains, varying growth temperature, and varying IPTG concentrations for induction and the OD_{600} at which induction was initiated. Unfortunately, none of these approaches was successful (data not shown).

Thus, we showed that MS-DesK expressed in inclusion bodies is resistant to SMA solubilization, indicating that a lipid environment is required for purification by SMA solubilization. If it would be possible to express MS-DesK and properly insert it in the membrane, the protein could be cross-linked in nanodiscs and its native oligomerization state could be visualized by SDS-PAGE. SMA would not interfere because the peptides would be larger than the SMA. Therefore, further optimization of the expression conditions will be worth exploring in the future. An alternative possibility would be to refold MS-DesK from inclusion bodies after further purification by sucrose gradient centrifugation [14], but this is far from straightforward.

Summarizing conclusion

The MS-DesK oligomerization state is crucial for its mechanism of sensing and signal transduction. Here, to determine the oligomerization state of MS-DesK, we explored the use of SMA, which solubilizes membranes into nanodiscs. Two approaches using these nanodiscs were investigated in this study. The first approach is based on the determination of the peptide/lipid ratio within purified nanodiscs. The second approach uses chemical cross-linking of the peptides within nanodiscs. The results indicate that both of these approaches could function as general methods to characterize oligomerization states. However, these methods require further optimization.

Materials & Methods

Materials

All chemicals and enzymes were purchased from Sigma-Aldrich unless otherwise indicated. 1,2-dioleoyl-*sn*-glycero-3-phosphocholine (DOPC) was obtained from Avanti Polar Lipids (Alabaster, AL). Synthetic peptides were obtained from Eurogentec (Seraing, Belgium) as > 95% pure peptides. Identity and purity were confirmed with Mass spectrometry and analytical HPLC. SMA2000 (styrene maleic anhydride, with a ratio of 2:1 and a M_w of 7.5 kD) copolymer was obtained as a kind gift from Cray Valley (Exton, PA). The cross-linking reagent dithiobis[succinimidylpropionate] (DSP) was purchased from Pierce Biotechnology (Rockford, IL) and Ni-NTA beads were from Thermo Fisher Scientific (Waltham, MA). Water was deionized and purified with a Milli-Q gradient water purification system from Millipore Corp. (Billerica, MA). All chemicals used were analytical grade.

Vesicle preparation

Samples were prepared as previously described [4]. Briefly, peptides (20 μM), dissolved in 0.5 mL trifluoroethanol were added to 0.5 mL of the phospholipid dispersion (0.5 mM) acquiring a final molar peptide/lipid ratio of 1/50. The lipid concentrations were determined by a phosphorus titration according to the method of Rouser [15]. Excess water was added and subsequently the samples were lyophilized after rapid freezing in liquid nitrogen. Vesicles were prepared by rehydrating the dry film at room temperature in buffer. For the cross-linking experiments 50 mM phosphate, 150 mM NaCl (pH 7.4) buffer was used and for the purification of His-WALP 50 mM Tris, 150 mM NaCl (pH 8) buffer was used. The hydrated vesicles were subjected to five freeze–thaw cycles.

SMA copolymer preparation and solubilization

The SMA2000 copolymer used throughout this study was prepared in exactly the same way as described in Swainsbury et al. [16] Briefly, a 5% (w/v) SMA2000 suspension in 1 M KOH was refluxed for at least 4 h after which the SMA was recovered by acid precipitation in 1.1 M HCl. The precipitated SMA was washed at least four times with 10 mM HCl. Finally, the SMA was lyophilized and stored at room temperature until required. 5% (w/v) SMA solutions used for experiments were prepared by dissolving lyophilized SMA in 50 mM Tris-HCl, after which the solution was adjusted to pH 8.0. Vesicles were solubilized with a final SMA concentration of ~0.1% (v/w). This corresponds to a SMA/phospholipid of 3:1 (w/w) (1:3.7 molar ratio). To separate the nanodiscs from free polymers, which interfere with Ni-NTA purification [8], 500 μL of the solubilized vesicles was loaded on a Superdex 200 10/300 GL size exclusion column (GE Healthcare) connected to an Äkta Prime Plus chromatography system (GE Healthcare).

Affinity purification & quantification

The solubilized vesicles, purified by size exclusion chromatography were incubated for at least 4 hours at 4 °C with the 0.5 mL of HisPur Ni-NTA agarose beads (Thermo Scientific). The beads were transferred to a gravity-flow column and washed twice with buffer containing 10 mM imidazole and once with buffer containing 50 mM imidazole. His-tagged peptides in nanodiscs were then eluted with buffer containing 300 mM imidazole. For quantification of the yields, samples containing SMA were 10× diluted in buffer, yielding a final SMA concentration of 0.01%. UV-VIS spectra of the samples were measured at 25 °C using a Lambda 18 spectrophotometer (PerkinElmer, Waltham, MA) equipped with a Peltier element.

Cross-linking

The cross-linking agent dithiobis[succinimidylpropionate] (DSP) was dissolved in DMSO and added to the sample in the appropriate amount to obtain the desired molar ratio. Subsequently the reaction mixture was incubated at room temperature for 30 minutes. Thereafter the reaction was stopped by adding 1M Tris, pH 7 to a final concentration of 50 mM and incubating for 15 minutes.

Analysis by SDS-PAGE

The nanodisc samples containing the cross-linked peptides were separated by non-reducing 10% Tricine-SDS-PAGE gel [17]. The peptides were visualized by coomassie brilliant blue r stain and detected with an ODYSSEY CLx scanner (Li-COR Biosciences, Lincoln, NE).

Gene expression & protein purification

For the expression of MS-DesK and KcsA, *E. coli* BL21 strains were used, either with a MS-DesK plasmid or with a KcsA plasmid. These strains were kindly provided by LE Cybulski and JM Dörr respectively. The proteins were expressed as described before [18]. These strains were grown in LB in a shaking incubator at 37 °C, 200 rpm. At an OD_{600} of 0.6, 1 mM IPTG was added. Induction was continued for 2 hours. Subsequently the cells were harvested by centrifugation at 4 °C. The cell pellets were resuspended in 10 mM Tris pH8, 10 mM Imidazole, 5 mM KCl. DNAse, lysozyme and protease inhibitor were added and the mixture was incubated on ice for 30 min. A 5% SMA solution, prepared as described above was added to a final concentration of 1.5% (w/v) and the mixture was sonicated using a tip sonicator (50% duty cycle, output 7-8, 8×10 pulses, on ice). The cells were incubated at room temperature, overnight. Insoluble fractions were removed by centrifugation and the supernatant was analyzed by SDS-PAGE and western blot analysis.

Analysis by SDS-PAGE and Western blot

The nanodiscs samples containing the MS-DesK and KcsA were analyzed 14% SDS-PAGE gels. The proteins were visualized by coomassie brilliant blue r stain and detected with an ODYSSEY CLx scanner (Li-COR Biosciences, Lincoln, NE) and by immunoblotting with an anti-His antibody.

Inclusion body isolation

The bacterial cell lysate was resuspended in 25 mM Tris (pH 7.4), 100 mM NaCl (buffer) and 0.5% Triton X-100 was added. The suspension was sonicated with a tip sonicator (on ice, 100% duty cycle, output 6, 5×20 seconds, 30 seconds cooling). The sample was washed 3 times by adding buffer with 2% Triton X-100 and subsequent centrifugation. The pellet was analyzed by SDS-PAGE.

References

[1] Aguilar PS, Hernandez-Arriaga AM, Cybulski LE, Erazo AC & de Mendoza D (2001) Molecular basis of thermosensing: A two-component signal transduction thermometer in *bacillus subtilis*. *Embo J* 20(7): 1681-1691.

[2] Gao R & Stock AM (2009) Biological insights from structures of two-component proteins. *Annu Rev Microbiol* 63: 133-154.

[3] Albanesi D, et al (2009) Structural plasticity and catalysis regulation of a thermosensor histidine kinase. *Proc Natl Acad Sci U S A* 106(38): 16185-16190.

[4] Cybulski LE, et al (2015) Activation of the bacterial thermosensor DesK involves a serine zipper dimerization motif that is modulated by bilayer thickness. *Proc Natl Acad Sci U S A* 112(20): 6353-6358.

[5] Cybulski LE, Martin M, Mansilla MC, Fernandez A & de Mendoza D (2010) Membrane thickness cue for cold sensing in a bacterium. *Curr Biol* 20(17): 1539-1544.

[6] Scheidelaar S, et al (2015) Molecular model for the solubilization of membranes into nanodisks by styrene maleic acid copolymers. *Biophys J* 108(2): 279-290

[7] Knowles TJ, et al (2009) Membrane proteins solubilized intact in lipid containing nanoparticles bounded by styrene maleic acid copolymer. *J Am Chem Soc* 131(22): 7484-7485.

[8] Dörr JM, et al (2016) The styrene-maleic acid copolymer: A versatile tool in membrane research. *Eur Biophys J* 45(1): 3-21.

[9] Jamshad M, et al (2015) Structural analysis of a nanoparticle containing a lipid bilayer used for detergent-free extraction of membrane proteins. *Nano Research* 8(3): 774-789.

[10] Kluger R & Alagic A (2004) Chemical cross-linking and protein–protein interactions—a review with illustrative protocols. *Bioorg Chem* 32(6): 451-472.

[11] Dörr JM, et al (2014) Detergent-free isolation, characterization, and functional reconstitution of a tetrameric K+ channel: The power of native nanodiscs. *Proc Natl Acad Sci U S A* 111(52): 18607-18612.

[12] Holt A & Killian JA (2010) Orientation and dynamics of transmembrane peptides: The power of simple models. *Eur Biophys J* 39(4): 609-621.

[13] Cortes DM & Perozo E (1997) Structural dynamics of the streptomyces lividans K+ channel (SKC1): Oligomeric stoichiometry and stability. *Biochemistry* 36(33): 10343-10352.

[14] Georgiou G & Valax P (1999) Isolating inclusion bodies from bacteria. *Methods Enzymol* 309: 48-58.

[15] Rouser G, Fleischer S & Yamamoto A (1970) Two dimensional thin layer chromatographic separation of polar lipids and determination of phospholipids by phosphorus analysis of spots. *Lipids* 5(5): 494-496.

[16] Swainsbury DJ, Scheidelaar S, van Grondelle R, Killian JA & Jones MR (2014) Bacterial reaction centers purified with styrene maleic acid copolymer retain native membrane functional properties and display enhanced stability. *Angew Chem Int Ed Engl* 53(44): 11803-11807.

[17] Schagger H (2006) Tricine-SDS-PAGE. *Nat Protoc* 1(1): 16-22.

[18] Van Dalen A, Hegger S, Killian JA, de Kruijff B (2002) Influence of lipids on membrane assembly and stability of the potassium channel KcsA. *FEBS Lett* 525(1-3):33–38.

6

Summarizing discussion

Summary

Despite their microscopic dimensions, bacteria have a significant impact on all life on earth. They inhabit various habitats as diverse as soil, water, acidic hot springs and Arctic environments. Furthermore, many bacteria live in symbiotic or parasitic relationships with animals and plants. With approximately 10^{30} bacteria on earth, they form a biomass which exceeds that of all plants and animals [1]. Bacteria recycle nutrients, influence the atmosphere and cause disease. To better understand the biological phenomena underlying the bacterial kingdom, several species or so-called model organisms are being extensively studied, assuming that bacteria share some fundamental mechanisms. On the basis of this assumption, discoveries made in the model organisms can provide insights into other organisms as well. Within these model organisms sensing and signaling is an intriguing topic, because it refers to the fundamental question how bacteria perceive the environment.

In nature, two-component systems (TCS) are ubiquitous to respond and adapt to environmental changes. They are particularly abundant in bacteria and archaea, but rarely seen in animals. Therefore, TCS are a potential target for antibiotics, and mechanistic understanding at a molecular level could help their development. The core of the mechanism of signal transduction among TCS is a phosphotransfer reaction between a histidine kinase (HK) and a response regulator (RR). The input is processed by the HK, which is the signaling component and the RR generates the cellular response [2, 3]. In this research, we investigated the bacterial two-component system DesKR that is involved in thermo-sensing [4]. It has the regular features of TCS, consisting of DesK, a homodimeric, membrane-bound sensor histidine kinase and DesR, a response regulator that triggers the bacterial response mainly by altering the expression of target genes [3].

The thermosensor DesK senses temperature inside the membrane [5] and therefore, protein-lipid interactions are key to understanding its mechanism of sensing and signal transduction. In principle, these interactions can be investigated by studying the proteins in their native lipid environment. However, this is not straightforward and reducing the complexity allows more systematic studies. DesK was reduced in complexity by capturing both sensing and signaling properties in a single transmembrane helix: the minimal sensor DesK (MS-DesK) [5]. In addition, the native lipid membrane was replaced by a synthetic model membrane. Thus, to investigate what exactly is sensed by MS-DesK and to explore how the signal is transmitted, we could systematically vary the properties of the lipids, as well as properties of the transmembrane segment. This model system approach was exploited in chapters 2 and 3, where MS-DesK transmembrane segments were investigated with different membrane thickness, lipid phase and bilayer charge. The model systems were studied with circular dichroism, tryptophan fluorescence molecular modeling and complementary *in vivo* functional studies were performed. With the results of these complementary techniques we observed a temperature dependent change in

conformation of the MS-DesK transmembrane helix and we were able to construct a molecular model for sensing and signal transduction of DesK.

To better mimic the *in vivo* situation, the synthetic lipids in the model membrane systems were replaced with lipid extracts from *B. subtilis* grown at relevant temperatures. These extracts were first characterized and we found temperature dependent regulation of the lipid acyl chain composition. Both the activity of a desaturase [4] and an iso-anteiso switching mechanism [6] were shown. In the model membrane systems with the *B. subtilis* lipids, no temperature dependent change in conformation of the MS-DesK transmembrane helix was observed. A possible explanation may be that the energetic barrier for reorientation of the helices is increased by the presence of branched side chains. In addition, owing to the attached cytosolic domain, the energetics of this barrier may be slightly different *in vivo*. The energetic barrier of the switch could for example be lowered because the linker region is more stable *in vivo*, reducing its interactions with the membrane. Finally, other proteins in the *B. subtilis* membrane affect the membrane properties, and could thereby lower the energetic barrier for reorientation of the MS-DesK transmembrane segment.

A very different model membrane system was used in chapter 5 to investigate the oligomerization state of MS-DesK. We explored the use of a styrene-maleic acid polymer (SMA), which solubilizes membranes into nanodiscs [7]. Two approaches with these nanodiscs were investigated in this study. The first approach is based on the biochemical characterization of purified nanodiscs with transmembrane peptides. The second approach uses chemical cross-linking of the peptides in the nanodiscs. The results show that both of these approaches are promising tools for the characterization of oligomerization states. These methods, however, require further optimization.

Molecular model of thermo-sensing of MS-DesK

The studies, described in this thesis resulted in a model of sensing and signal transduction of MS-DesK, as illustrated in Figure 1. The thermosensor is present as a dimer and senses the temperature within the membrane. MS-DesK does not respond to temperature per se, but presumably to a decrease in membrane fluidity and a corresponding increase in membrane thickness. The response consists of elongation of the MS-DesK transmembrane helix, aligning three serine residues at one side of the helix, forming a serine zipper motif. The exposure of this zipper motif triggers a reorientation of the helices to allow optimal interhelical H-bonding. The end result is the formation of a stable and continuous helix from the membrane to the cytoplasm, favoring the kinase conformation of the sensor, allowing for the phosphorylation of DesR, which results in the expression of a desaturase.

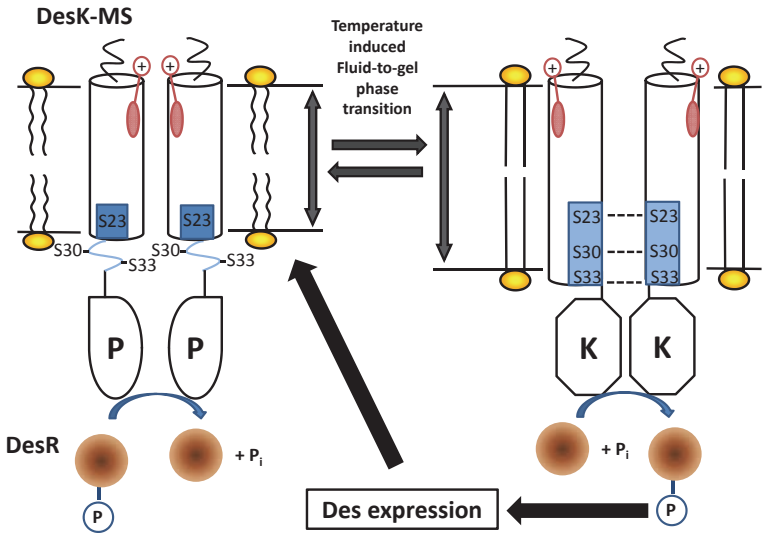

Figure 1. Schematic representation of the mode of action of MS-DesK. Its transmembrane segment (MS-TMS) contains an N-terminal charged hydrophilic motif (K10, N12; red), the so-called sunken-buoy (SB) motif. The sidechains of these residues limit the further downward lateral movement of the MS-TMS by snorkeling to the hydrophilic membrane interface. The C-terminus of the transmembrane part contains a hydrophilic motif of three serine residues (S23, S30, S33; blue). In a fluid membrane these serines interact with the hydrophilic interface (left). On a decrease in temperature, the membrane becomes thicker and an extra turn of the helix folds inside the membrane, resulting in the formation of a serine zipper motif (right). This motif can form intrahelical hydrogen bonds that shield the hydroxyl groups from the hydrophobic core of the membrane. The reorientation, necessary for this interaction, will lead to a change in the C-terminal domain (DesKC) from the phosphatase to the kinase state, allowing the phosphorylation of DesR. Phosphorylated DesR induces the expression of a desaturase, which increases the fluidity of the membrane, resulting in phosphatase activity of DesK.

The piston model as a mechanism for signal transduction

The proposed reorientation of the MS-DesK transmembrane helices may include changes in rotational angle, small piston-like movements and/or changes in tilt angle between the helices. These type of events have been proposed to be involved in transmembrane signaling of chemoreceptors and histidine kinases [8-12], combined in a small-magnitude piston-type helix sliding displacement, which is ideally suited for transmembrane signaling for several reasons. Signaling events typically provide relatively little energy capable of doing conformational work. A helix sliding displacement requires little driving energy as long as its magnitude is less than ~2 Å, so that specific side chain contacts and ridges-grooves packing between adjacent helices are largely maintained. Furthermore the signal has to be transduced over relatively large distances. Helix bends, rotations, or tilts could more easily be quenched by the flexibility of helices over these distances, whereas the rigid backbone of the helices allows for a piston displacement to be transmitted throughout the entire helix length. Additionally, a small 1-2 Å displacement would be large enough to directly regulate the on-off switching of a kinase active site [13].

Comparing models of signal transduction of DesK

How would our sensing and signaling model, together with a signal transduction mechanism with a small piston-like movement, compare to existing models for DesK signal transduction? Several models have been developed and will be discussed below.

The first model is derived from crystal structures [14]. A three state model was proposed for the flow of the phosphate group from DesK to DesR which proposes that the phosphatase-competent state of DesK has a stable coiled-coil structure protruding from the membrane and the ATP-binding domains are attached to the core, preventing histidine phosphorylation. A large conformational change of the coiled-coil results in reorientation of the core and release of the ATP-binding domains, which are now able to phosphorylate the histidine residue, hence the kinase-competent state. The actual binding of the phosphate group to the histidine results in yet another conformation, which allows for binding of DesR and subsequent transfer of the phosphate group. The membrane induces the differences between the phosphatase-competent state and the kinase-competent state, which are comparable with the switching from the phosphatase state to the kinase state in our model. But, based on the crystal structures, a rotation of almost 180° would be required to flip one helix over to the other side for the switch. Such a relatively large reorientation contradicts our model, in which more subtle rearrangements are sufficient for the switch. We favor subtle rearrangements for several reasons. If a large rotational displacement could be induced by the membrane, it is likely to be dampened by the helix flexibility. Furthermore the coiled-coils in the crystal structures are the N-terminus of

the protein, where the crystal structure could be unrealistic because of crystal-crystal contacts stabilizing an otherwise unfavorable conformation. Another consideration is that the crystal structures of the phosphatase and the kinase-competent state are specific mutants of DesKC, in which the essential phosphorylatable histidine residue is mutated to mimic the two different states of the protein. These mutations change the properties of this essential residue, which could have an effect on the folding of the protein, amplifying the differences between the two states. Additionally, the conformational flexibility of ATP-binding domain could be regulated by the membrane, which is absent in the crystallization study. The ATP-binding domains are located close to the membrane and in the crystal structure a conserved tryptophan, an arginine and several lysines protrude outwards, and possibly interact with the membrane. Therefore one should be careful to build a model of signal transduction based on these crystal structures only.

Recently, the kinase- and the phosphatase states of this three state, crystal structure-derived model were refined with molecular dynamics simulations [15]. The coiled-coils from the phosphatase-competent state and the kinase-competent state were further extended towards their N-termini according to the amino acid sequence of MS-DesK and several mutants. These extended models were embedded in membranes of varying thickness, resulting in two different types of structures for the phosphatase and kinase-competent states. The large differences between these structures, which are a direct result of the differences between their crystal structures, can be described as unwinding of the coiled-coil, involving a large rotation. The model of unwinding is supported by functional studies on DesK mutations. However the triple mutants described would also fit our model with the piston-like displacement for signal transduction. For example, the mutant in which two serines from the serine zipper are mutated is locked in the "kinase-off" state, similar to the serine zipper mutants we studied in chapter 2. However, a crucial mutant in our study, with a strengthened serine zipper with an extra serine residue, is locked in the "kinase-on" state, which is hard to explain in the context of the model of unwinding. Another model recently proposed involves an unfolding event of the charged linker region for signal transduction [16]. This model of unfolding is based on mutants in this region, and secondary structure measurements on corresponding peptides of the linker region in model membrane systems. Such method of signal transduction would be compatible with our model, but to support this mechanism more experimental evidence is required.

Influence of charge on the activity of DesK

Several charged residues of MS-DesK are crucial for the activity switch form phosphatase to kinase. An N-terminal lysine is essential and was hypothesized to anchor the transmembrane domain to the membrane-water interface [5]. Furthermore, at the intracellular side of the helix several charged residues are essential [16]. Next to the charge of the protein, the charge of the membrane was found to have an effect on DesK activity [17]. However, the switch between the "kinase-on" and "kinase-off" state was unaffected by the charge of the membrane lipids, which is in agreement with our observation in chapter 3, that the MS-DesK transmembrane segment is subject to a temperature dependent structural change in both zwitterionic and negatively charged lipids. These observations further support the choice of zwitterionic lipids in the model systems used throughout this research. Also, possible effects on the membrane charge by variations in head group composition of *B. subtilis* that were observed in chapter 4 are unlikely to disturb the mechanism of sensing and signal transduction. Finally, it should be noted that positively charged residues are often found at the intracelluar membrane-water interface, driving the correct transmembrane topology of the protein [18, 19].

Prolines in transmembrane helices

Prolines are considered helix breaking residues in soluble proteins [20]. Yet they are often found in transmembrane helices, where they induce a kink. There are many indications that such kinks could have functional importance in membrane proteins, for instance for dimerization of transmembrane helices [21]. Indeed, single proline mutations in MS-DesK favor the "kinase off" state, independent of temperature, highlighting the importance of the proline residues for MS-DesK. These prolines are possibly important sites for MS-DesK dimerization. The kinks in the backbone of transmembrane segments could induce a dimerization site, aligning neighboring residues for favorable interactions. On the other hand, kinks could prevent steric hindrance when the serine zipper is formed.

On the properties sensed by DesK

DesK was originally called a thermosensor because the temperature was found to influence its activity [4]. Because DesK plays a role in fluidity maintenance, it was suggested that perhaps it could sense the fluidity itself, rather than sensing the temperature. Indeed, in less fluid membranes increased activity of DesK was identified, independent of temperature [22, 23]. Membrane thickness, which is significantly increased in the gel phase [24], was also identified as a cue for DesK sensing [5]. In chapter 2 and 3 we found that both fluidity and thickness of the membrane, but not temperature itself, cause a similar reorientation of the MS-DesK transmembrane

segment. Furthermore, in chapter 4 we observed that the *B. subtilis* membrane lipids undergo a phase transition at temperatures where DesK is active. These findings support the view that membrane fluidity is sensed by DesK, presumably owing to corresponding changes in membrane thickness, although other possible mechanisms cannot be ruled out yet.

One such possibility is that DesK senses anomalies during the phase transition. For instance, phase separation of lipids was also suggested to be a membrane property sensed by DesK, because increased activity of DesK was found in synthetic lipids around the phase transition temperature [17]. It was argued that liquid and gel-phase coexist at the lipid phase transition [25], thereby forming microdomains that could result in redistribution of the proteins, which in turn could result in protein conformational changes. Such mechanism has been observed for some signaling proteins [26]. In our studies we observed a phase transition for *B. subtilis* lipids at temperatures where DesK is active. Additionally, DesK was found to be permanently inactive in the gel phase, possibly owing to aggregation [17]. The inactivity in the gel phase also correlates with the behavior of MS-DesK transmembrane peptides observed in chapter 3. The small deviations we found in the gel phase were argued to be artifacts of the ordered acyl chains of the gel phase.

Another property that might be sensed by DesK is the hydration of the membrane, which is much lower in the gel phase than in fluid membranes [25]. Once the membrane becomes less hydrated the kinase active conformation of MS-DesK might be induced, until lowered hydration levels induce aggregation. However, increased hydration levels have been observed as an anomaly during the phase transition [27], which would suggest an active conformation in increased hydrated membranes.

Finally it is possible, and perhaps even most likely, that DesK senses a combination of all the above mentioned properties. However, to investigate the hydration or phase separation in the membrane without changing other properties is experimentally very challenging. An option would be to use molecular dynamics (MD) simulations. In MD simulations these properties are still interconnected, but the simulations can provide direct information on hydration and phase separation inside the membrane. The molecular modeling method Docking Assay For Transmembrane components (DAFT) [28], was especially developed to identify preferred binding orientations within the membrane. DAFT involves multiple coarse-grained simulations to find the most populated dimer conformations. Subsequently, the dimers can be investigated at an atomistic level. This method was used in this study to investigate the dimer interfaces of the MS-DesK transmembrane helix [29] and would be suitable to further explore the MS-DesK dimer conformations as function of hydration levels or phase separation phenomena.

On the oligomerization of MS-DesK

MS-DesK is believed to function as a dimer for several reasons. First, many two-component systems were found to function as a dimer [30, 31]. Furthermore the intracellular domain of DesK was crystallized as a dimer. In chapter 1 we performed molecular dynamics simulations that indicate dimerization of the MS-DesK transmembrane helix. If MS-DesK forms dimers, a potential problem could arise in the model membrane systems with transmembrane peptides because the orientation cannot be controlled. Although we designed the peptides with the charged linker region which may be expected to promote the formation of parallel dimer, we cannot exclude anti-parallel dimer formation. However, we did not observe indications of two populations in our data and therefore we suspect an insignificant anti-parallel dimer population.

The MS-DesK oligomerization state was investigated in chapter 5 with the use of a styrene-maleic acid polymer (SMA). SMA solubilizes membranes into nanodiscs, which were used for two different approaches. The first approach is based on the observation that proteins are solubilized in nanodiscs of similar size, in their native oligomerization state [7]. If transmembrane peptides are solubilized in a similar fashion, it should be possible to examine the oligomerization state by analysis of the peptide/lipid ratio in purified peptide-containing nanodiscs. However, we found the purification of the peptide-containing nanodiscs with nickel-affinity chromatography to be problematic, possibly because the polymer interferes with the His-tag binding to the nickel-affinity column. Therefore, future alternative purification methods could use other tags (Strep tag, FLAG tag, etc.) to separate the peptide.

The second approach to investigate the MS-DesK oligomerization state is based on chemical cross-linking of the peptides within the nanodiscs. However, owing to the presence of SMA in the samples, the visualization of the cross-linked products was problematic. Here, the purification of the cross-linked products might be further explored, for example using protein precipitation with acetone or detergents. The solubilization of full-length MS-DesK in nanodiscs was tested in chapter 5. However, the formation of inclusion bodies was found to be incompatible with the SMA solubilization. Optimized expression, preventing the formation of inclusion bodies and successful solubilization with SMA, would result in multiple analysis options. For example the use of mass spectrometry and NMR could provide insight in preferential interactions of MS-DesK with surrounding lipids and the molecular structure and dynamics of this system.

Epilogue

The insights in the molecular mechanism of sensing and signal transduction of the two-component system DesK presented in this study are yet another step in understanding biological membranes at a molecular level. Such insights into the molecular basis of life provided information on many fundamental biological processes because the three-dimensional molecular structures of biomolecules are related to their function [32]. This structure function relationship in biology became evident through the determination of the first structures of biomolecules, such as the discovery of the double helical structure of DNA, which allows for the mechanism of replication by unwinding and copying one of the strands [33, 34]. The visualization of protein structures started with myoglobin and hemoglobin, followed by many enzyme structures in the 1960s, which ultimately reinforced the structure function relationship [35, 36].

The significance of basic structures was realized before visualization on molecular resolution was possible. Cell theory emerged in the 19th century, recognizing that the cell is the basic structural unit of life. However, for this understanding, many observations and technical innovations were necessary during the nearly two centuries following the first observation of cells through a microscope by Hooke and van Leeuwenhoek [37, 38]. Optical instruments were developed at that time from grinded and polished lenses to microscopes, magnifying objects to almost 300×, which allowed investigation of life on a smaller scale than ever before. These developments exemplify the success of the scientific method, which developed in the 17th century because of a scientific revolution inspired by faith in logic [39, 40]. The development of the scientific method at that time is regarded as the birth of modern science [39, 40]. The modes of acquiring knowledge about nature were transformed revolutionary and three important pillars of science as we know it emerged. The role of mathematics was extended, inspired by Kepler and Galileo, to an ongoing process of mathematization of nature. The speculative systems of natural philosophy of Aristotle amongst others were gradually displaced by so-called corpuscularian thinkers such as Descartes by an atomistic natural philosophy with a novel concept of motion, coinciding with the concepts developed by Galileo. Finally, investigation upon accurate description and practical application was gradually transformed into a fact-finding, practice-oriented mode of experimental science as described by Francis Bacon [39].

The faith in logic and careful observation that allowed the scientific revolution of the 17th century emerged in the European Renaissance [39, 40]. Great thinkers of that period seemed to possess unquenchable curiosity and feverishly inventive imagination, and they were willing to change traditional methods. These polymaths often excelled in many fields, which reflected the ideals of the humanists of the time. A gentleman of that era was expected to speak several languages, play a musical instrument, write poetry, and so on, thus fulfilling the Renaissance ideal. The idea of

a universal education was essential to master these diverse subjects; hence the word 'university' was used to describe an institute of learning. Leonardo da Vinci, often described as the archetype of the Renaissance man, was an innovator in many fields, arts and sciences alike [41, 42].

However, the hypothesis of the scientific method is the intelligibility of the universe. We learned from experience that the world is logically structured – or science would be a waste of time. However, does logic apply to the fundamental basis of our existence? [43, 44]

> Rationalism is a view of life which is based on Hegel's motto: the rational is real, real is rational, and therefore assumes that the outness in its totality can be understood by the ratio. This includes that the ideal society can be achieved through understanding and control. Nature is seen as a source of raw materials and energy, as well as chaos that requires reorganization. The aesthetic experience is reduced to a fringe of life, the mystical experience is considered theology. The rational function is a wonderful human instument, but rationalism is a sin against humanity. The identification of philosophy with the rational interpretation of the universe, is the most threatening consequence of rationalism.
> (Ulrich Libbrecht)

A model relates to reality as a map to the land. The map provides us with information of the land and gives an overview. But the map is not the land. A description of reality always uses a language. Thus, science is itself a language that is useful to understand certain properties of the universe, but the scientific description is not reality itself.

Thus, from marvel and wonder about the universe, humanity came to disclosure and experience of the universe in many ways. But the description is a language, and experience is emotion, they are not the phenomenon itself. Fortunately, we can return to the marvel and wonder.

> The purpose of a fish trap is to catch fish,
> And when the fish are caught the trap is forgotten.
>
> The purpose of a rabbit snare is to catch rabbit,
> And when the rabbits are caught the snare is forgotten.
>
> The purpose of words is to convey ideas.
> When the ideas are grasped the words are forgotten.
> (Chuang-tzu)

References

[1] Whitman WB, Coleman DC & Wiebe WJ (1998) Prokaryotes: the unseen majority. *Proc Natl Acad Sci U S A* 95 (12): 6578–83.

[2] Stock AM, Robinson VL & Goudreau PN (2000) Two-component signal transduction. *Annu Rev Biochem* 69: 183-215.

[3] Gao R & Stock AM (2009) Biological insights from structures of two-component proteins. *Annu Rev Microbiol* 63: 133-154.

[4] Aguilar PS, Hernandez-Arriaga AM, Cybulski LE, Erazo AC & de Mendoza D (2001) Molecular basis of thermosensing: A two-component signal transduction thermometer in *bacillus subtilis*. *Embo J* 20(7): 1681-1691.

[5] Cybulski LE, Martin M, Mansilla MC, Fernandez A & de Mendoza D (2010) Membrane thickness cue for cold sensing in a bacterium. *Curr Biol* 20(17): 1539-1544.

[6] Suutari M & Laakso S (1992) Unsaturated and branched chain-fatty acids in temperature adaptation of *bacillus subtilis* and bacillus megaterium. *Biochim Biophys Acta* 1126(2): 119-124.

[7] Dörr JM, et al (2016) The styrene-maleic acid copolymer: A versatile tool in membrane research. *Eur Biophys J* 45(1): 3-21.

[8] Matthews EE, Zoonens M & Engelman DM (2006) Dynamic helix interactions in transmembrane signaling. *Cell* 127(3): 447-450.

[9] Gao R & Lynn DG (2007) Integration of rotation and piston motions in coiled-coil signal transduction. *J Bacteriol* 189(16): 6048-6056.

[10] Casino P, Rubio V & Marina A (2010) The mechanism of signal transduction by two-component systems. *Curr Opin Struct Biol* 20(6): 763-771.

[11] Zhang Z & Hendrickson WA (2010) Structural characterization of the predominant family of histidine kinase sensor domains. *J Mol Biol* 400(3): 335-353.

[12] Casino P, Rubio V & Marina A (2009) Structural insight into partner specificity and phosphoryl transfer in two-component signal transduction. *Cell* 139(2): 325-336.

[13] Falke JJ & Erbse AH (2009) The piston rises again. *Structure* 17(9): 1149-1151.

[14] Albanesi D, et al (2009) Structural plasticity and catalysis regulation of a thermosensor histidine kinase. *Proc Natl Acad Sci U S A* 106(38): 16185-16190.

[15] Saita E, et al (2015) A coiled coil switch mediates cold sensing by the thermosensory protein DesK. *Mol Microbiol* 98(2): 258-271.

[16] Inda ME, et al (2014) A lipid-mediated conformational switch modulates the thermosensing activity of DesK. *Proc Natl Acad Sci U S A* 111(9): 3579-3584.

[17] Martin M & de Mendoza D (2013) Regulation of *bacillus subtilis* DesK thermosensor by lipids. *Biochem J* 451(2): 269-275.

[18] von Heijne G (1992) Membrane protein structure prediction. hydrophobicity analysis and the positive-inside rule. *J Mol Biol* 225(2): 487-494.

[19] Bogdanov M, Xie J & Dowhan W (2009) Lipid-protein interactions drive membrane protein topogenesis in accordance with the positive inside rule. *J Biol Chem* 284(15): 9637-9641.

[20] Thou PY & Fasman GD (1978) Prediction of the secondary structure of proteins from their amino acid sequence. *Advan Enzymol* (47): 45-148.

[21] von Heijne G (1991) Proline kinks in transmembrane α-helices. *J Mol Biol* 218(3): 499-503.

[22] Cybulski LE, et al (2002) Mechanism of membrane fluidity optimization: Isothermal control of the *bacillus subtilis* acyl-lipid desaturase. *Mol Microbiol* 45(5): 1379-1388.

[23] Martin N, Lombardia E, Altabe SG, de Mendoza D & Mansilla MC (2009) A lipA (yutB) mutant, encoding lipoic acid synthase, provides insight into the interplay between branched-chain and unsaturated fatty acid biosynthesis in *bacillus subtilis*. *J Bacteriol* 191(24): 7447-7455.

[24] Janiak MJ, Small DM & Shipley GG (1979) Temperature and compositional dependence of the structure of hydrated dimyristoyl lecithin. *J Biol Chem* 254(13): 6068-6078.

[25] Cevc G & Marsh D (1987) Phospholipid Bilayers: Physical Principles and Models (Wiley-Interscience, New York)
[26] Lopez D & Kolter R (2010) Functional microdomains in bacterial membranes. *Genes Dev* 24: 1893–1902.
[27] Honger T, Mortensen K, Ipsen JH, Lemmich J, Bauer R & Mouritsen OG (1994) Anomalous swelling of multilamellar lipid bilayers in the transition region by renormalization of curvature elasticity. *Phys Rev Let*, 72: 3911–3914
[28] Wassenaar TA, et al (2015) High-throughput simulations of dimer and trimer assembly of membrane proteins. the DAFT approach. *J Chem Theory Comput* 11(5): 2278-2291.
[29] Cybulski LE, et al (2015) Activation of the bacterial thermosensor DesK involves a serine zipper dimerization motif that is modulated by bilayer thickness. *Proc Natl Acad Sci U S A* 112(20): 6353-6358.
[30] Stock AM, Robinson VL & Goudreau PN (2000) Two-component signal transduction. *Annu Rev Biochem* 69: 183-215.
[31] Gao R & Stock AM (2009) Biological insights from structures of two-component proteins. *Annu Rev Microbiol* 63: 133-154.
[32] Stryer L (1995) Biochemistry (W.H. Freeman and Company, New York).
[33] Watson JD & Crick FH (1953) Molecular structure of nucleic acids; a structure for deoxyribose nucleic acid. *Nature* 171(4356): 737-738.
[34] Watson JD & Crick FH (1953) Genetical implications of the structure of deoxyribonucleic acid. *Nature* 171(4361): 964-967.
[35] Kendrew JC, Bodo G, Dintzis HM, Parrish RG, Wyckoff H & Phillips DC (1958) A three-dimensional model of the myoglobin molecule obtained by x-ray analysis. *Nature* 181(4610): 662-666.
[36] Perutz MF, Rossmann MG, Cullis AF, Muirhead H, Will G & North AC (1960) Structure of haemoglobin: a three-dimensional Fourier synthesis at 5.5-Å resolution, obtained by X-ray analysis. *Nature* 185(4711): 416-422.
[37] Hooke, R. (1665). Micrographia, or, Some physiological descriptions of minute bodies made by magnifying glasses: With observations and inquiries thereupon. (J. Martyn and J. Allestry, London).
[38] Leewenhoeck A (1677) Observation, communicated to the publisher by Mr. Antony van Leewenhoeck, in a Dutch letter of the 9 Octob. 1676 here English'd: concerning little animals by him observed in rain-well-sea and snow water; as also in water wherein pepper had lain infused. *Phil. Trans.* 12, 821–831.
[39] Cohen HF (2010) How modern science came into the world – Four civilizations, one 17th-century breakthrough. (Amsterdam University Press, Amsterdam).
[40] Dijksterhuis EJ (1950) De mechanisering van het wereldbeeld. (Meulenhoff, Amsterdam).
[41] Nicholl C (2004) Leonardo da Vinci – The flights of the mind. (Allen Lane, London).
[42] Müntz E (1898) Leonardo da Vinci – Artist, thinker and man of science. (W. Heinemann, London)
[43] Libbrecht U (2001) Burger van de wereld - Inleiding tot een wereldbeschouwing. (Damon, Budel)
[44] Libbrecht U (2001) Inleiding comparative filosofie. (Van Gorcum, Assen)

&

Addendum

Nederlandse samenvatting

List of publications

Curriculum Vitae

Dankwoord

Nederlandse samenvatting

Sinds mensenheugenis proberen wij te begrijpen hoe de wereld om ons heen functioneert. Deze zoektocht vloeit voort uit de verwondering over alles wat we om ons heen kunnen waarnemen. Bijdragen aan ons begrip van de natuur zijn van alle tijden. De ontwikkeling van de wiskunde, filosofie en sterrenkunde gaat terug tot de oude beschavingen van Griekenland, Egypte, Mesopotamië, de Indusvallei, China en de Maya's. Tijdens de Europese Renaissance veranderde men geleidelijk de traditionele methoden en werd de logica als maat van alle dingen genomen. De wens van zowel kunstenaars als wetenschappers om de zaken weer te geven zoals ze zijn - in tegenstelling tot het verder uitbouwen van bestaande theorieën - leidde tot zorgvuldig observeren en experimenteren onder gecontroleerde omstandigheden. Om de kwaliteit van zijn schilderijen te verbeteren ontleedde Leonardo da Vinci systematisch tientallen lijken en maakte prachtige, realistische tekeningen waarmee hij de menselijke anatomie in meer detail weergaf dan ooit tevoren. Vesalius, een beroemde anatoom, huurde kunstenaars in om illustraties van zijn dissecties te maken. In de 17e eeuw culmineerden de nieuwe opvattingen en werkwijzen van de Renaissance in een wetenschappelijke revolutie en werd de moderne praktijkgerichte experimentele wetenschap geboren. Nieuwe paradigma's ontstonden in de natuur- en sterrenkunde en door de uitvinding van de microscoop konden voor het eerst cellen worden waargenomen. Die cellen werden erkend als basiseenheden van alle organismen en de zogenaamde celtheorie ontstond, bestaande uit drie stellingen. 1) Alle levende organismen bestaan uit één of meer cellen, 2) de cel is de basiseenheid van structuur en organisatie en 3) alle cellen komen voort uit reeds bestaande cellen. In de 19e eeuw werd de celtheorie algemeen aanvaard, maar een intrigerende vraag bleef: wat is de aard van het celmembraan, het vlies om de cel, dat selectief transport van stoffen de cel in en uit mogelijk maakt en daardoor feitelijk de cel definieert? Het zou tot de 20e eeuw duren voordat zowel de chemische samenstelling als de structuur van het celmembraan werden ontrafeld. We weten nu dat het celmembraan hoofdzakelijk uit lipiden en eiwitten bestaat.

Vele eigenschappen van het celmembraan worden bepaald door de lipiden. Lipiden zijn opgebouwd uit een hydrofobe staart en een hydrofiele kopgroep. In waterige oplossingen hebben de hydrofobe staarten de neiging om te aggregeren, zodat de verstoring van de energetisch gunstige waterstofbruggen minimaal is. Dit verschijnsel wordt het hydrofobe effect genoemd en het is de drijvende kracht voor lipiden om structuren te vormen zoals micellen of bilagen. De meeste lipiden in waterig milieu vormen spontaan bilagen, dat wil zeggen twee lagen met de staarten bij elkaar in een hydrofobe kern en de hydrofiele kopgroepen gericht naar de waterige omgeving. In biologische membranen zijn de lipiden geordend in bilagen. Deze bilagen zijn zeer impermeabel voor ionen en de meeste polaire moleculen, met uitzondering van water. Door deze eigenschappen is de bilaag een uitstekende barrière tussen de binnen- en

de buitenkant van de cel. Veel stoffen moeten echter op een gecontroleerde manier de cel binnenkomen of verlaten. Voor deze en andere functies zijn cellen afhankelijk van een andere component van het membraan: de membraaneiwitten.

Het grootste deel van de dynamische processen die plaatsvinden in biologische membranen wordt uitgevoerd door membraaneiwitten. Deze eiwitten bevinden zich aan het membraanoppervlak of ze doorkruisen het membraan waardoor ze ingebed zijn in het membraan. De in het membraan geïntegreerde eiwitten hebben een karakteristieke structuur, meestal gevormd door één of meerdere membraan-overspannende α-helices. Deze helices zijn bijvoorbeeld betrokken bij de vorming van kanalen en pompen die zorgen voor selectief transport over het membraan. Bij receptoren en sensoren zijn transmembraan helices verantwoordelijk voor het overdragen van informatie over het membraan, wat resulteert in activering of de-activering van vitale cellulaire processen. Hierbij is de interactie tussen eiwitten en lipiden in het bijzonder van belang. Daarom is, naast de studie van membraaneiwitten zelf, onderzoek naar hoe deze eiwitten worden beïnvloed door de lipide omgeving van cruciaal belang.

Celmembranen zijn zeer dynamische structuren en worden wel voorgesteld als een tweedimensionale vloeistof. Individuele lipide- en eiwitmoleculen kunnen diffunderen in het vlak van het membraan. Anderzijds is diffusie loodrecht op het membraanvlak, ofwel de translocatie van een molecuul naar de tegenover liggende monolaag in het membraan, een veel trager proces. De viscositeit of vloeibaarheid van het membraan is een biologisch belangrijke eigenschap. Membraaneiwitten kunnen alleen functioneren in een vloeibaar membraan. In stuggere membranen worden belangrijke functies als transport en signaaltransductie verstoord wat uiteindelijk celdood tot gevolg heeft. Daarom wordt de vloeibaarheid van het membraan zorgvuldig gereguleerd in alle organismen. De vloeibaarheid van het membraan wordt onder andere beïnvloed door de temperatuur en de samenstelling van het membraan. Daarom reguleren bacteriën hun membraansamenstelling afhankelijk van de omgevingstemperatuur. Die regulering van membraanvloeibaarheid in bacteriën is het hoofdonderwerp van dit proefschrift.

Ondanks hun microscopisch kleine afmetingen hebben bacteriën een belangrijke invloed op alle leven op aarde. Hun leefomgeving varieert van de bodem of het water tot zure warmwaterbronnen of Arctische omgevingen. Verder leven bacteriën ook in symbiotische of parasitaire relaties met dieren en planten. Met ongeveer 10^{30} bacteriën op aarde, vormen ze een biomassa die veel groter is dan die van alle planten en dieren samen. Bacteriën recyclen voedingsstoffen, hebben invloed op de biosfeer en veroorzaken ziekte. Voor een beter begrip van de biologische mechanismen in het bacteriële koninkrijk worden verschillende zogenaamde modelorganismen uitgebreid bestudeerd, met de verwachting dat ontdekkingen in deze organismen inzicht geven in het functioneren van andere organismen. Binnen deze modelorganismen is detectie

en signalering een intrigerend onderwerp, omdat het ingaat op de fundamentele vraag hoe bacteriën hun omgeving waarnemen. Beter begrip van de processen die betrokken zijn bij detectie en signalering kan leiden tot nieuwe antibiotica, omdat we dan kunnen onderzoeken hoe we deze processen kunnen verstoren.

In dit proefschrift is het bacteriële thermostaateiwit DesK van de bacterie *Bacillus subtilis* onderzocht. Dit is een sensor die zich in het membraan van de bacterie bevindt en daar verlaging van de omgevingstemperatuur kan meten. Temperatuurverlagingen hebben en verstarrend effect op het membraan. Daarom is het van levensbelang voor de bacterie dat een verlaagde temperatuur gemeten wordt en dat, als reactie daarop, direct meer vloeibare componenten aan het membraan worden toegevoegd. DesK reageert dan ook op een verlaagde temperatuur door een cascade in werking te stellen die resulteert in verhoging van het aantal vloeibare componenten in het membraan. Hierdoor wordt de verlaagde membraanvloeibaarheid als gevolg van de temperatuur gecompenseerd.

Omdat DesK de temperatuur binnen in het membraan waarneemt, zijn eiwit-lipide interacties cruciaal voor het mechanisme van detectie en signaaltransductie. In principe kunnen deze interacties worden onderzocht door eiwitten in hun oorspronkelijke lipide omgeving te bestuderen. Dit is echter niet eenvoudig en maakt systematische studies bijna onmogelijk. Gelukkigerwijs werd in 2010 een vereenvoudigde zogenaamde minimale sensor van DesK (MS-DesK) ontdekt, die de bestudering van dit thermostaateiwit vergemakkelijkt. MS-DesK heeft slechts één transmembraan helix in plaats van vijf. Als ook het complexe mengsel van membraanlipiden vervangen wordt door synthetische lipiden, ontstaat een membraansysteem met sterk gereduceerde complexiteit, een zogenaamd model membraansysteem. Deze modelsystemen zijn voor onderzoek naar het mechanisme van DesK zeer geschikt omdat zowel de detectie als de signaaltransductie plaats vindt binnen het membraan en omdat DesK specifieke membraaneigenschappen waarneemt die in model systemen systematisch gevarieerd kunnen worden zodat de bijdrage van elke eigenschap kan worden onderzocht. Eiwit-lipide interacties zijn hierbij van cruciaal belang, omdat deze interacties direct verantwoordelijk zijn voor de activatie van DesK.

De benadering met model membraansystemen werd gebruikt in de hoofdstukken 2 en 3, waar het MS-DesK transmembraan segment werd onderzocht in membranen met verschillende dikte, lipide-fase en lading. De modelsystemen werden bestudeerd met circulair dichroïsme, tryptofaan fluorescentie en moleculaire simulaties, aangevuld met *in vivo* activiteitsbepalingen. Met behulp van deze complementaire technieken vonden we een temperatuurafhankelijke verandering in conformatie van de MS-DesK transmembraan helix en konden we een moleculair model van de detectie en signaaltransductie van DesK construeren, dat verderop behandeld zal worden.

Om het systeem meer overeen te laten komen met de *in vivo* situatie, werden de synthetische lipiden in de model membraansystemen vervangen met lipide extracten van *B. subtilis* bacteriën. Deze extracten werden eerst gekarakteriseerd en we vonden een temperatuurafhankelijke regulatie van de lipid samenstelling. Het resultaat van de activiteit van twee mechanismen om de vloeibaarheid te verhogen werd waargenomen: verlaging van het verzadigingsniveau van de lipiden en verandering van het vertakkingspatroon van de lipiden. In de model membraansystemen met de *B. subtilis* lipiden werd echter geen temperatuurafhankelijke verandering in conformatie van de MS-DesK transmembraan helix waargenomen. Een mogelijke verklaring kan zijn dat de heroriëntatie van de MS-DesK helices wordt gehinderd door de aanwezigheid van de *B. subtilis* lipiden. Bovendien heeft MS-DesK *in vivo* een intracellulair domein, dat binding van de C-terminus van de MS-DesK transmembraan helix met het membraan zou kunnen voorkomen, waardoor de heroriëntatie van de helix makkelijker zou kunnen worden. Tot slot zouden andere eiwitten in de *B. subtilis* membraan invloed kunnen hebben op de heroriëntatie van het MS-DesK transmembraan segment.

In hoofdstuk 5 werd de oligomerizatietoestand van MS-DesK onderzocht met behulp van een heel ander model membraansysteem. We onderzochten het gebruik van een styreen maleïnezuur polymeer, dat membranen oplost in zogenaamde nanodiscs. Twee manieren om deze nanodiscs te gebruiken werden in deze studie onderzocht. De eerste benadering is gebaseerd op de biochemische karakterisering van gezuiverde nanodiscs met transmembraanpeptiden. De tweede benadering maakt gebruik van chemisch cross-linken van de peptiden in de nanodiscs. De resultaten tonen dat deze beide methoden veelbelovende hulpmiddelen zijn voor de karakterisering van oligomerizatietoestanden van eiwitten. Verdere optimalisatie is echter noodzakelijk.

De studies in dit proefschrift resulteerde in een model van detectie en signaaltransductie van MS-DesK. Het thermostaateiwit vormt een dimeer en detecteert de temperatuur binnen in het membraan. MS-DesK reageert niet op temperatuur zelf, maar vermoedelijk op een afname van membraanvloeibaarheid en een overeenkomstige stijging van membraandikte. Als reactie verlengt de MS-DesK transmembraan helix, wat drie serine residuen aan één zijde van de helix brengt. Zo wordt een zogenaamd serine-rits motief gevormd. Het contact van deze hydrofiele serine-rits met de hydrofobe membraan is energetisch ongunstig. Een heroriëntatie van de helices maakt optimale vorming van waterstofbruggen mogelijk tussen de twee helices van de MS-DesK dimeer. Het eindresultaat is de vorming van een stabiele en continue helix van het membraan naar het cytoplasma, waardoor de kinase conformatie van de sensor gevormd wordt. Dit heeft de fosforylering van een respons regulator tot gevolg, waardoor een desaturase tot expressie komt dat door incorporatie van dubbele bindingen in bestaande lipiden de membraanvloeibaarheid weer verhoogd.

De precieze aard van de heroriëntatie van de transmembraan helices van de MS-DesK dimeer kan nog niet met zekerheid worden vastgesteld. Mogelijk zijn kleine rotaties, schuivende bewegingen en / of veranderingen in tilt tussen de helices betrokken bij de signaaltransductie. Er wordt inderdaad verondersteld dat dit soort bewegingen betrokken is bij verschillende detectie en signaaltransductie mechanismen. Maar verder onderzoek moet uitwijzen welke bewegingen daadwerkelijk betrokken zijn bij het doorgegeven van het signaal naar het intracellulaire domein van DesK.

List of publications

Structural properties of the transmembrane helices of the thermosensor DesK are regulated by both length and phase state of the surrounding lipids. **J. Ballering**, T.E. Rijpma, M.E. van Eck and J.A. Killian. *Manuscript in preparation*

Activation of the bacterial thermosensor DesK involves a serine zipper dimerization motif that is modulated by bilayer thickness. **J. Ballering**, L.E. Cybulski, A. Moussatova, M.E. Inda, D.B. Vazquez, T.A. Wassenaar, D. de Mendoza, D.P. Tieleman, J.A. Killian. *Proceedings of the National Academy of Sciences (PNAS)*, Volume 112, Issue 20, 6353-6358, 19 May 2015.

Aspergillus niger RhaR, a regulator involved in L-rhamnose release and catabolism. B.S. Gruben, M. Zhou, A. Wiebenga, **J. Ballering**, K.M. Overkamp, P.J. Punt, R.P. de Vries. *Applied Microbiology and Biotechnology*, Volume 98, Issue 12, 5531-5540, 28 February 2014.

Crystal structure and collagen-binding site of immune inhibitory receptor LAIR-1; unexpected implications for collagen binding by platelet receptor GPVI. T.H.C. Brondijk, T. de Ruiter, **J. Ballering**, H. Wienk, R.-J. Lebbink, H. van Ingen, R. Boelens, R.W. Farndale, L. Meyaard and E.G. Huizinga. *Blood*, Volume 115, Issue 7, 1364-1373, 18 February 2010.

Structural insight into the recognition of the H3K4me3 mark by the TFIID subunit TAF3. H. van Ingen, F.M.A. van Schaik, H. Wienk, **J. Ballering**, H. Rehmann, A.C. Dechesne, J.A.W. Kruijzer, R.M.J. Liskamp, H.Th.M. Timmers and R. Boelens. *Structure*, Volume 16, Issue 8, 1245-1256, 6 August 2008.

Curriculum Vitae

Joost Ballering was born March 1st 1981 in Leiden. After obtaining his secondary school VWO diploma at the Stedelijk Gymnasium Leiden, he studied chemistry at Utrecht University. During his study, he was secretary of the board of "Beta Bedrijvendagen" (2003/2004), organizing the Utrecht University science career event. Furthermore, he was chairman of the board of student soccer club "USVV Odysseus '91" (2005/2006). He continued his study in Utrecht with the master Biomolecular Sciences, where he performed two research internships. In his minor research project, at the NMR spectroscopy research group under the supervision of prof. dr. A.M.J.J. Bonvin, he explored the allostery of the Lactose Repressor Protein by analyzing molecular dynamics simulations. A major research project was performed at the Crystal and Structural Chemistry group under the supervision of dr. E.G. Huizinga concerning expression, crystallization and NMR binding studies of the immunoreceptor LAIR. After graduation (2009) he started his PhD project at the Membrane Biochemistry & Biophysics group under the supervision of prof. dr. J.A. Killian. The molecular insights into the mechanism of sensing and signal transduction of the thermosensor DesK, obtained during this project are described in this thesis, and were regularly presented at (inter)national conferences. During his PhD, he supervised five bachelor students and two master students on DesK related research projects and he assisted students in several theoretical and practical courses. Furthermore, Joost was chairman of the PhD council and member of the executive board of studies of the Graduate School of Life Sciences.

Dankwoord

Dit werk had onmogelijk tot stand kunnen komen zonder de medewerking, hulp en steun van een groot aantal mensen. Bovendien was het mede dankzij jullie dat ik met plezier gewerkt heb en zoveel heb geleerd. Kortom, ik wil hier graag de mensen bedanken die mij een fantastische promotietijd bezorgd hebben. Mijn grootste dank gaat uit naar mijn promotor. Antoinette, je zag in dat DesK een uitstekend praktijkvoorbeeld is van de door jou zo uitgebreid bestudeerde model transmembraan peptiden. Ik heb veel bewondering voor je kennis over membranen en de interessante projecten die daaruit voortgevloeid zijn. Je bood me de gelegenheid de resultaten overal te presenteren, inclusief drie maal bij de Biophysical Society meeting in de VS. Dat vond ik stuk voor stuk geweldige en leerzame ervaringen. Ik maakte kennis met jouw netwerk: bekende en zeer gewaardeerde collegae in het membraanonderzoek. Dat jij één van hen bent, werd onderstreept toen de Avanti EBSA Award vorig jaar aan jou werd toegekend. Ik ben je ook dankbaar voor alle aansporingen, zonder welke ik nu waarschijnlijk nog bezig was, maar je besefte ook dat het soms niet sneller kon en minder werken na de geboorte van Eva was geen probleem. Tijdens het schrijven heb ik ook veel van jou geleerd, waardoor het verhaal in dit proefschrift goed loopt met de juiste nadrukken en nuances. Er was ook altijd ruimte voor ontmoetingen, in de vorm van etentjes met collegae en je hebt ervoor gezorgd dat Larisa hier een jaar kon werken.

Daarnaast wil ik de leescommissie bestaande uit Maarten Egmond, Marc Baldus, Bernd Helms, Joost Holthuis en Tsjerk Wassenaar hartelijk bedanken voor het kritisch lezen van mijn proefschrift.

I want to thank my dear colleagues in Argentina: Larisa and Diego, the pioneers of DesK. Without your work and particularly the discovery of the minimal sensor, my project would not have existed in the first place. Larisa, I enjoyed your stay in Utrecht and it brought me insight and understanding of the molecular biological techniques you use. I particularly enjoyed your typical South-American liveliness, always yearning for new projects. In addition, I owe many thanks to my coworkers in Canada: Anastassiia en Peter. Your simulations were a valuable addition to the project and I hope to see many more in the future. Anastassiia, I enjoyed working with you. Your cheerful attitude and willingness to explore were perfect ingredients to persist at the Biophysical Society meetings from early morning until late in the evening and I equally enjoyed your visits to the Netherlands.

Hierbij wil ik ook alle collegae van de vakgroep bedanken. Martijn, je leerde mij de weerbarstige praktijk van lipiden en membranen. De fijne kneepjes van Rouser en Bligh & Dyer. Er moest ook altijd geborreld worden. De Cie en je zelfgestookte pastis zijn wat mij betreft legendarisch. Samen met Marlies, Mandy, Joep en Ruud hebben jullie altijd het lab draaiende gehouden, ondanks de bureaucratie en bezuinigingen

van de UU. Maar wel met de hulp van onze onmisbare secretaresses Irene, Barbara, Cecile, Caroline en Noortje.

Daarnaast wil ik de studenten bedanken die meegewerkt hebben aan dit project. Aike, Joanne, Melissa, Tom, Lidia, Antoine, Ineke, Mariëtte en Thomas, bedankt voor jullie inzet en de gezelligheid in het lab en daarbuiten.

Onze vakgroep heeft heel wat veranderingen ondergaan. Toen ik begon, waren wij Chemical Biology and Organic Chemistry. Ik herinner mij een warm onthaal en gezelligheid in en buiten het lab met de Chemical Biology collegae van die tijd: Yvonne, Erica, Tania, Nick, Nicole, Tami, Diana, Ben en Eefjan. Jacques, you were like a mentor to me, teaching me everything about biophysics and poster design. I enjoyed your company, particularly at the Biophysical Society meetings in the US, where you introduced me to many colleagues, sharing a beer or two. Daarnaast waren er de immer fanatieke voetbaltoernooien van katalyse, waar wij een welkome aanvulling waren op het Organic Catalysis team met Jacco, Peter, Manuel en studenten – leve de derde helft. Paulien, Inge, Yao en Remko, als collega AIO's van het eerste uur hebben we naast het harde werken ook een hoop lol gemaakt en ik denk met plezier terug aan alle conferenties, feestjes, (kerst)diners en gezelligheid. Remko, dankzij jou heb ik het squashen ook weer opgepakt en ik hoop dat we dat nog vele jaren kunnen doen. Ik ben blij dat je mij ook als paranimf wilt assisteren tijdens mijn verdediging.

Na de verhuizing gingen we verder als Biochemie van Membranen. Vervolgens kwam de fusie met Membraan Enzymologie en die leverde weer een aantal gezellige nieuwe collegae op. We gingen verder als Membraan Biochemie & Biofysica. Thanks to Maarten, Tine, RK, Rob, Hanka, Toon, Joost H, Matthijs, Per, Steven, Gabi, Patricia, Greg, Samuel, Stefan, Sabine, Lisette, Jonas, Xue, Amrah, Saran, Mike, Juan, Kees and Marre, for many inspiring talks, a great atmosphere in the group and legendary conference parties. Sam, thanks for your NMR efforts and intellectual, British discussions with high cultural content. Saran, thanks for your inspirations from India.

Dan rest mij het gehele SMALP team met Martijn, Kees, Marre, Jonas, Juan en Stefan te bedanken. Jonas, thanks for helping me out with column purifications and CD, critical comments and figures, which pimped chapter 5 of this thesis, helping me with the PNAS submission procedure, smooth succession as the Bijvoet representative, fruitful discussions and fun evenings. Looks like everything you touch here turns to gold and with you we gained an excellent scientist and talkative colleague. Juan - I hate proteins - Dominguez Pardo, you filthy misogynist (look up that term, it will be of great use to you) thanks for introducing good food and bad talk to the coffee table. It was great having you as roommate and I will miss our discussions regarding work, food drink and the good life. I might even miss your Spanish swearing. En tot slot SMALPer van het eerste uur: Stefan. Bedankt Stefan, voor het broodnodige fysisch chemisch tegengewicht in de groep. Ik vond het SMALP project van het begin af aan interessant en veelbelovend, ook dankzij

jou bijdrage, waarbij je altijd tot op de bodem wilde gaan. Helaas zijn DesK samen met SMA nog niet tot grote hoogte gekomen maar we hebben toch zeker een aanzet kunnen doen. Ik heb enorm genoten van jou als kamergenoot, nooit te beroerd om de lolbroek uit te hangen. Niet gehinderd door enige terughoudendheid naar collegae met meer aanzien of senioriteit wist jij altijd weer hilarische situaties te laten ontstaan. Ik kon alles met jou delen, tot dochterleed aan toe en ik ben blij dat je paranimf wilt zijn bij de verdediging van dit proefschrift.

Verder wil ik een aantal collegae van andere vakgroepen bedanken. Michal, Mans, Megan, bedankt voor goede verhalen, treiterige discussies en een goed uitzicht. Arjan en Mies, dank voor jullie hulp met de massaspectrometers en DSC. Ik wil de leden van de Bijvoet PhD commissie en de Graduate of Life Sciences PhD commissie graag bedanken voor een leuke en leerzame tijd. Reinout en Saskia, de activiteiten van het Bijvoet en de Graduate School waren een succes dankzij jullie.

Buiten de werksfeer waren er vrienden en familie, die ik graag wil bedanken voor de broodnodige afleiding en ontspanning. Peter M, Peter D, Koert, Rijnette, Dianne, Quintin, aka The Ballistics, bedankt voor de geweldige muziekervaringen. De GVR: Ewold, Joep, Steven, Meile, Siddharth, Ivo, Arno en Vicencio, bedankt voor alle trips en stapavonden en vooral de lol. De jaarclub: Ramon, Thomas, Gerlof, Constant, Sjors, Johannes, Pascal, Joost, Joost, Joost…., ook wij hadden aan stapavonden lol en uitjes geen gebrek. Hanna, Oscar en Sophie, onze paden zullen elkaar wel blijven kruisen. Jan, onze keuken en badkamer zijn nog steeds tiptop en Els bedankt dat je het hele manuscript hebt doorgeworsteld en de (taal)fouten eruit hebt gehaald. Lars, bedankt voor je commentaren en goede sauternes.

Ik wil hier ook mijn familie bedanken voor alle steun en toeverlaat. Oma, Anne, Tijs, Gea, Yvette, Sonja, Stefan, Bart en Sanne, bedankt voor jullie interesse en gezelligheid. Hans en Hannie, bij jullie is het als een tweede thuis. Bedankt voor alle oppas, verrijkende en ver reikende, alles-met-alles-verbindende discussies, vergezeld van uitstekende wijnen en spijzen, die uiteraard ook altijd weer onderwerp van discussie zijn.

Papa en Mama, bedankt voor jullie onvoorwaardelijke steun. Ik leerde van jullie keuzes te maken op basis van mijn hart en de wereld met een open blik tegemoet te treden.

Lieve Sandra, ik ben onbeschrijflijk blij dat ik bij jou ben. Zonder jou was ik überhaupt niet aan deze promotie begonnen. Bedankt voor je steun en ik houd van je perfectionisme en rusteloosheid en heb ze ook nodig. Ik geniet nog steeds van onze geweldige reizen en van ons samenzijn als gezinnetje met onze lieve, lieve baby Eva. Het is mijn grootste geluk dat ik haar mag zien opgroeien. Ik houd van jullie en zal altijd van jullie blijven houden.